



AGE-HARDENING OF A COPPER-COBALT  
AND A COPPER-IRON ALLOY

By

ROBERT BRUCE GORDON

B. S. University of Rochester

1935

Submitted in Partial Fulfillment of the  
Requirements for the Degree of  
DOCTOR OF SCIENCE  
from the  
Massachusetts Institute of Technology  
1939

Signature of Author        **Signature redacted**       

Department of Metallurgy, May 1939

Signature of Professor        **Signature redacted**         
in Charge of Research

Signature of Chairman of Department        **Signature redacted**         
Committee on Graduate Students

✓

TABLE OF CONTENTS

38

	Page
Acknowledgments . . . . .	v
I. Introduction . . . . .	1
1. The Problem . . . . .	1
2. Plan of Attack . . . . .	2
II. Summary . . . . .	3
III. Review of Literature . . . . .	5
1. Choice of Alloys . . . . .	5
2. Equilibrium Diagrams . . . . .	6
3. Theories of Age-Hardening . . . . .	12
4. Aging of Copper-Iron and Copper-Cobalt Alloys . . . . .	15
5. Magnetic Properties of Copper-Iron Alloys . . . . .	16
6. Summary . . . . .	20
IV. Preparation of Materials . . . . .	22
1. Preparation of Alloys . . . . .	22
2. Preparation of Specimens . . . . .	25
V. Heat Treatment . . . . .	27
1. Solution Treatment . . . . .	27
2. Aging Treatments . . . . .	31
VI. Measurements . . . . .	33
1. Hardness . . . . .	33
2. Lattice Parameter . . . . .	33
3. Electrical Resistance . . . . .	35
4. Magnetic Measurements - General . . . . .	37
5. Magnetic Susceptibility . . . . .	40
6. Remanent Magnetic Moment . . . . .	44
7. Microstructure - Electrolytic Polishing . . . . .	51
VII. Presentation of Results . . . . .	56
1. General . . . . .	56
2. Aging at 250° C . . . . .	57
3. Aging at 375° C . . . . .	59
4. Aging at 550° C . . . . .	61

TABLE OF CONTENTS (continued)

	Page
VII. Presentation of Results (continued) . . . . .	64
5. Aging at 700° C . . . . .	64
6. Microstructure of Copper-Iron Alloy . . . . .	71
7. Microstructure of Copper-Cobalt Alloy . . . . .	72
VIII. Correlation and Interpretation of Results . . . . .	85
1. Copper-Cobalt Alloy . . . . .	85
2. Copper-Iron Alloy . . . . .	90
IX. Conclusions . . . . .	95
X. Recommendations for Further Work . . . . .	97
XI. Bibliography . . . . .	99
XII. Biographical Note . . . . .	102
XIII. Appendix . . . . .	103
Experimental Data . . . . .	104
Abstract . . . . .	1 - 4

LIST OF ILLUSTRATIONS

Figure		Page
1	The Copper-Iron Diagram (Hansen) . . . . .	7
2	Solid Solubility of Iron in Copper	
	(a) Tammann and Oelsen . . . . .	8
	(b) Hanson and Ford . . . . .	9
3	Specific Magnetization of Copper-Iron Alloys (Tammann and Oelsen) . . . . .	9
4	The Copper-Cobalt Diagram (Hansen) . . . . .	10
5	Solid Solubility of Cobalt in Iron (Tammann and Oelsen) . . . . .	11
6	Hardness Changes in Copper-Iron Alloys (Hanson and Ford) . . . . .	15
7	Hardness of Copper-Iron Alloys (Tammann and Oelsen) . . . . .	17
8	Paramagnetic Susceptibility vs. Reheating Temperature (Tammann and Oelsen) . . . . .	18
9	Hardness and Susceptibility Changes During 700° C Aging (Tammann and Oelsen) . . . . .	19
10	The Melting Furnace with Mold in Position . . . . .	22
11	Furnace for Solution Treatment and Quench in Hydrogen Atmosphere . . . . .	29
12	Back Reflection Patterns of Alloys Compared with That of Pure Copper . . . . .	34
13	Apparatus for Measuring Electrical Resistance . . . . .	36
14	Typical Magnetization Curves . . . . .	37
15	Composite Magnetization Curve . . . . .	39
16	The Gouy Method for Measuring Susceptibility . . . . .	40
17	Apparatus for Measuring Susceptibility . . . . .	42

LIST OF ILLUSTRATIONS (continued)

Figure		Page
18	Magnet for Magnetizing Remanence Specimens . . . . .	45
19	Method for Measuring Remanence . . . . .	47
20	Apparatus for Measuring Remanence . . . . .	48
21	Close-up of Magnetometer . . . . .	49
22	Electrolytically Poletched Sample at 2500 Diameters . .	52
23	Apparatus for Electrolytic Poletching . . . . .	53
24	Aging Curves of Copper-Cobalt Alloy at 250° C . . . . .	67
25	Aging Curves of Copper-Iron Alloy at 250° C . . . . .	67
26	Aging Curves of Copper-Cobalt Alloy at 375° C . . . . .	68
27	Aging Curves of Copper-Iron Alloy at 375° C . . . . .	68
28	Aging Curves of Copper-Cobalt Alloy at 550° C . . . . .	69
29	Aging Curves of Copper-Iron Alloy at 550° C . . . . .	69
30	Aging Curves of Copper-Cobalt Alloy at 700° C . . . . .	70
31	Aging Curves of Copper-Iron Alloy at 700° C . . . . .	70
32	Microstructure of Copper-Iron Alloy at 375° C . . . . .	74
33	Microstructure of Copper-Iron Alloy at 550° C . . . . .	76
34	Microstructure of Copper-Iron Alloy at 700° C . . . . .	79
35	Microstructure of Copper-Cobalt Alloy at 375° C . . . . .	81
36	Microstructure of Copper-Cobalt Alloy at 550° C . . . . .	82
37	Microstructure of Copper-Cobalt Alloy at 700° C . . . . .	83

## ACKNOWLEDGMENTS

The author wishes to thank the following men for their help in various stages of the work.

Professor Morris Cohen suggested the problem and supervised the investigation in all its stages.

Professor Carle R. Hayward provided the cathode copper and the use of the melting furnace.

Mr. George P. Swift helped in making the alloys.

Dr. Cyril S. Smith of the American Brass Co. arranged for the hot rolling of the forgings.

Professor F. Bitter provided apparatus and facilities for making the magnetic measurements. He and Dr. A. R. Kaufmann gave valuable advice on the experimental technique and interpretation of the magnetic measurements.

Professor John T. Norton gave advice on the X-ray diffraction work.

Professor Igor N. Zavarine gave advice on problems of heat treatment.

The Dow Chemical Co. provided the Dowtherm through the courtesy of Mr. W. A. Melching.

Mr. Walter M. Saunders, Jr., made the chemical analyses.

## I. INTRODUCTION

### 1. The Problem

Age-hardening is a term used to describe a metallurgical phenomenon which is now recognized as being of quite common occurrence. A large number of alloys exhibit the solid solubility-temperature relationship necessary for age-hardening, namely, an increasing solubility of one phase in another with increasing temperature. With these alloys there exists the possibility of quenching a solid solution from an elevated temperature and retaining it in a supersaturated condition at room temperature. Upon subsequent aging, the alloy proceeds towards equilibrium at a rate dependent upon the aging temperature. If the temperature is sufficiently low, it is possible by various measurements to follow the decomposition of the supersaturated solution and the ultimate attainment of the equilibrium state.

The problems associated with age-hardening are of universal interest and importance. The large increase in hardness and strength accompanying the aging of certain alloys first attracted the attention of metallurgists, and many alloys of commercial importance have been developed. From a theoretical viewpoint, the question of what changes in structure occur during aging is among the most fundamental in the field of physical metallurgy. The work to be reported here was directed towards the solution of this problem.

Many alloys and property changes have been studied in an attempt to associate the hardening with some particular stage in the aging process. This has led to investigations of the changes in the arrangement of the solute atoms prior to their precipitation as discrete particles. Other studies have been made concerning the nature of the precipitation process and the location of the precipitated phase. Although progress has been made, the great need at the present time is for data of a fundamental nature that can be explained by modern theories of the solid state. It was with this thought in mind that the present investigation of the mechanism of age-hardening was begun.

## 2. Plan of Attack

Among the physical phenomena best explained by our present knowledge are those of the magnetic properties of matter. The results of magnetic measurements during aging might therefore lend themselves, more readily than others, to interpretation in terms of atomic arrangement and aggregation. To make full use of these advantages, it was decided to study the age-hardening of alloys in which a ferromagnetic phase would be precipitated from a paramagnetic solid solution. Thus, the maximum possible change would be obtained. The magnetic properties should provide a good criterion for the beginning of precipitation and, if the aging process is sufficiently uniform, it might be possible to follow changes in the supersaturated solid solution prior to precipitation. Changes in hardness, electri-



cal resistance, lattice parameter and microstructure will be observed to aid in the evaluation of the magnetic results.

## II. SUMMARY

Binary alloys of copper with 3.2 percent cobalt and 2.4 percent iron were quenched from 1040° C and aged at temperatures of 250°, 375°, 550° and 700° C for times ranging from 3 seconds to a thousand hours. The progress of aging was studied by following the changes in hardness, electrical resistance, magnetic susceptibility, remanence and microstructure. The results showed a striking similarity in the aging mechanism of the two alloys. Both undergo a two-stage precipitation process, which is shown by microscopic evidence to occur first at the grain boundaries and then within the grains. The microstructure was examined on specimens that were polished and etched electrolytically to avoid any disturbances due to mechanical polishing.

Hardness increases slightly during the first stage and markedly during the second. Resistance decreases considerably in the first stage, but to an even greater extent at the start of general pre-

cipitation. The grain boundary precipitate is ferromagnetic in both alloys. The general precipitate, which is probably a face-centered cubic transition phase, is ferromagnetic in the copper-cobalt alloy but paramagnetic in the copper-iron alloy. The paramagnetic iron-rich phase transforms into a ferromagnetic form, probably the stable body-centered cubic phase, after prolonged aging at high temperatures. This change is clearly shown by the magnetic measurements. The initial cobalt-rich precipitate may likewise transform into its stable hexagonal close-packed phase, but the magnetic change is small since both forms are ferromagnetic.

Although no pre-precipitation effects of the duralumin type were found, the probable occurrence of face-centered transition phases leads to the conclusion that such a stage is likely but is masked by the non-uniformity of the aging process.

### III. REVIEW OF LITERATURE

#### 1. Choice of Alloys

A survey of the available binary equilibrium diagrams was made to locate the most promising alloys for the present investigation. The requirements were grouped under two headings (a) suitability for magnetic work and (b) susceptibility to age-hardening. Under the first category the most important qualification was that the alloy should contain a ferromagnetic phase in equilibrium with a paramagnetic phase. The first requirement for age-hardening was that the ferromagnetic phase be increasingly soluble in the other with increasing temperature. Other considerations were the ability to suppress the transformation during the quench and to age at a suitable rate. These were important for a theoretical study of the aging process and especially for the use of the magnetic measurements.

The magnetic requirements narrowed the search to those alloys of iron, cobalt and nickel with other metals which consisted of two phases - one rich and one poor in the ferromagnetic element. Aside from several alloys with previous metals, the only systems found to satisfy this requirement were those of copper with cobalt and iron. At room temperature these alloys consist of mixtures of the two terminal solid solutions. The copper-rich solutions are paramagnetic and the iron and cobalt-rich solutions are ferromagnetic. The copper-rich alloys of these two systems also satisfied the principal requirement for age-hardening, namely, a solid solubility

increasing with temperature. There was less certainty about the ability to prevent completely the precipitation of the ferromagnetic phase during quenching. The rates of aging remained to be determined.

After choosing the systems to be studied, the next step was the selection of particular compositions to work with. The aim was to obtain the maximum degree of age-hardening and still be able to dissolve completely the ferromagnetic phase. In this way it was thought it would be easier to detect various stages in the hardening process if any existed. From the previous work of other investigators, which are reported later in this chapter, it was decided that these requirements were best met by binary alloys of copper with 3 percent cobalt and with 2.5 percent iron.

## 2. Equilibrium Diagrams

The best diagram for copper-iron alloys based on the review of the existing literature by M. Hansen<sup>1</sup> is given in Figure 1. The solid solubility of iron in copper was determined microscopically by Hanson and Ford<sup>2</sup> and magnetically by Tammann and Oelsen<sup>3</sup> with the results as shown in Figures 2(a) and 2(b). The microscopic results shown by the squares and triangles in Figure 2(a) agree rather well with the curve determined magnetically.

The magnetic determination of solid solubility was made by measuring the specific magnetization of a series of alloys quenched from various temperatures. The results, plotted in Figure 3, show

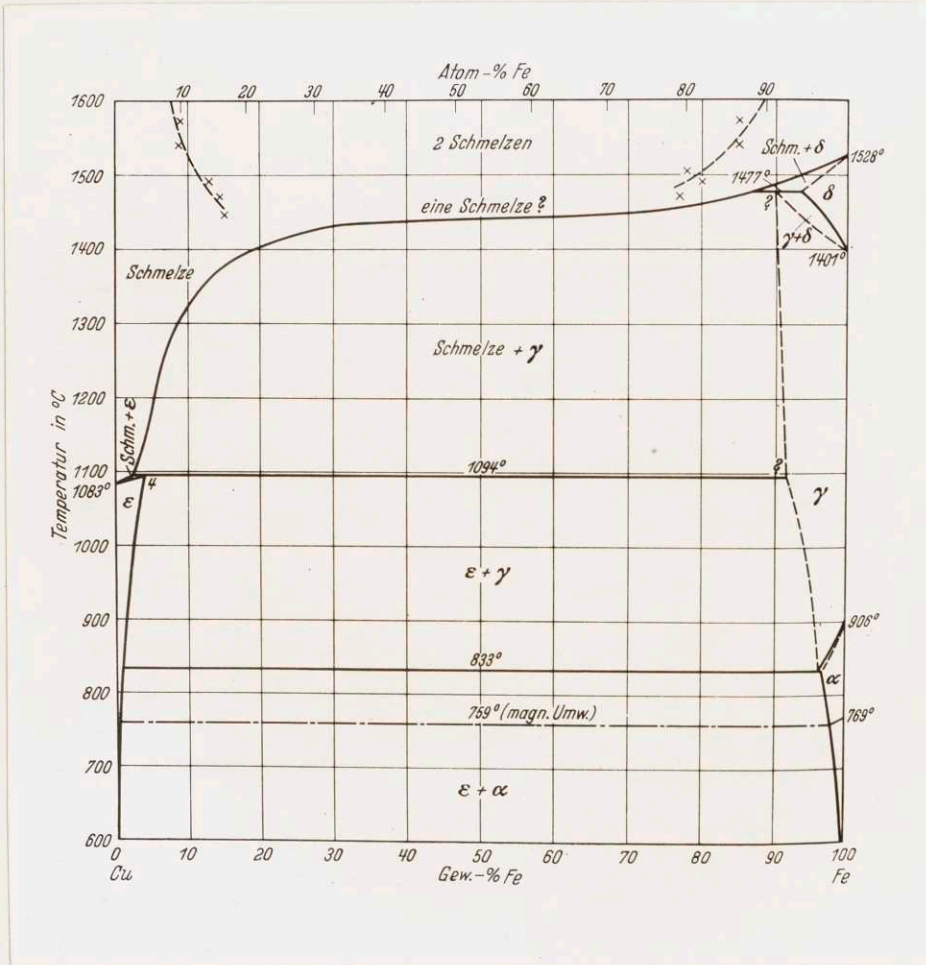


Fig. 1. The Copper-Iron Diagram (Hansen)

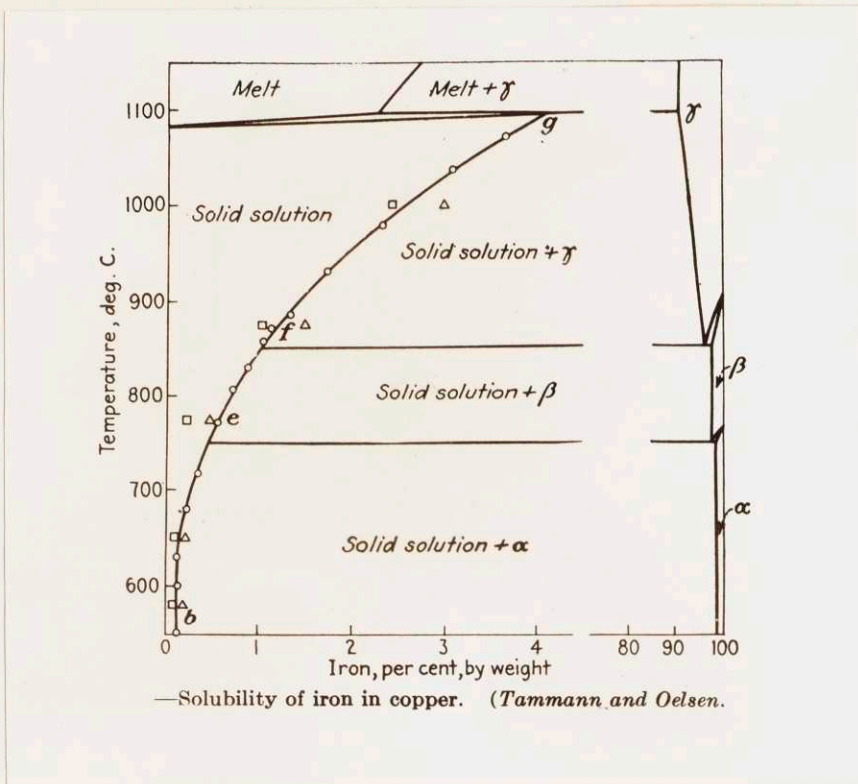
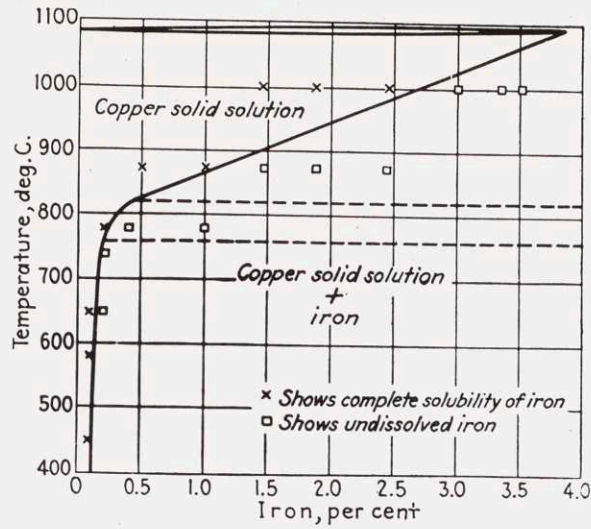


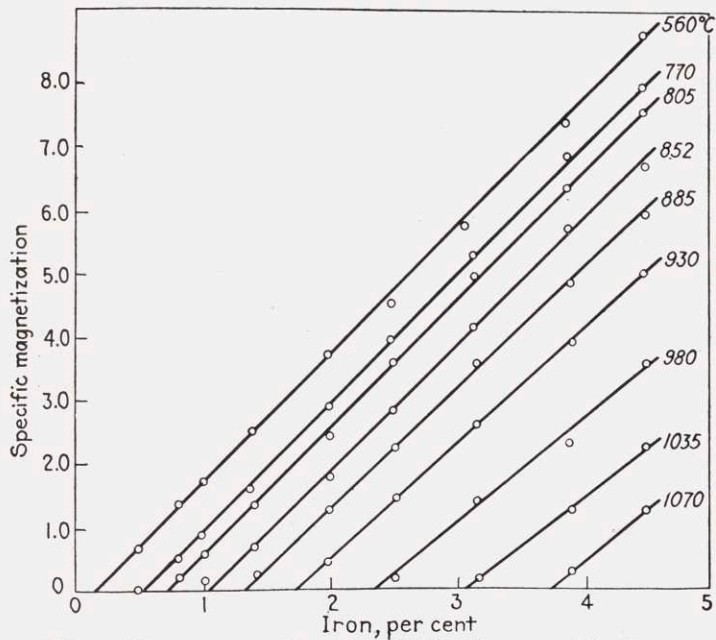
Fig. 2(a). Solid Solubility of Iron in Copper

a linear relation at every temperature between magnetization and percent iron in the heterogeneous field. The extremely small magnetization of the saturated solid solution (0.002) could not be shown on this scale and was neglected. The solubility at any temperature was taken as the value at the intersection of the isothermal magnetization curve with the concentration axis. The accuracy of this magnetic work was claimed to be  $\pm 0.02$  percent iron.

Fig. 2(b) Solid Solubility of Iron in Copper



—Solubility of iron in copper. (Hanson and Ford.)



—Effect of iron on magnetic susceptibility of copper-rich alloys quenched from temperatures shown. (Tammann and Oelsen.)

Fig. 3. Specific Magnetization of Copper-Iron Alloys

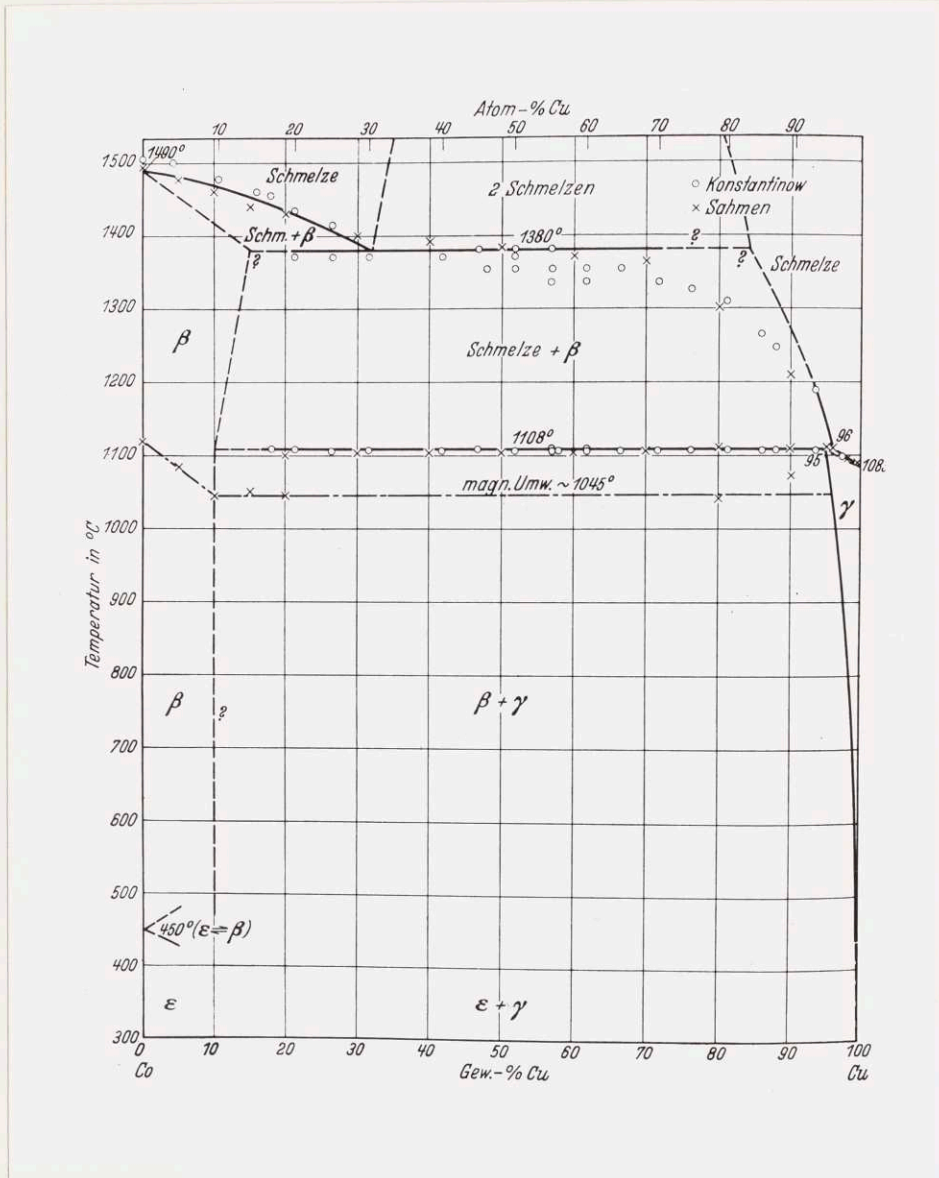


Fig. 4. The Copper-Cobalt Diagram (Hansen)



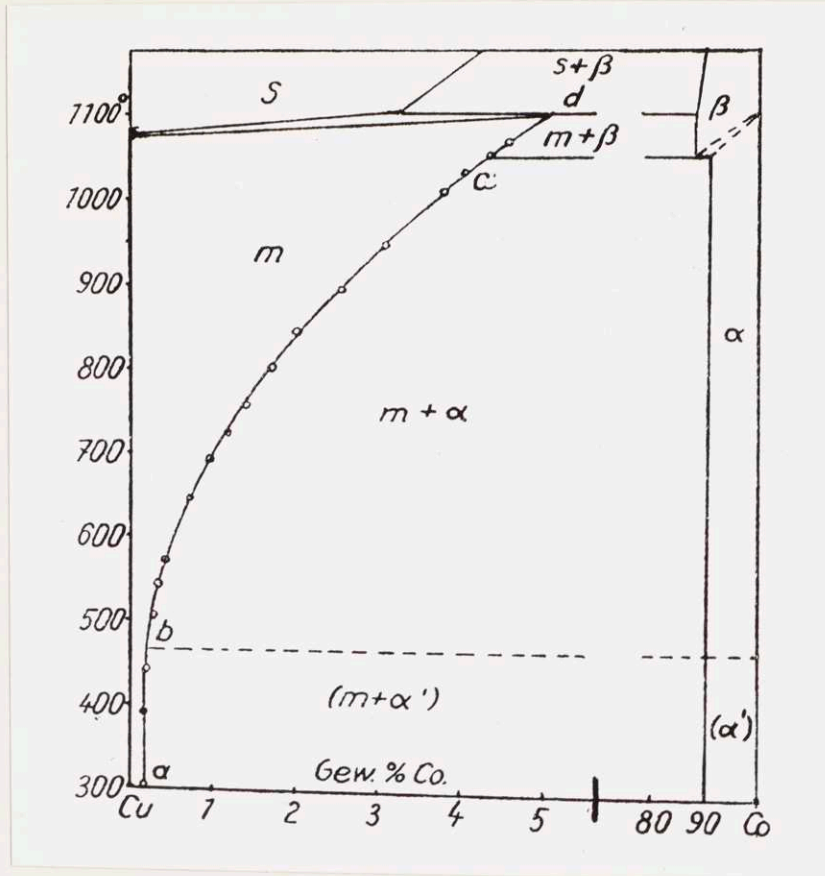


Fig. 5. Solid Solubility of Cobalt in Iron (Tammann and Oelsen)

The diagram for copper-cobalt alloys based on the literature survey of Hansen<sup>1</sup> is given in Figure 4. The solid solubility of cobalt in copper was determined magnetically by Tammann and Oelsen<sup>3</sup> in the manner described above. Their results are shown in Figure 5. From 700° to 1070° C the solubility of cobalt is about one per cent greater than that of iron in copper. Although it was not possible to determine the solubility of either cobalt or iron at low temperatures, extrapolation showed it to be quite small.

### 3. Theories of Age-Hardening

The literature on the general subject of age-hardening is voluminous and no attempt will be made to give a complete review here. A number of excellent reviews have appeared recently of which the latest is that of Gaylor<sup>4</sup>. The first explanation of age-hardening was given by the theory of Merica, Waltenburg and Scott<sup>5</sup> which attributed the hardening to a critical dispersion of precipitated particles. This simple precipitation theory adequately explained the observed changes in a number of alloys. However, other alloys showed hardening before the occurrence of the changes in electrical resistance, lattice parameter and dilation, usually associated with precipitation. This fact led Merica<sup>6</sup> to propose a new theory in which the hardening was explained as due to segregations or "knots" of solute atoms on the solid solution lattice. Thus, certain alloys were believed to harden by precipitation while others hardened by "knot" formation. Working with silver-copper alloys, Cohen<sup>7</sup> was able to produce both types of hardening depending on the temperature of aging. He formulated a theory that the mechanism of aging was the same at all temperatures, and that hardening could be caused both by "knot" formation and by precipitation, thus producing double peaks in the hardness curves. At about the same time, Gaylor<sup>8</sup>, working principally with aluminum alloys, came to approximately the same conclusions.

Other investigators, notably Fink and Smith<sup>9</sup>, have opposed these views and have attempted to explain double-aging peaks and other anomalies by the simple precipitation theory. By using a special etching technique they were able to show precipitation in the early

stages of the aging of aluminum alloys. They found that quenching stresses caused localized precipitation to take place at grain boundaries and along slip planes. Hence they ascribed the two hardness peaks as due to a non-uniform precipitation process. In a recent paper, Cohen<sup>10</sup> has found still an earlier stage in the hardness which can be attributed to "knot" formation. The concensus of opinion at the present time seems to be that property changes do occur prior to precipitation. However, we are hampered by the inability to predict on theoretical grounds what the changes in physical properties should be during the "knot" stage.

Despite this uncertainty about the early stages of aging, much progress has been made towards an understanding of the later stages, involving precipitation, where the maximum property changes occur. In line with the work in Germany of Dehlinger<sup>11</sup>, Köster and Dannöhl<sup>12</sup>, Volk, Dannöhl and Masing<sup>13</sup> and others, age-hardening alloys may be classified according to the character of the precipitation process as follows. (a) Homogeneous or uniform precipitation where all regions in a sample precipitate at the same rate. (b) Heterogeneous or non-uniform precipitation where the precipitation rate is accelerated in certain regions such as the grain boundaries and along slip planes. In the first class, the lattice parameter shifts steadily from the value corresponding to the supersaturated solution to that of the stable solution. The microstructure shows a general precipitate distributed at random throughout the grains. In the second class, two sets of lines appear in the X-ray pattern, the positions of which remain unchanged during aging. One set, due to the supersaturated solu-

tion, gradually decreases in intensity, while the other, due to the stable solution, gradually increases. The microstructure shows a heterogeneous mixture of precipitate and stable solution forming in areas at the grain boundaries which gradually grow at the expense of the unchanged supersaturated solution within the grains. Gold-nickel alloys<sup>12</sup> are examples of this kind of precipitation.

Another type of heterogeneous precipitation occurs in beryllium-copper and in cobalt-nickel-copper alloys<sup>13</sup> where the grain boundary areas grow to a certain extent and then stop, while the center of the grain undergoes a uniform precipitation. Dehlinger ascribes the initiation of both types of heterogeneous processes to stresses at the grain boundaries and the continuation to an "autocatalytic" acceleration. In the gold-nickel alloys this acceleration may be the result of distortion due to a 12 percent change in lattice parameter at the edge of the heterogeneous regions. But this hypothesis does not account for the behavior of the cobalt-nickel-copper alloys. Masing<sup>14</sup> offers the following explanation: The supersaturated solution contains nuclei of molecular dimensions due to strong undercooling. An increased molecular mobility produces larger nuclei at the boundaries which have a greater thermodynamic stability and hence grow at the expense of those within the grain. These alloys have only a 2 percent change in lattice parameter so there is little distortion to continue the growth of the precipitated boundary areas. Precipitation within the grain eventually reaches a point where the difference in stability is too small to promote further growth of the boundary regions.

4. Aging of Copper-Iron and Copper-Cobalt Alloys

The literature on the age-hardening of copper-rich copper-iron and copper-cobalt alloys is extremely meager. Hanson and Ford<sup>2</sup> made a few aging treatments on a 0.7 percent iron. They also studied the effect of iron on the recrystallization temperature of copper. Their results are shown in Figure 6.

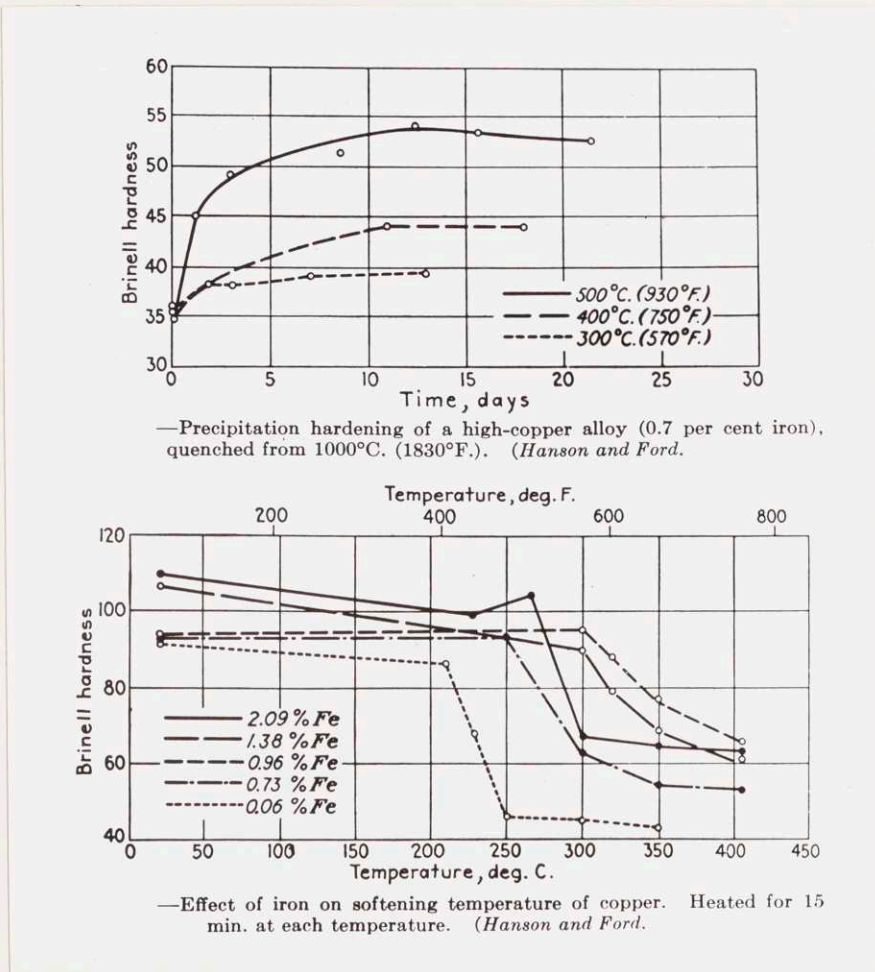


Fig. 6. Hardness Changes in Copper-Iron Alloys

M. G. Corson<sup>15</sup> studied the hardness and electrical resistance changes after different thermal and mechanical treatments of some copper-cobalt alloys. He found that 2.5 percent cobalt gave maximum hardening and that 62,000 pounds per square inch tensile strength and 105 Brinell were obtainable. Over-aged samples showed the maximum conductivity of 55 percent standard. A 0.90 percent cobalt alloy chill cast showed precipitated particles in an irregular network within the grains that Corson described as dendritic. After annealing for 6 hours at 950° C and water quenching, this same alloy showed large twinned crystals with rounded bumpy grain boundaries.

C. S. Smith<sup>16</sup> reported the unusual hardening obtained by air cooling a 3.58 percent cobalt alloy from 900° C. When cooled from 900° to 600° C in 100 seconds, this alloy aged to the maximum hardness obtainable by quenching and tempering. This was attributed to the low diffusion rate of cobalt in copper. This caused a very slow rate of crystal growth which, combined with a high rate of nuclei formation at elevated temperatures, resulted in a large number of tiny particles effective in producing hardening.

##### 5. Magnetic Properties of Copper-Iron Alloys

Tammann and Oelsen<sup>3</sup> determined the changes in hardness and in magnetic properties of a series of copper-rich copper-iron alloys after various thermal and mechanical treatments. Referring to Figure 7, where the diameter of Brinell impression is plotted vs. percent iron, alloys with less than 1.5 percent iron were paramagnetic after slow cooling (curve B) but were more weakly paramagnetic and softer after

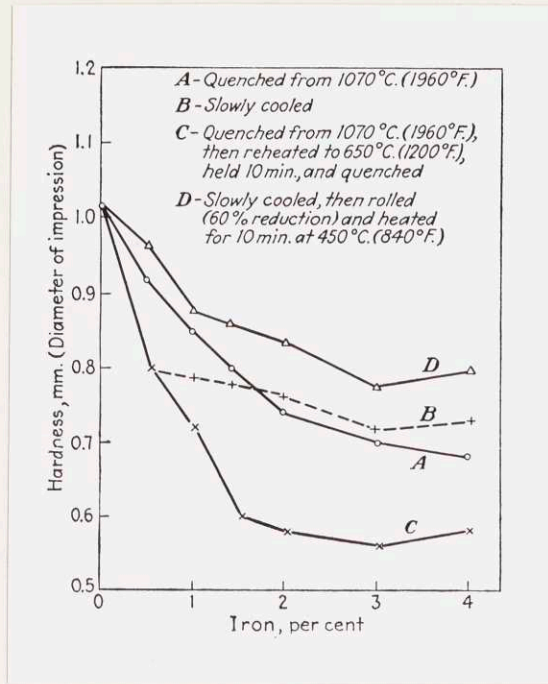


Fig. 7. Hardness of Copper-Iron Alloys  
(Tammann and Oelsen)

quenching from 1070° C (curve A). Alloys with from 1.5 to 3 percent iron were weakly ferromagnetic after slow cooling (curve B) but were paramagnetic and harder after quenching (curve A). By quenching from 1070° C and reheating 10 minutes at 650° C all the alloys exhibited minimum paramagnetism and maximum hardness (curve C). By cold rolling slowly cooled alloys and annealing at 450° C to remove the work hardening, all were ferromagnetic and in the softest condition. (D)

A horizontal balance of the Weiss-Foex type was used to measure magnetization and susceptibility. The force  $f$  on a small specimen of mass  $m$  placed in a field with a gradient  $\frac{\delta H}{\delta y}$  is given by the equation:

$$f = m s \frac{\delta H}{\delta y} = m \chi_H \frac{\delta H}{\delta y}$$

where

$s$  = specific magnetization

$\chi$  = mass susceptibility

Both quantities can be converted to the corresponding quantities per unit volume by multiplying by the density of the alloy. The authors did not state how they distinguished the paramagnetic state from the ferromagnetic. Apparently they merely used the absolute value of susceptibility, as determined in a field of 8300 oersteds, as their criterion.

Tammann and Oelsen studied the effect of heating the paramagnetic alloys for 20 minutes at various temperatures and quenching. The susceptibility of alloys with less than 1.5 percent iron, which did not become ferromagnetic after slow cooling, is shown in curves A, B, C and D of Figure 8.

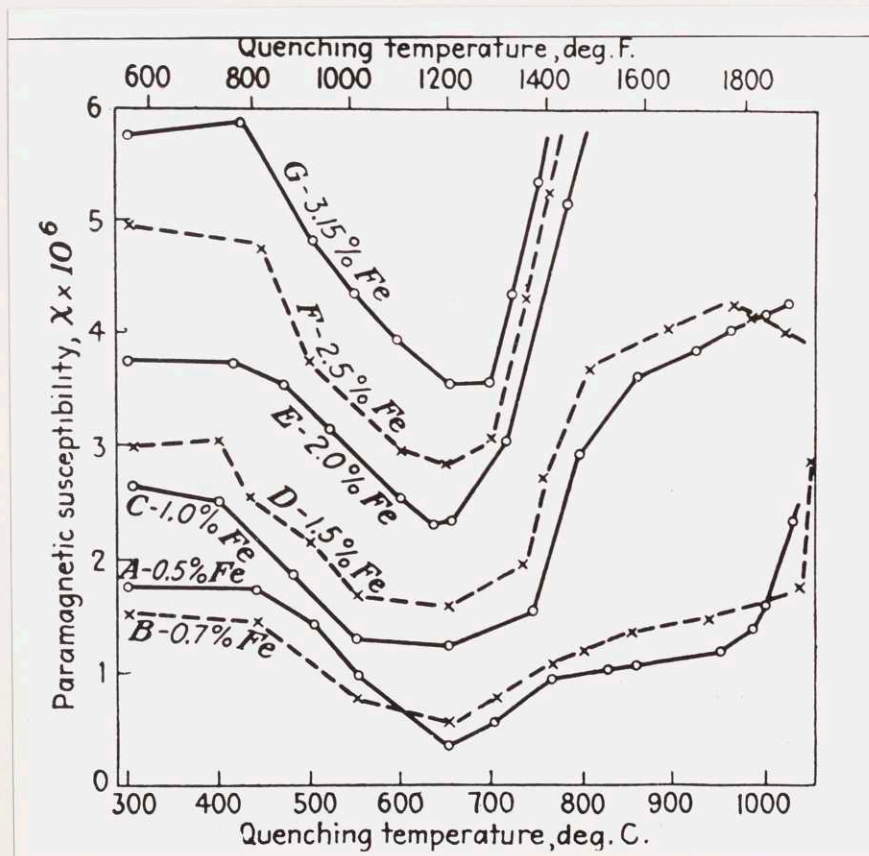


Fig. 8. Paramagnetic Susceptibility vs. Reheating Temperature (Tammann and Oelsen)



The susceptibility decreased with temperature, confirming the fact that no ferromagnetic phase was precipitating. Alloys with from 1.5 percent to 3 percent iron were quenched to convert them to the paramagnetic state, then reheated for 20 minutes and quenched. The susceptibility values are shown in curves E, F and G. All alloys showed a minimum susceptibility at 650° C and this minimum became more pronounced with increasing iron content.

The only data given by Tammann and Oelsen of a type similar to that of the present work is shown in Figure 9.

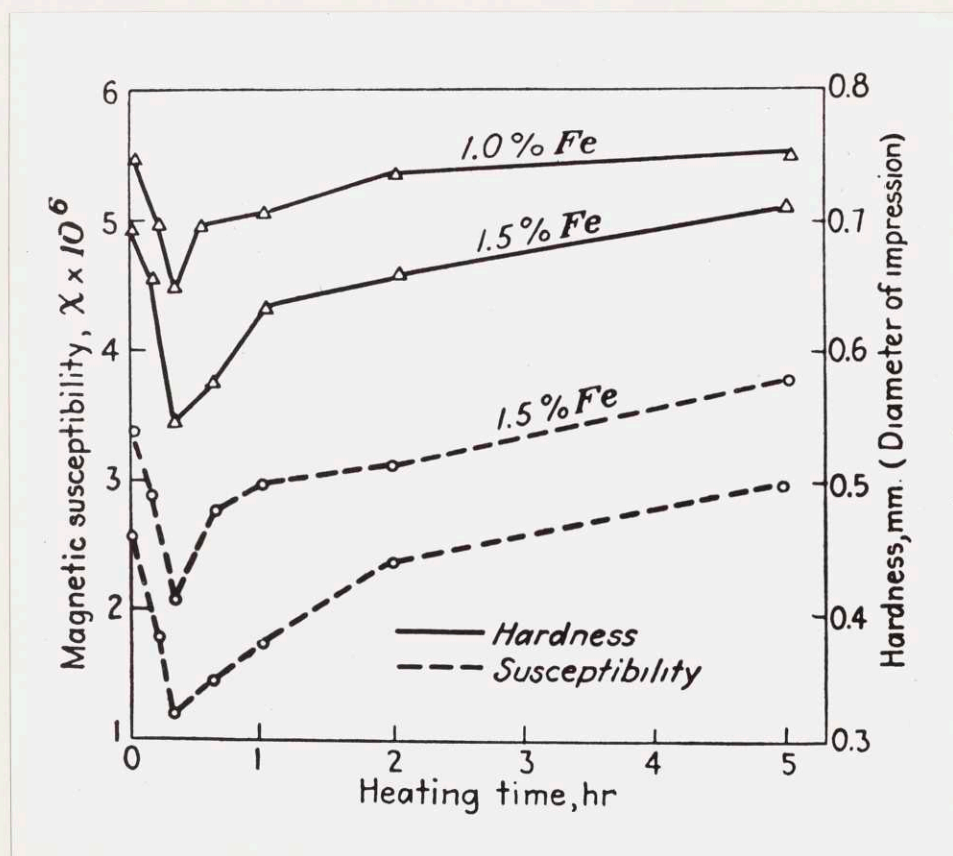


Fig. 9. Hardness and Susceptibility Changes during 700° C Aging (Tammann and Oelsen)

The hardness (diameter of Brinell impression) and susceptibility are plotted vs. time for alloys with 1.0 and 1.5 percent iron quenched and aged at 700° C. The hardness rose to a maximum and the susceptibility fell to a minimum after 15 minutes. Then the hardness decreased and the susceptibility rose. These alloys became ferromagnetic after 50 hours aging at 700° C when they were presumably completely softened.

Although the work of Tammann and Oelsen reported above has an important bearing on the age-hardening of copper-iron alloys, they made no statements concerning this aspect of their work. However, in another paper, Tammann<sup>17</sup> reviewed the data shown in Figures 6 and 7. He stated that the association of maximum hardness and minimum paramagnetic susceptibility was evidence that the hardening was due to changes taking place in the solid solution prior to precipitation. He thus assumed that the absence of a ferromagnetic phase also meant the absence of any precipitate. This important point will be discussed later after considering the results of the present investigation.

## 6. Summary

After a careful review of the literature, it was decided that copper-rich alloys containing 3 percent cobalt and 2.5 percent iron showed possibilities of having the most desirable combination of magnetic properties and age-hardenability. The copper-cobalt and the copper-iron equilibrium diagrams are not known with any great degree of accuracy but the solid solubilities of cobalt and iron in copper have been determined magnetically by Tammann and Oelsen with considerable precision. The copper-rich ends of the diagrams are of primary

importance to the present investigation but it is also of interest that both iron and cobalt have allotropic modifications. At elevated temperatures both are face-centered cubic while at room temperature iron is body-centered cubic and cobalt is hexagonal close-packed. This fact may play an important role in the precipitation of an iron-rich or a cobalt-rich phase from the face-centered copper-rich solution.

There is general agreement among various investigators that the mechanism of aging is the same at all temperatures. Uncertainty exists, however, as to the actual effects of the pre-precipitation stage on physical properties. Studies attempting to reach an answer to this problem are complicated by the microscopic non-uniformity of aging in most alloys. Hence the property changes occurring during aging are the summation of the effects of several overlapping stages and they may vary with every alloy studied.

There has been little published information on copper-iron or copper-cobalt alloys with a direct bearing on the present work except for the magnetic investigations of Tammann and Oelsen. Their results pointed out the possibility of iron precipitating in a paramagnetic form when copper-iron alloys are cold rolled after quenching from above 850° C. Although the authors do not explain their aging results, it is also possible to attribute this behavior to paramagnetic iron.

#### IV. PREPARATION OF MATERIALS

##### 1. Preparation of Alloys

The alloys were made by melting under charcoal in a clay-graphite crucible and bottom-pouring into a chill mold. Cathode copper of high commercial purity was cut into small pieces, pickled and carefully washed. The cobalt was in the form of commercial rondelles with a stated purity of 98.47 percent cobalt. The iron was high purity electrolytic iron in the form of thin sheet.

The melting furnace, shown in Figure 10, was designed by Prof. C. R. Hayward. The steel shell was lined with insulating brick inside of which was placed the winding of Kanthal resistance wire. The

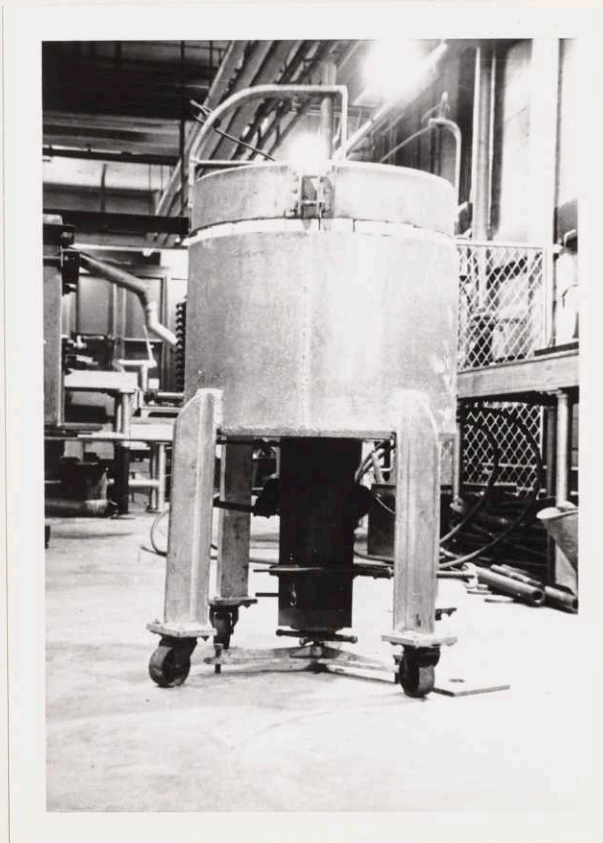


Fig. 10. The Melting Furnace with Mold in Position

crucible had a tapered hole in the bottom into which was fitted a long graphite stopper rod that extended up through the top of the furnace. Provision was made for insertion into the crucible of a thermocouple in a silica protection tube and a graphite stirring rod. A heavy split steel mold  $1\frac{1}{2}$  inches square inside was clamped together and jacked up tight against the bottom of the furnace with an asbestos gasket as a seal. When the melt was ready for pouring the stopper rod was raised, allowing the metal to flow into the mold beneath.

The first copper-cobalt melt, with a nominal content of 3 percent cobalt, was made by melting weighed amounts of copper and cobalt under charcoal. The ingot was cast after holding the molten alloy at  $1150^{\circ}\text{C}$  for one hour. Chemical analysis showed 2.29 percent cobalt at the top and 2.00 percent cobalt at the bottom, indicating segregation and incomplete solution of the cobalt in the melt. For this reason it was decided to make a hardener alloy containing 15 percent cobalt. This alloy was made by melting in a clay-graphite crucible in an Arsem vacuum furnace under a vacuum of 2 mm. mercury. When the copper had melted, gas started to be evolved and continued to do so for a period of 6 hours with the temperature between  $1150^{\circ}$  and  $1200^{\circ}\text{C}$ . The gas was probably carbon monoxide from a reaction between graphite and the oxygen in the cobalt. The furnace was shut off with the temperature at  $1250^{\circ}\text{C}$  and the melt was allowed to solidify in the furnace. The resultant ingot showed practically complete solution of the cobalt. The microstructure consisted of blue dendrites of primary

beta plus a uniform fine dispersion of beta particles precipitated during the slow cooling.

The final copper-cobalt alloy, with a nominal composition of 3 percent cobalt, was made by melting this hardener alloy of approximately 15 percent cobalt with cathode copper in the electric resistance furnace under a cover of charcoal. The melt was held at 1200° C for 2 hours and stirred every 15 minutes with a graphite rod. It was cooled to 1150° C, stirred vigorously and chill cast. The resultant ingot weighed 3130 grams and had a pipe about 1 inch deep which was cropped off. Radiographs were made in two directions and they showed a very sound ingot with the exception of a large blowhole near the bottom. The lower quarter of the ingot was discarded, leaving a 7 inch length of sound material weighing 2260 grams. Ten gram samples were machined from the top and bottom surfaces for chemical analysis. The top showed 3.18 and 3.21 percent cobalt in two determinations while the bottom showed 3.19 and 3.24 percent. Thus if there was any segregation it was of the order of the experimental error in analysis. The top also showed 0.03 percent carbon, 0.02 percent iron and less than 0.01 percent nickel with 0.02 percent carbon, 0.02 percent iron and less than 0.01 percent nickel in the bottom. These impurities probably were introduced in the cobalt and charcoal used.

The copper-iron alloy had a nominal composition of 2.5 percent iron and a weight of 3500 grams. The iron was rolled up in sheet copper to protect it during melting. The pieces of cathode were then charged and covered with large lumps of charcoal. The charge

was melted in  $2\frac{1}{2}$  hours and was held at  $1200^{\circ}$  C for two hours. The silica protection tube broke off at the liquid level and a small amount of the chromel-alumel thermocouple was melted. The charge was cooled to  $1150^{\circ}$  C and poured. The ingot had a blistered surface and a small sinkhead, probably due to the low pouring temperature. The radiograph showed a sound ingot except for a thread-like blowhole in the bottom center. The top and bottom were cropped off to give a 7 inch length of sound material weighing 2180 grams.

Ten gram samples were machined from the bottom and top surfaces for chemical analysis. The top showed duplicate determinations of 2.43 and 2.40 percent iron while the bottom showed 2.40 and 2.40 percent iron. Four determinations gave 0.01 percent nickel. From the composition of the thermocouple and the weight melted, it was estimated that the maximum possible contamination of the melt was 0.1 percent nickel and 0.01 percent chromium. The small amount of nickel found in the analysis shows that only a small percentage of the melted thermocouple went into the alloy. In fact, there may have been no contamination since the copper-cobalt alloy, which was melted without incident, also showed 0.01 percent nickel. The percent copper found in each sample made up the balance of 100 percent within the experimental error.

## 2. Preparation of Specimens

The copper-cobalt and the copper-iron ingots were milled to about  $1\frac{3}{8}$  inches square to remove surface defects. They were then cut into two pieces. One piece of each ingot was forged to a  $\frac{3}{4}$  inch

square while the other was forged to a strip  $5/8$  inches thick and  $1\frac{1}{4}$  inches wide. The ingots were heated to  $1500^{\circ}$  F before, and were reheated several times during, the forging. They forged very nicely and no cracks were produced. The forgings were then pickled to remove the scale and the surface defects and seams were chipped and filed out.

The forgings were given a homogenizing anneal in vacuo at  $1600^{\circ}$  F for 12 hours. They were then hot rolled by the American Brass Co. through the courtesy of Dr. C. S. Smith. The square forgings were rolled to a rod  $\frac{1}{4}$  inches square with rounded edges. The rectangular forgings were hot rolled to strip  $3/16$  inches thick. The strips were pickled and cold rolled to a thickness of 0.118 inches and a width of  $1\frac{1}{4}$  inches. Specimens  $\frac{1}{2}$  inch wide were cut from these strips for the hardness and microscopic work.

The  $\frac{1}{4}$  inch rods were annealed at  $1600^{\circ}$  F for 1 hour and then cold swaged through 5 sets of dies in successive passes. The reduction in area from 0.250 inches to 0.079 inches (0.2 mm.) diameter amounted to 90 percent and was accomplished without any difficulty. These small rods were cut into 4 inch lengths which served as specimens for the electrical resistance and magnetic measurements.



## V. HEAT TREATMENT

### 1. Solution Treatment

Considerable difficulty was encountered in giving the alloys a satisfactory solution heat treatment prior to aging. According to the data of Tammann and Oelsen<sup>3</sup>, the solution temperature for 3.2 percent cobalt is 960° C (1760° F) and for 2.4 percent iron is 985° C (1805° F). Due to the extremely rapid transformation rate in these alloys it was found necessary to quench from much higher temperatures in order to retain the supersaturated solid solution. The great sensitivity of the magnetic measurements gave a very good criterion for solution of the cobalt and iron, while electrical resistance measurements indicated the successfulness of the quench in keeping the cobalt and iron in solution.

One of the first problems was the prevention of oxidation of the specimens since magnetic oxides of iron and cobalt might affect the magnetic results. The first treatments of the copper-cobalt alloy were made in an electric resistance furnace at temperatures of 970° C (1780° F) to 1010° C (1850° F). An atmosphere of carefully purified nitrogen was used, but some oxidation of the specimens always occurred, perhaps during the quenching operation. After treatments of from 1 to 12 hours, some particles of undissolved cobalt were still visible under the microscope. The specimens were then treated in a furnace heated by Globar resistance elements to temperatures up to 1070° C (1958° F). At these higher temperatures, treatments of 1 to 3 hours seemed to give complete solution as judged

by microscopic evidence. A graphite-clay muffle protected the specimens from oxidation in the furnace, but again they had to be quenched in air. Water and brine were first tried as the quenching liquid but an 8 percent solution of sodium hydroxide was finally chosen as giving the best results. Despite attempts to adhere to a uniform quenching procedure, small variations in the rapidity of the quench caused large changes in the as-quenched values of electrical resistance and magnetic susceptibility.

The results of this preliminary work pointed to the desirability of designing a special furnace in which the specimens could be heated and quenched in a non-oxidizing atmosphere and in which variations in the quenching procedure would be reduced to a minimum. In accordance with these ideas the vertical tube furnace shown in Figure 11 was constructed.

The furnace was built inside of a long steel tube, 3 inches in diameter, so that the resistance winding as well as the specimen would be in a hydrogen atmosphere. In this way the furnace could be operated at temperatures up to 1070° C with a chromel winding. The tube was lined with insulating brick which supported a winding, uniformly spaced on an alundum muffle 1 inch in diameter and 2 feet long. The furnace leads were taken out through a pipe in the side which served as the hydrogen inlet. A cooling coil around the tube protected the rubber stopper at the top. The temperature variation over a 4 inch length was about 10° C. The chromel-alumel couple was protected by a fused quartz tube. However, at the temperature used, the quartz apparently allowed some hydrogen to reach the couple

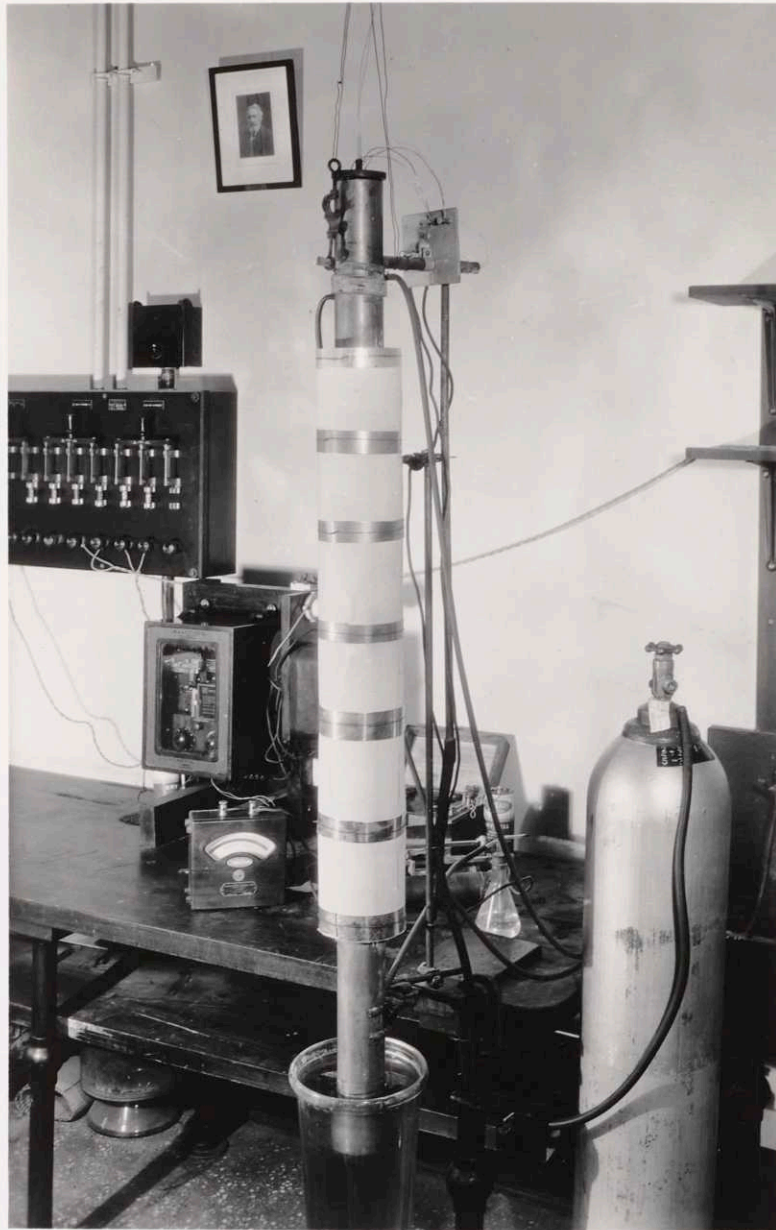


Fig. 11. Furnace for Solution Treatment and Quench in Hydrogen Atmosphere

and affect its calibration. For this reason the couple was calibrated at the melting point of chemically pure sodium chloride before each run. The lower end of the furnace tube was immersed directly in the quenching liquid and the hydrogen was taken out through a small glass U-tube. The specimens were in a hydrogen atmosphere at all times including the quench and a perfectly bright surface was obtained.

A special method was used for holding and releasing the specimens so that the quench could be as nearly automatic as possible. A fine iron wire holding the specimen was supported by another fine wire connected to two leads passing through the rubber stopper. When 220 volts were impressed across these leads, the connecting wire burnt out and released the wire holding the specimen. The specimen fell through a distance of about 3 feet into the quenching bath. A method of agitating the specimen or the liquid to increase the quenching rate would have been desirable but was difficult to accomplish without breaking the liquid seal of the furnace. As a substitute the quenching bath was made 2 feet deep so that the specimens were cooled to a considerable extent before reaching the bottom.

This furnace solved the problem of heating the specimens at a temperature high enough to dissolve the cobalt and iron without oxidation of the surface. Specimens were heated at about 1040° C (1900° F) for 1 to 6 hours but the time at temperatures over 1 hour made no noticeable change in microstructure or properties. Despite efforts to make the quench as rapid as possible, considerable

scatter was found in hardness, resistance and susceptibility. The samples with low hardness or high resistance were assumed to have received the best quench and were used for aging. This difficulty in obtaining reproducible quenched values is believed to be inherent in these alloys due to their extremely high transformation rate.

## 2. Aging Treatments

The quenched specimens were aged at temperatures of 250°, 375°, 550° and 700° C for periods ranging from a few seconds to a thousand hours. Liquid baths were used in order to bring the specimens quickly up to temperature and insure accuracy in timing the short intervals of aging. A temperature of 250° C was obtained by boiling Dowtherm A\* in a small pot equipped with a water-jacketed reflux condenser open to the atmosphere. A temperature of 375° C was obtained by boiling Dowtherm C\* in a similar pot placed in an electric resistance furnace. This material is solid below 100° C and care had to be exercised to prevent the air cooled condenser from plugging up. Both of these boiling liquids were very satisfactory in that they gave constant temperatures and did not attack the specimens in any noticeable way.

---

\* Dowtherm A is the eutectic mixture of diphenyl  $(C_6H_5)_2$  and diphenyl oxide  $(C_6H_5)_2O$ . Dowtherm C is a mixture of the approximate composition  $(C_6H_5)_3$ . They may be obtained from the Dow Chemical Co., Midland, Michigan.

The higher aging temperatures of 550° and 700° C were obtained with a salt bath which melted at about 500° C. The pot type furnace was held by an automatic controller to  $\pm 5^\circ$  C. The bath was stirred to prevent the existence of a temperature gradient. After periods of an hour or more the specimens began to show signs of corrosion by the salt, so a method of protecting them had to be devised. It was discovered that simply by wrapping several layers of copper sheet around the specimens, they were practically unattacked, even after long periods of time. The copper wrapping apparently dissolved preferentially and although the specimens were in contact with the salt it was possible to preserve a metallographic polish for some time.

Since the measurements were all made at room temperature, the aging treatments were interrupted at suitable intervals by quenching in water.

## VI. MEASUREMENTS

### 1. Hardness

In order to get a rapid quench the hardness specimens were made as small as possible. Since the specimens were quite soft after quenching their thickness had to be great enough to avoid an anvil effect on the hardness reading. The surface area had to be large enough to enable a sufficient number of readings to be taken during the aging runs. The size finally adopted was  $\frac{1}{2}$  inch by  $1\frac{1}{4}$  inch and 0.118 inches thick. As a result of the high temperature of the solution treatment the specimens were very coarse grained. This caused an unavoidable scatter in the hardness as quenched and during the early stages of aging. The hardness runs were made on two specimens which had the same initial hardness. At suitable intervals readings were taken, one on each side of both specimens, and the average value was recorded. The Rockwell F scale with a 60 kilogram major load and a 1/16 inch steel ball was used. The machine was checked with a block of known hardness before each series of readings on the specimens. The results were recorded to the nearest half division but are not considered accurate to better than  $\pm 2$  units.

### 2. Lattice Parameter

A few lattice parameter measurements were made on the hardness specimens after various treatments. The back reflection method with copper radiation from a Hagg tube was used. The apparatus and method have been described elsewhere by Norton<sup>18</sup>. An annealed sample of

oxygen-free copper gave a lattice parameter of 3.6073 A. U. as compared with the accepted value for pure copper of 3.6077 A. U., showing that the apparatus was set up accurately.

The copper-cobalt samples gave lattice parameters, varying from 3.6040 to 3.6108 A. U., which showed no regular change during aging at 375° or 550° C. The lines were sharp but seemed to give values of lattice parameter both above and below that for copper. In Figure 12 are reproduced the patterns of a quenched sample and one aged 100 hours at 375° C in comparison with one of annealed, pure copper.

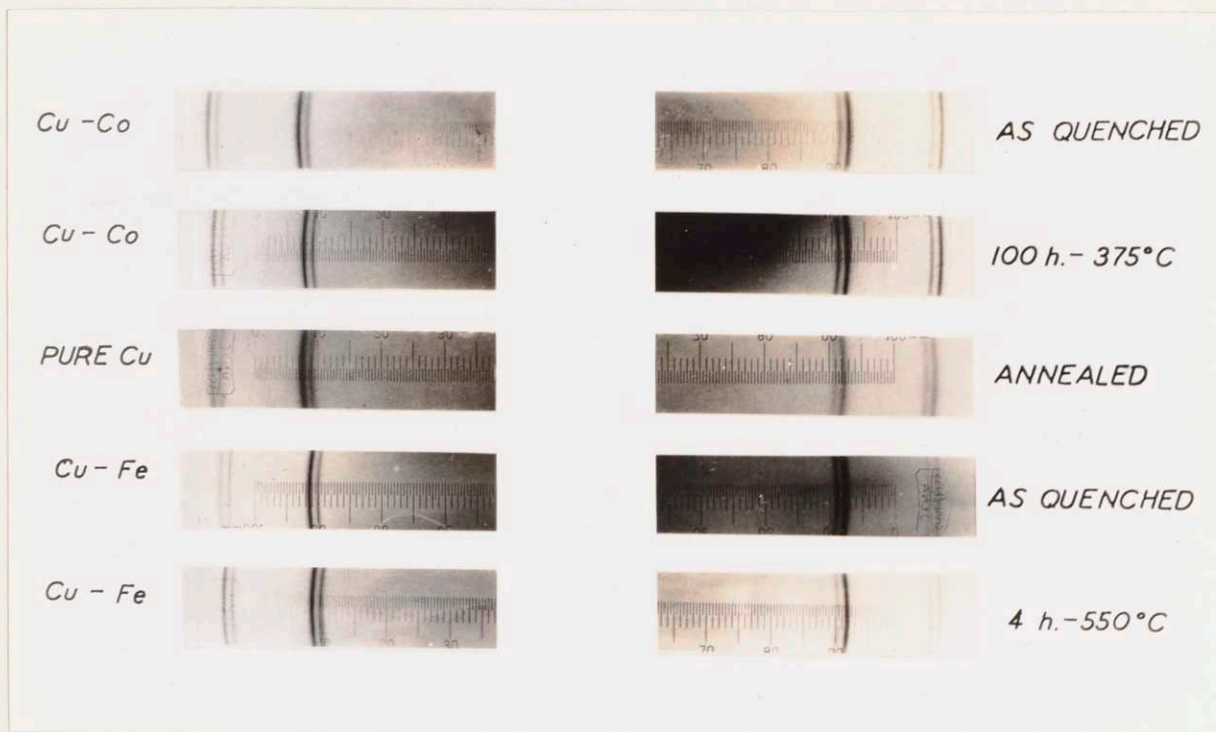


Fig. 12. Back Reflection Patterns of Alloys Compared with That of Pure Copper



Various copper-iron samples gave lattice parameters from 3.6031 to 3.6048 A. U. An aging run at 565° C showed no consistent changes. The patterns of a quenched sample and one aged 4 hours at 550° C are shown in Figure 12.

Since the atomic radii of copper, iron and cobalt are nearly the same, no large change in the parameter of these alloys is to be expected. However, one might expect precision measurements to show a small reproducible change on aging. This was not found to be true. The results show a wide degree of scatter which may perhaps be due to varying amounts of quenching strains in the lattice. It might be possible to measure and correct for these strains by taking measurements with the specimen at different angles to the X-ray beam. The coarse grain size would make this very difficult due to an inability to rotate the specimen through an angle great enough to give smooth lines on the X-ray pattern.

### 3. Electrical Resistance

Electrical resistance measurements were made on small rods 0.079 inches (0.2 mm.) in diameter and 4 inches long. The experimental set up is shown in Figure 13. The specimen was placed in a holder which clamped it against two knife edges 3 inches apart. The potential leads were attached to the knife edges while the current leads were attached to the ends of the rod. The resistance of the rod between the knife edges was measured by a Kelvin double bridge capable of an absolute accuracy of 0.1 percent. The specimen and holder were immersed in an oil bath which was equipped with a stirrer and a means for maintaining the temperature at 25° C  $\pm$  0.1°.

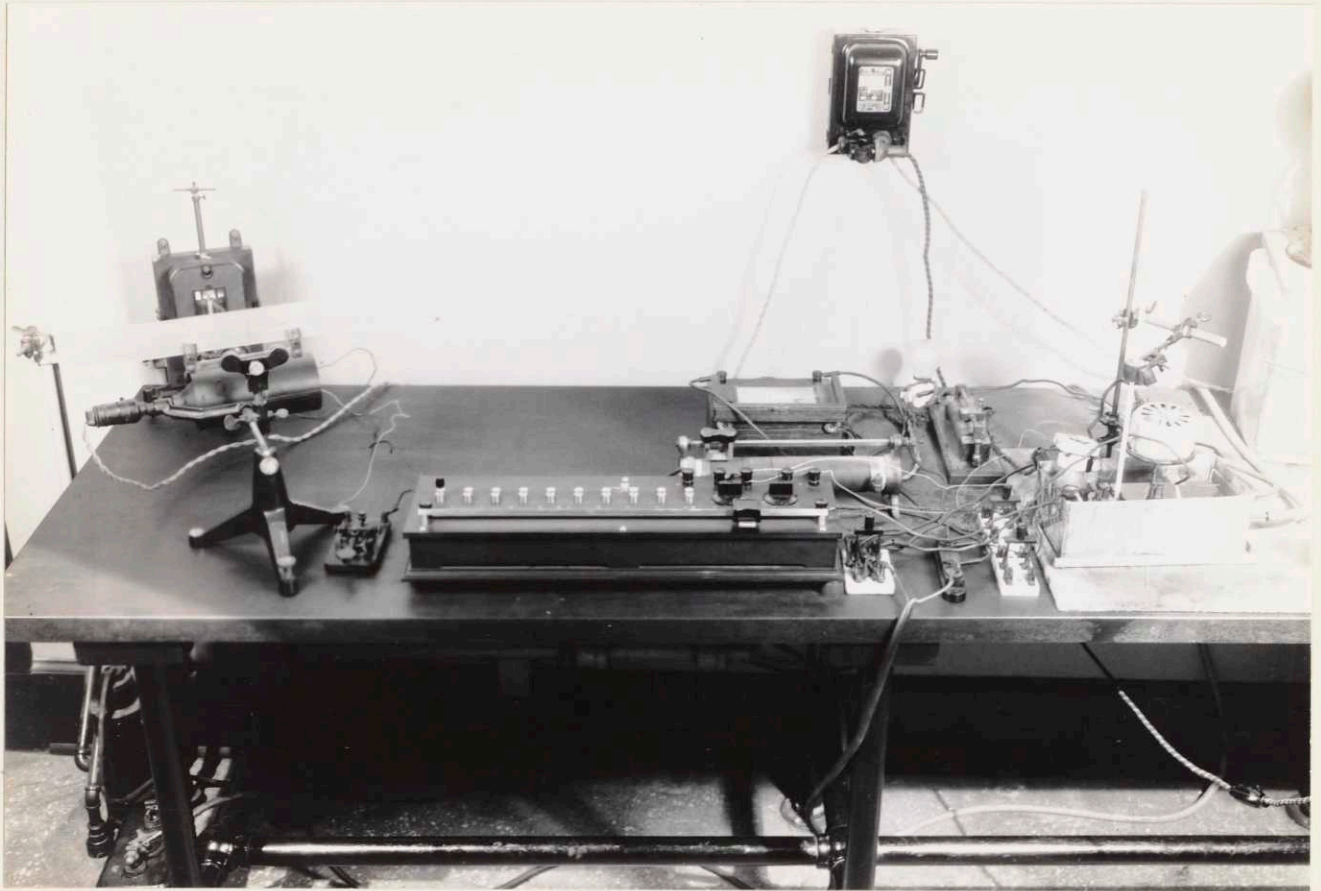


Fig. 13. Apparatus for Measuring Electrical Resistance

Because of the large changes occurring during aging the relative accuracy of the measurements (about 0.1 percent) was more than sufficient. Had it been possible to clamp the knife edges permanently on the specimen and keep a fixed gauge length the relative accuracy might have been increased to 0.01 percent. It was not convenient to do this because of the high aging temperatures and the necessity of using salt baths. Furthermore, the same specimens were also used for the magnetic measurements and could not be encumbered with permanently attached knife edges.

#### 4. Magnetic Measurements - General

Before discussing the actual magnetic measurements made in this investigation, it will be desirable to review some of the fundamental concepts involved. Magnetism is a universal property of matter and we can distinguish two classes of substances: (a) those which are more permeable than a vacuum and are attracted into a magnetic field are called paramagnetic, (b) those which are less permeable and are repulsed by a magnetic field are called diamagnetic. Ferromagnetism represents a special strong case of paramagnetism. All ferromagnetics become paramagnetic above a certain temperature known as the Curie point.

Para- and diamagnetic substances in general show an intensity of magnetization  $I$  which is proportional to the field  $H$ . Ferromagnetics, on the other hand, are distinguished not only by the high value of magnetization acquired in low fields but also by the non-linear relation between  $I$  and  $H$ . Furthermore, ferromagnetics can be magnetized to a saturation value with moderately high field strengths, while paramagnetics cannot be saturated in the highest fields yet obtained.

In Figure 14 are plotted the magnetization curves of ferromagnetic alpha

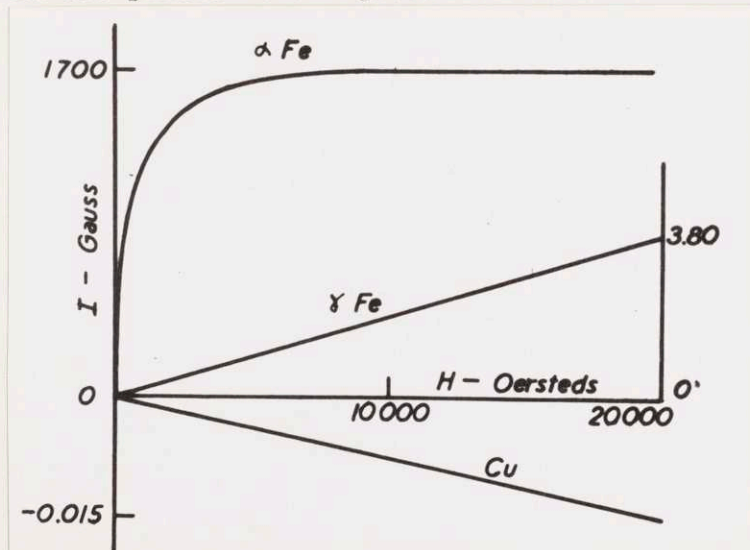


Fig. 14. Typical Magnetization Curves

iron, paramagnetic gamma iron and diamagnetic copper. Notice especially the difference in scales used. Thus in a field of 20,000 oersteds alpha iron shows a magnetization of 1700 gauss compared to 3.8 gauss for gamma iron<sup>19</sup> and -0.015 gauss for copper<sup>20</sup>.

The numerical data of weakly magnetic material is usually given by the susceptibility. Volume susceptibility  $\underline{K}$  is the ratio of  $I/H$  or the slope of the magnetization curve. For example, the values of  $K$  for gamma iron and copper are about  $190 \times 10^{-6}$  and  $-0.75 \times 10^{-6}$  respectively. Specific or mass susceptibility  $\chi$  equals  $K$  divided by the density. For dia- and paramagnetics the susceptibility is constant and independent of field strength. With ferromagnetics the susceptibility varies with the field and cannot be given as a characteristic of the material. The ferromagnetization also depends on previously applied fields because of magnetic hysteresis. Thus, if a ferromagnetic is magnetized to saturation and then removed from the field, it will exhibit a remanent magnetization.

If an alloy contains two phases, one dia- or paramagnetic and the other ferromagnetic, it is possible to separate their individual contributions to the total magnetization by measuring the field dependence of magnetization. However, this method will work only when the two contributions are of the same order of magnitude. For illustration, let us assume the case shown in Figure 15 where we have the paramagnetism of phase A superimposed on the ferromagnetism of phase B to give the magnetization curve C found experimentally. Thus the true saturation magnetization of phase B is 0.4 gauss. If we assume pure B to have a saturation magnetization of 1000 gauss, then the percent

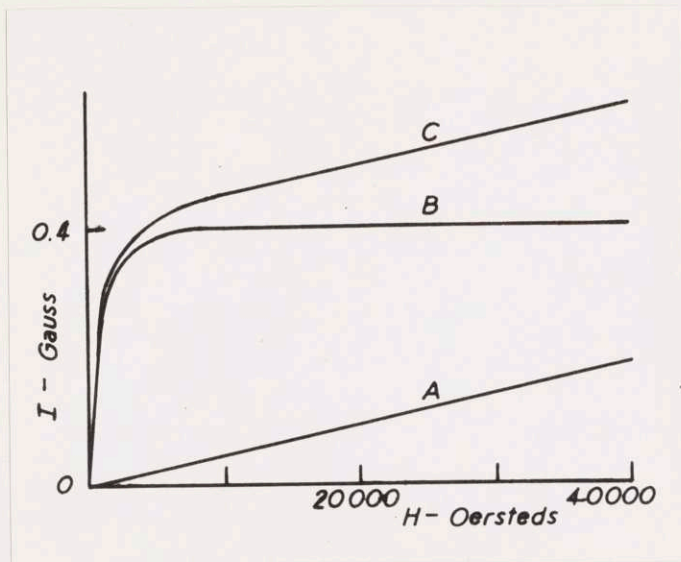


Fig. 15. Composite Magnetization Curve

of B by volume =  $0.4/1000 \times 100 = 0.04$  percent. Then the values of curve A divided by 0.9996 represent the true paramagnetism of pure A. If the percentage of the ferromagnetic constituent is very large then the paramagnetism will be relatively too small to detect while if it is extremely small it will be difficult to find the ferromagnetism. Quite high field strengths are necessary to attain the precision necessary for quantitative work of this kind.

In the present investigation a different method, designed to give a qualitative picture of the structural changes during aging, has been used. As quenched, the copper-cobalt and copper-iron alloys are largely paramagnetic with only small traces of ferromagnetism due to imperfect quenching. During aging a ferromagnetic phase precipitates from the paramagnetic solid solution. Thus there are two changes to be distin-

guished: (a) changes in the amount of the ferromagnetic precipitate and (b) changes in paramagnetic susceptibility of the copper-rich solution. In order to do this two different magnetic properties were measured, apparent magnetic susceptibility and remanent magnetic moment. The first measures the over-all magnetization of the aggregate, while the second measures the magnetization of the ferromagnetic phase alone. By comparing these two properties it is possible to obtain a qualitative interpretation of the magnetic results. What these quantities actually mean will be discussed in the section immediately following.

#### 5. Magnetic Susceptibility

The volume susceptibility  $K$  was measured by the Gouy method which is shown schematically in Figure 16.

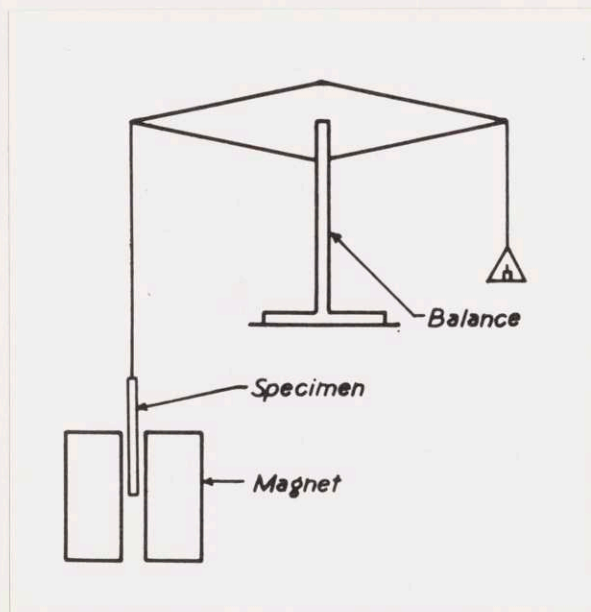


Fig. 16. The Gouy Method for Measuring Susceptibility

A cylindrical specimen, of uniform cross-sectional area  $A$ , is suspended from one arm of a sensitive balance so that one end of the specimen is in a homogeneous magnetic field  $H$  while the other is in a region of negligible field. If we let  $I$  equal the intensity of magnetization and let  $\frac{\delta H}{\delta x}$  equal the field gradient along the axis of the specimen, then the force  $dF$  on any infinitesimal segment of volume  $dv$  is:

$$dF = I \frac{\delta H}{\delta x} dv \quad \text{and}$$

substituting  $A dx$  for  $dv$   $dF = A I dH$

The total force on the specimen

$$F = A \int_0^H I dH$$

For a paramagnetic substance  $K$  is independent of  $H$  so one may write

$$\begin{aligned} F &= A \int_0^H K H dH \\ &= \frac{1}{2} A K H^2 \quad \text{and} \\ K &= \frac{2F}{A H^2} \end{aligned}$$

Thus the susceptibility is directly proportional to the force on the specimen. The force  $F = Wg$  where  $W$  is the change in weight when the field is applied and  $g$  is the gravitational constant. So

$$K = \frac{2Wg}{A H^2}$$

The above derivation applies only to paramagnetic substances. As mentioned before, the copper-iron and copper-cobalt specimens always contained varying amounts of a ferromagnetic phase. Hence the quantity  $K$  calculated according to the formula given above will be called apparent susceptibility. It is an over-all value which, at a given field strength, will not yield a quantitative determination of the phases

present. However, by determining this quantity at different field strengths it is possible to calculate both the true paramagnetic susceptibility of the copper-rich solution and the amount of the ferromagnetic phase. In order to do this successfully it is necessary that the specimen and the apparatus meet the requirements as stated in the previous section.

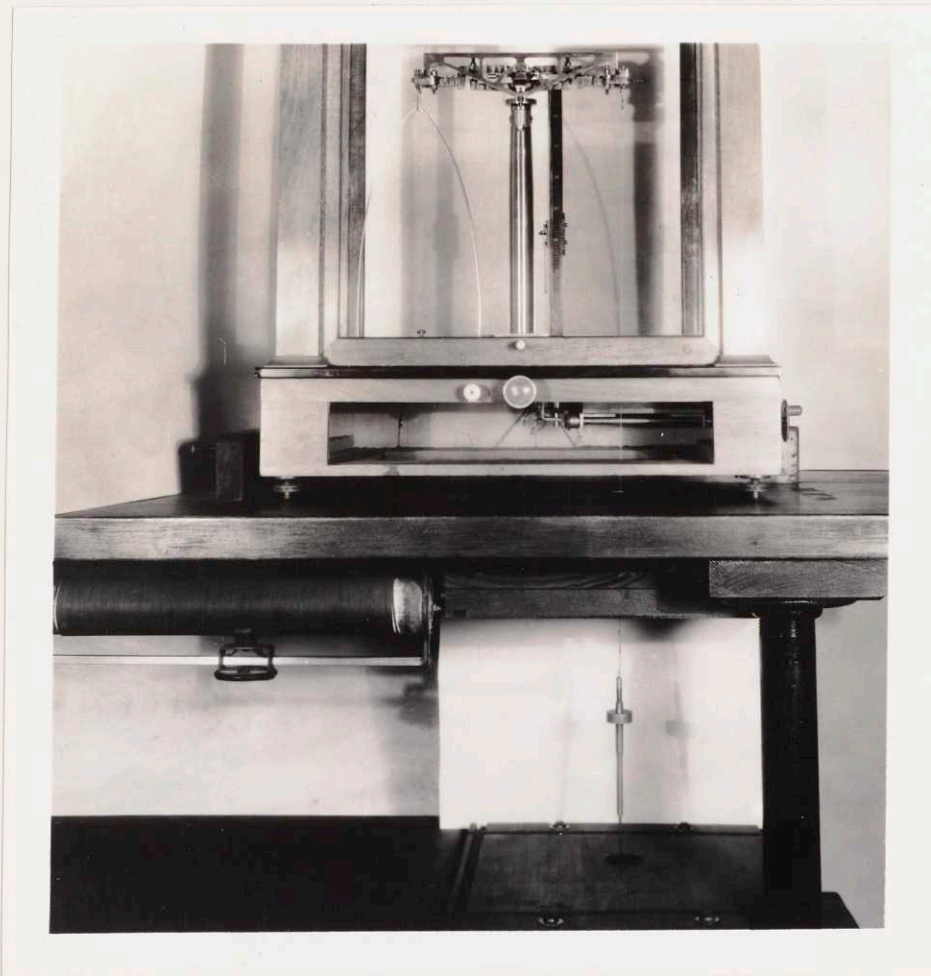


Fig. 17. Apparatus for Measuring Susceptibility

A view of the apparatus is shown in Figure 17. The wooden enclosure has been removed to show the specimen holder and part of the specimen. The balance was a standard analytical type and could be read



to 0.1 milligrams which corresponded to about 0.1 percent of the change in weight  $W$  actually measured in the paramagnetic samples. The small cylindrical specimen was suspended from one arm of the balance by a fine wire which passed through a hole drilled through the bottom of the balance cabinet and the table supporting it.

The specimen was positioned so that the lower end was at the center of the magnet. This was done by reading the deflection of the balance pointer when the specimen end was slightly below center and bottoming on a brass rod in the core of the magnet. The location of this rod and the length of the suspension wire were adjusted so that when the specimen was balanced it would be in the center and sufficiently above the rod to allow a small amplitude of swing. The position of the specimen could thus be reproduced to a degree greater than necessary because the field was uniform over an appreciable distance.

The magnet was of the air core type, designed and developed by Dr. F. Bitter. It consisted essentially of a small coil of copper sheet 1 inch wide and 0.013 inches thick wound about a brass tube of  $\frac{1}{4}$  inch inside diameter. The successive turns were insulated by layers of Glyptal paint. The coil was surrounded by a water jacket on both ends and on the outer circumference except where the electrical contacts were made. The other electrical connection was made on the brass tube. The power source was a direct current generator which supplied 1000 amperes at 25 volts.

The magnet was calibrated by a method due to Kaufmann<sup>21</sup> and a linear relation between current and field strength was found as expected. A current of 740 amperes and a field of 15,000 oersteds was

controlled by variable rheostats in the field circuit of the generator. The field current of the generator was read on a potentiometer across a fixed resistance and adjustments were made during the course of taking measurements to keep this value constant. Despite this precaution the magnetic field did fluctuate as shown by variations in the weight of the specimen of the order of several milligrams. This may perhaps be attributed to leakage currents through the insulation of the magnet coil. Because of this varying field at constant current the reproducibility of the susceptibility was reduced to about 1 or 2 percent. When the specimens became strongly magnetic after aging at high temperatures, they tended to stick to the sides of the magnet and accurate weighings were impossible to obtain.

Although the specimens were 4 inches long so that the upper end would extend above the outer case of the magnet, probably less than half of this length was actually in a field of any great strength. The quenched specimens showed different values for susceptibility when they were turned end for end. Accordingly the specimens were suitably marked and the susceptibility measurements during the aging runs were all made with the same end in the magnet.

#### 6. Remanent Magnetic Moment

The same specimens used for measuring resistance and susceptibility were magnetized in a large, air core magnet at 10,000 oersteds and then placed in an apparatus which measured the remanent magnetization. The magnet is shown in Figure 18. It consisted of a coil of sheet copper 0.010 inches thick and 12 inches wide with a diameter

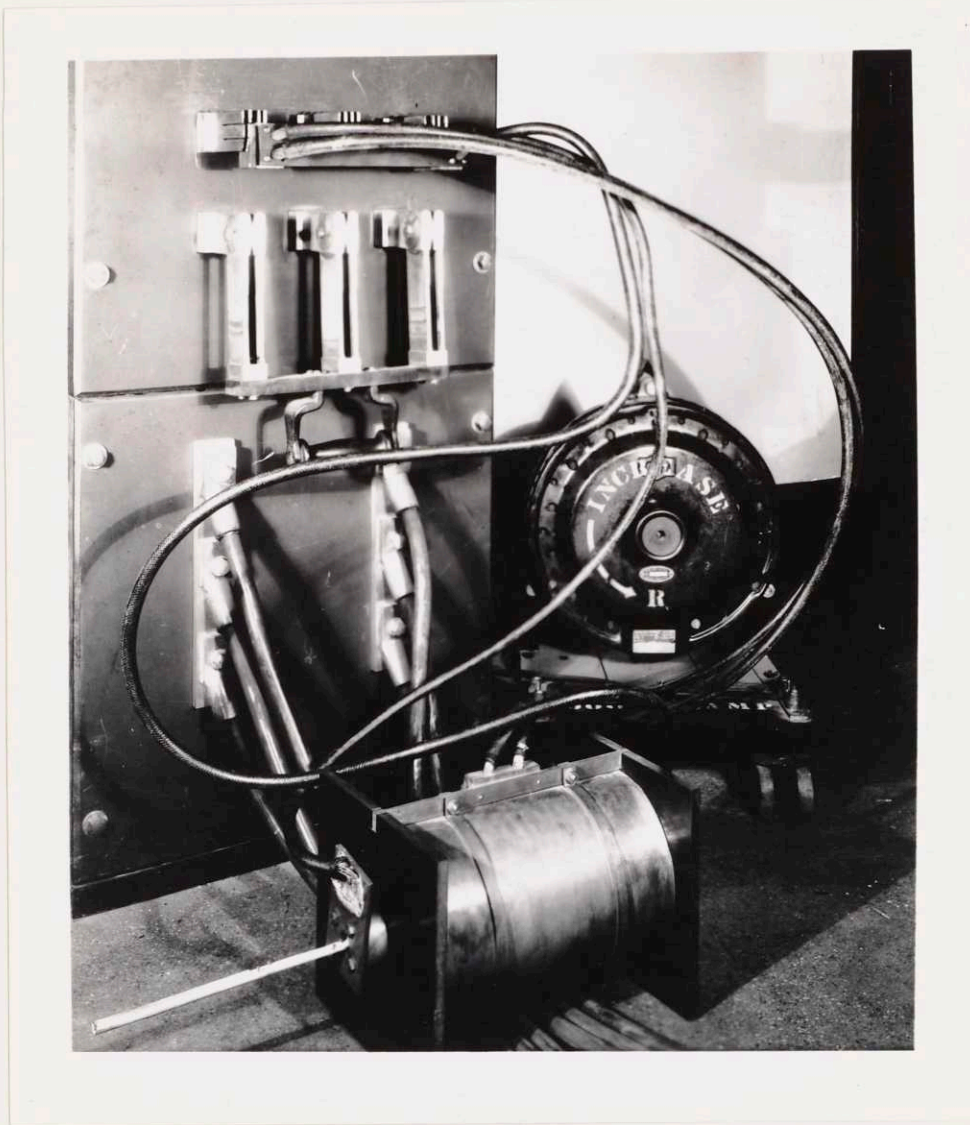


Fig. 18. Magnet for Magnetizing Remanence Specimens

inside of  $3/4$  inches and outside of 10 inches. The turns were insulated by fish paper. A current of 1000 amperes gave a field of 10,000 oersteds which was probably fairly uniform over a 4 inch length

in the center. A temperature rise of  $1^{\circ}$  C per second was calculated so that it was only possible to run the magnet for short periods without burning out the insulation. The specimens were placed in a holder so that they were always in the same position in the magnet.

It was found that the specimens had to be magnetized very carefully in order to obtain accurate results. After some preliminary work the following standard procedure was adopted. The specimens were always magnetized in the same direction so that any effect of the previous magnetization during the susceptibility measurement would be constant. The field was raised from zero to 10,000 oersteds and then alternated between 10,000 and 3,000 oersteds four times. This was necessary to insure complete magnetization. Apparently the shape or size of the small ferromagnetic particles was such that they were not easily magnetizable.

The method for measuring the remanent magnetic moments is illustrated schematically in Figure 19. A general view of the apparatus is shown in Figure 20 and a close-up of the magnetometer in Figure 21. The magnetometer consisted of two Helmholtz coils and a specimen holder on the end of a slender glass fiber. The coils were designed and placed so that, when carrying the same current in the same direction, they produced a uniform magnetic field over a large space. The specimen was suspended so as to be perpendicular to the direction of the field and at a point midway between the coils and on their center line. On the upper part of the specimen holder was a small mirror which reflected the light from a lamp onto a glass scale at a fixed

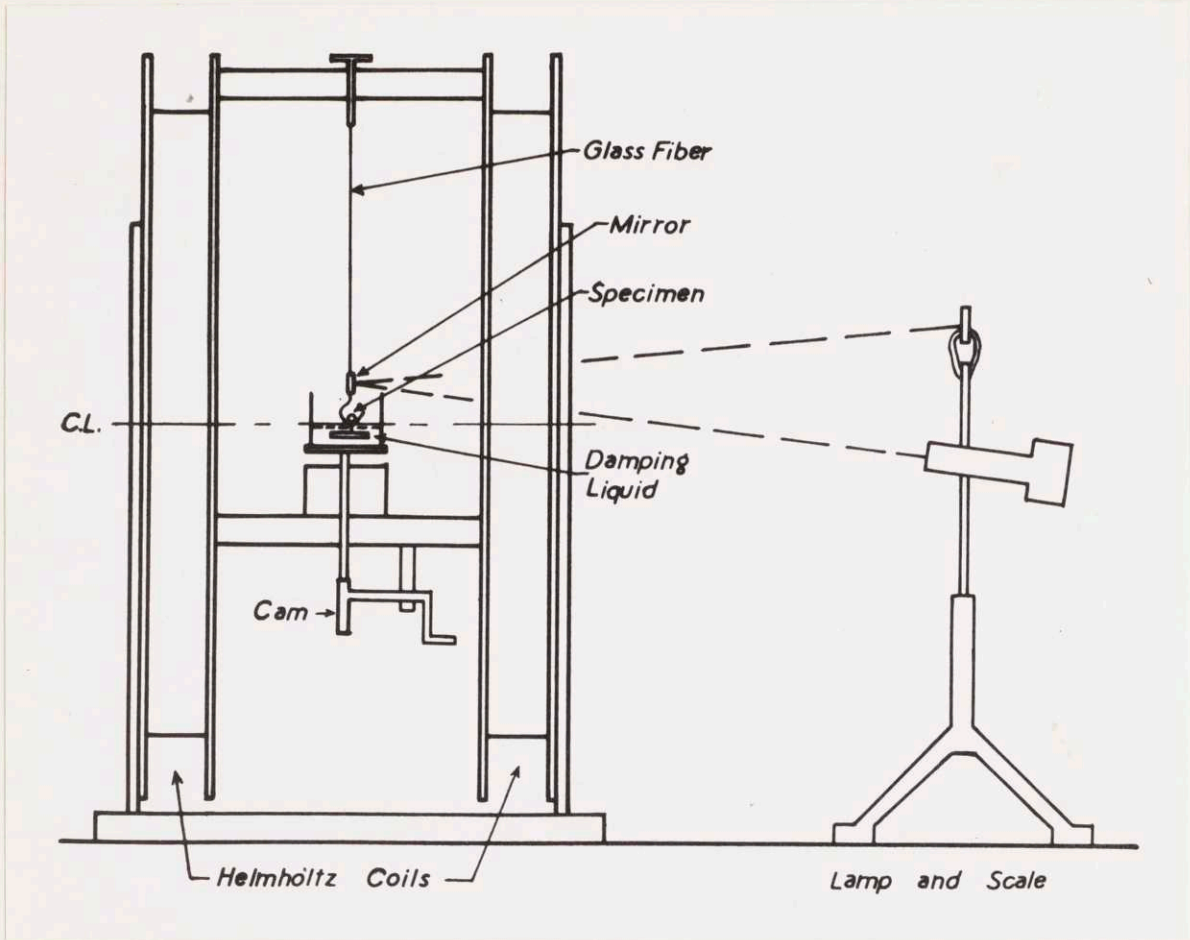


Fig. 19. Method for Measuring Remanence

distance. The lower part of the holder was immersed in a glass dish of oil of the correct viscosity for slightly under critical damping.

The specimen was placed in the holder by laying it across the glass dish at its topmost position and then lowering the dish by a cam arrangement until the specimen was carefully deposited on the holder. When the field was applied the specimen rotated through a small angle which caused a deflection of the light beam on the glass scale. The torque exerted on the specimen and on the glass fiber is the same and we may equate these two expressions:

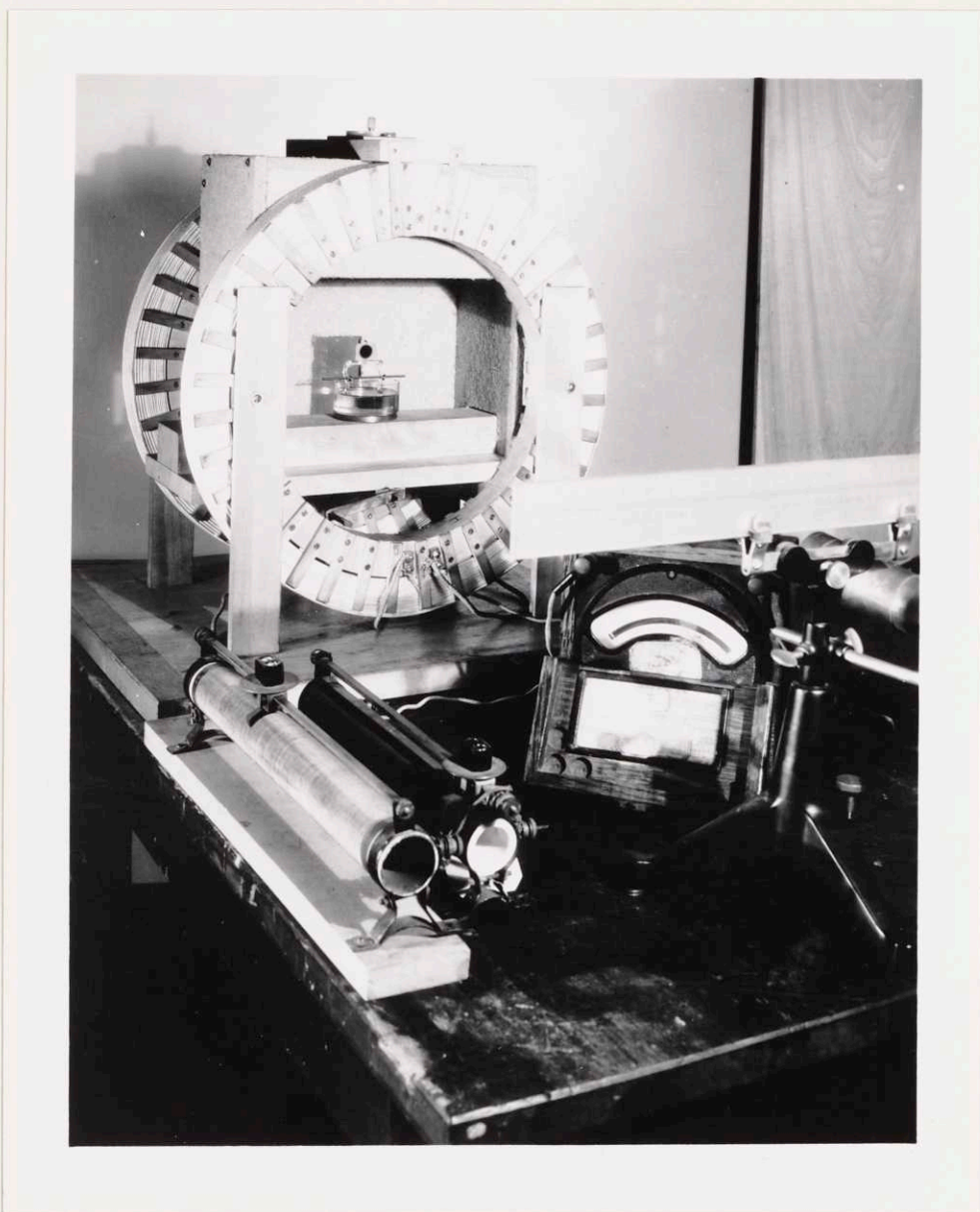


Fig. 20. Apparatus for Measuring Remanence

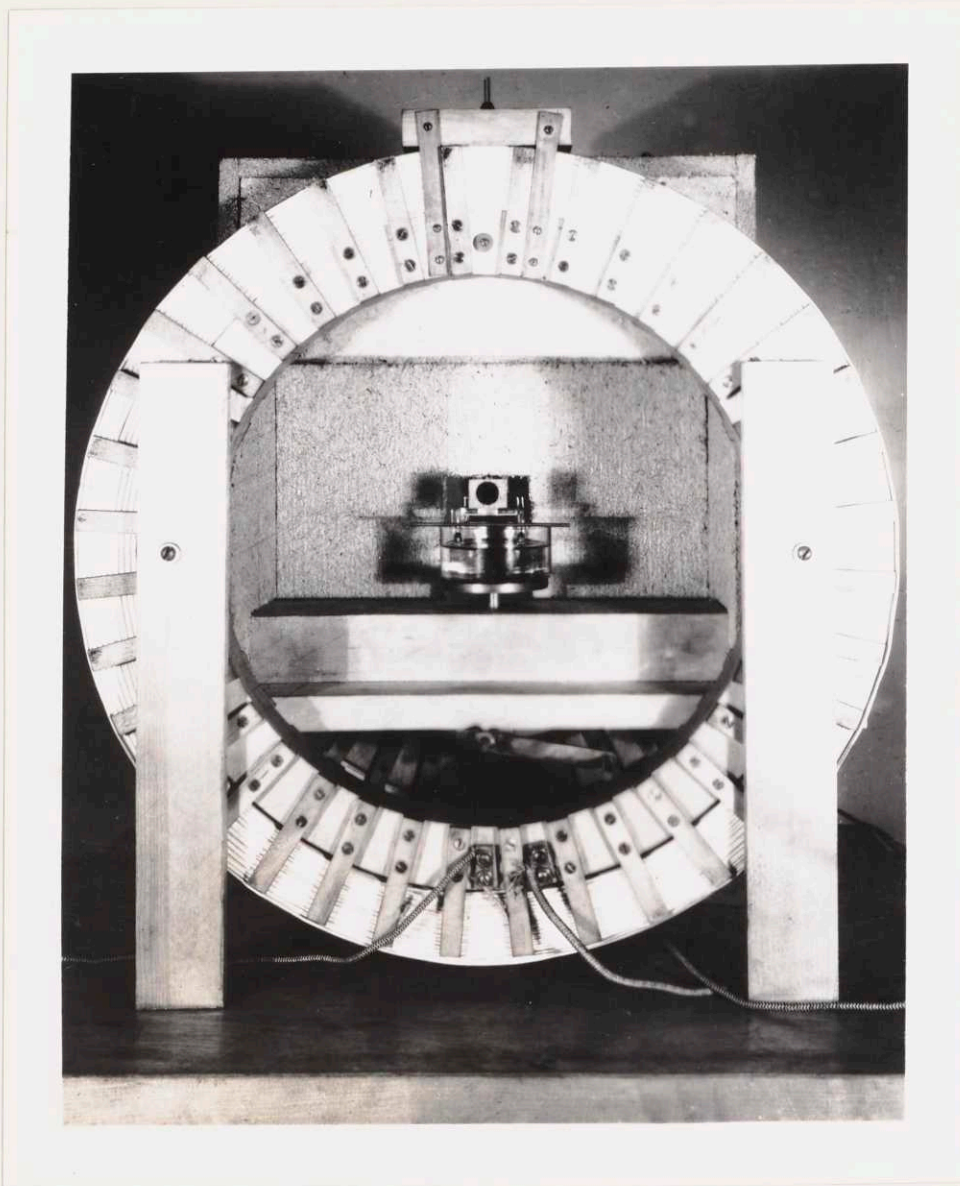


Fig. 21. Close-Up of Magnetometer

$$M H \sin \theta = C \phi$$

where

M = remanent magnetic moment

H = field strength

$\theta$  = angle between specimen and field

C = torsional constant of fiber

$\phi$  = angle of twist

If we let

$$H = a i \quad \text{and}$$

$$\phi = \tan^{-1} \frac{D}{b}$$

where

a = constant

i = current in Helmholtz coils

D = scale deflection

b = scale distance

then  $M a i \sin \theta = C \tan^{-1} \frac{D}{b}$

Since  $\theta$  is nearly  $90^\circ$  and  $\phi$  is nearly  $0^\circ$  we may write as a close approximate

$$M a i = \frac{C D}{b}$$

and

$$M = \frac{C D}{a b i} = C' \frac{D}{i}$$

Thus the remanent magnetic moment is directly proportional to the quantity  $D/i$  and with a constant current it is directly proportional to the deflection.

The currents used in operation of the magnetometer varied from 0.005 to 5 amperes depending upon the condition of the specimen. The object was to have the deflection great enough to measure accurately and still keep it on the scale. It was necessary always to place the specimens in the same direction because of the torque from the earth's field. Since they were always magnetized the same this kept the de-



flection on the same side of the zero point and the effect of the earth's field was constant. In the early stages of aging where the remanent moment was small, the earth's field of about 0.5 oersteds was negligible compared to the 100 oersteds produced by 5 amperes through the Helmholtz coils. However, in later stages where there was a considerable amount of ferromagnetic precipitate, the deflection from the earth's field was greater than that produced by 0.005 amperes in the coils. Thus it was found necessary to line up the magnetometer so that the specimen, in its zero position, would point towards magnetic north. With these precautions the reproducibility of the results was about 1 to 3 percent depending upon the condition of the sample. This relative accuracy was sufficient to follow the large changes occurring during aging.

#### 7. Microstructure - Electrolytic Poletching

The microstructure was studied on samples that were polished electrolytically by the method originated by Jacquet<sup>22</sup> and used on copper by Lowery, Wilkinson and Smare<sup>23</sup>. After polishing, a slight change in the voltage of the cell produced an electrolytic etch. Hence the term poletching refers to the polishing and etching of a sample in successive stages of the same process. There are descriptions in the literature of the electrolytic polishing of a number of pure metals and solid solutions but there is no reference to the successful polishing of heterogeneous alloys. The samples used in the present investigation were homogeneous as quenched but became heterogeneous with the precipitation of a second phase during aging. However, no difficulty

was encountered in poletching them satisfactorily, even when considerable amounts of precipitate were present. An example of what can be done by this method of polishing and etching is shown in Figure 22 which is a photomicrograph showing grain boundary precipitate in the copper-iron alloy at 2500 diameters.

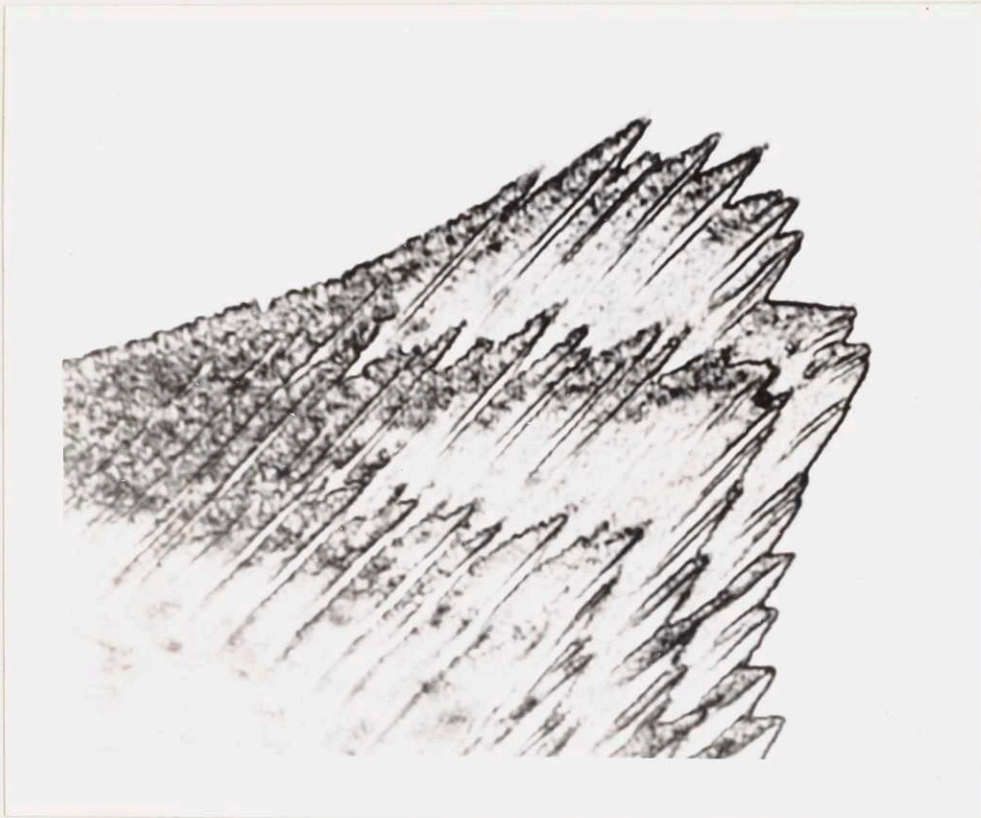


Fig. 22. Electrolytically Poletched Sample at 2500 Diameters

The apparatus required is surprisingly simple. It is shown schematically in Figure 23.

The hardness specimens were held in a fixture and given a rough metallurgical polish on one end. Care was taken to produce a flat surface but no special attention was given to the elimination of scratches on the final velvet lap. The specimen was then mounted in

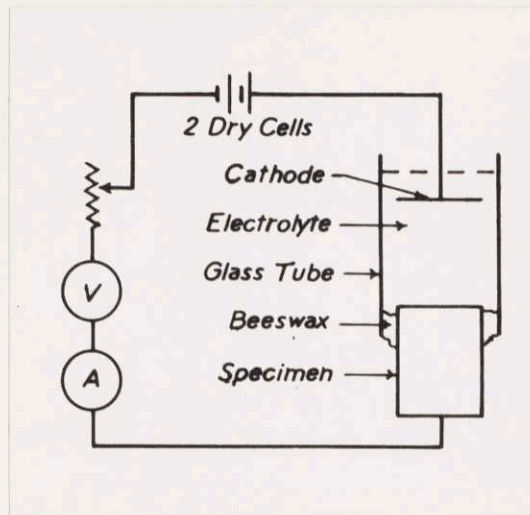


Fig. 23. Apparatus for Electrolytic Poletching

the small piece of glass tubing with beeswax as shown in Figure 22. The wax was kept as close to the polished surface as possible without smearing it. Although the surface to be examined was about  $1/8$  by  $1/2$  inch, the area actually polished, and which determined the current in the cell, was the total surface area above the wax. This area varied from sample to sample. The sides could have been protected with a lacquer but this was deemed to be unnecessary since the method adopted was rapid and gave excellent results. The cathode was a small sheet of copper placed parallel to, and about a half inch above, the specimen. The electrode distance was not critical. The electrolyte was ortho-phosphoric acid with a specific gravity of 1.30 to 1.40. Above 1.40 the electrolyte was too viscous to allow gas bubbles to escape and below 1.30 the voltage characteristics of the cell were different.

In the operation of the cell, three definite stages are observed while increasing the voltage with a rheostat. (a) Voltage and current rise together, gas is evolved at the cathode, and the specimen begins to etch. (b) At about 1.6 volts, the voltage jumps suddenly to 1.8, followed a moment later by a steady drop in current from about 0.2 to 0.1 amperes. The specimen starts to polish and the etch from (a) disappears rapidly. With the rheostat unchanged, the voltage rises slowly to about 2.0 volts and the current drops to about 0.07 amperes. Polishing continues under these stable conditions. (c) Further increase in voltage with the rheostat causes a proportional increase in current and gas is evolved at the anode as well as the cathode. Gas bubbles adhering to the polished surface cause uneven polishing and pitting.

The technique adopted was designed to polish the specimen in stage (b) and then etch it in stage (a). Hence the voltage was raised rapidly from zero to 1.8 volts to diminish the etching and establish stable conditions for polishing. Polishing was continued for from 5 to 10 minutes. Then the voltage was dropped to 0.6 and the specimen allowed to etch to the desired extent, usually for two or three minutes. The cell was disassembled and the specimen washed in water and alcohol and dried in a warm air blast.

Several precautions are necessary to insure the desired results. The etching prior to polishing is harmless but apparently necessary. If the voltage is raised too rapidly at the start, both the etching and polishing stages are suppressed, and the first occurrence is that of gas evolution from the specimen. After polishing is established,

the voltage sometimes creeps high enough to introduce the third stage. Occasionally the voltage drops to a point where etching occurs, but this is rare because of the fact that polishing conditions may be carried down to about 1.2 volts. So it is best to adjust the voltage from time to time during polishing. The final etching may be done at voltages as high as 1.0 volts but the rate is too rapid to control. On the other hand, with voltages below 0.4 volts, the etching is very slow.

The formation of some pits and humps on the polished surface seems to be unavoidable. The former are probably due to inhomogeneities in the sample while the latter are due to dirt or bubbles on the surface. However, these disadvantages are greatly outweighed by the advantages of electrolytic poletching. By this method, it is possible to prepare a flat, highly polished surface, free from scratches and the effect of mechanical work. This is especially important in following the progress of aging since the usual polishing operation may cause precipitation on the surface. In the present investigation the specimens were ground and polished prior to the solution heat treatment. They were then electrolytically poletched at suitable intervals during the aging process and only required a light repolish on the velvet lap from time to time. Thus it is believed that the changes observed are real and not influenced by the polishing operation.

## VII. PRESENTATION OF RESULTS

### 1. General

The results of this investigation are given in Figures 24 to 31. The experimental data is included in the appendix. For each aging temperature, the changes in hardness, electrical resistance, magnetic susceptibility and remanence are plotted against aging time in hours. A logarithmic time scale is used in order to compress the results of the longer intervals and still show the changes during the short intervals. The same scales are used for both alloys and the graphs are arranged so that, at each aging temperature, a direct comparison can be made between the copper-cobalt and the copper-iron alloy. This is desirable because of the striking similarities in the hardness and resistance changes of the two alloys. On account of this similarity in the kinetics of the precipitation process, the marked differences in the magnetic properties become even more interesting.

Hardness values are given as Rockwell F numbers, with the diameter of the circles equal to one unit. Resistance is plotted as percent of quenched value, since it is not the absolute values, but the direction and magnitude of the changes which are important for our purposes. The diameter of the circles represents one percent change. Both magnetic properties are also given in relative units. Due to the large changes in these properties and the importance of showing the early stages, it was necessary to plot them on a logarithmic scale. Remanence is given as the logarithm of the ratio of  $D/i$  (see section VI - 6), which is proportional to remanent magnetic moment. Susceptibility is

given as the logarithm of percent of quenched value. Wherever, in this discussion, the term susceptibility is used, it means apparent susceptibility as defined in a previous section. As with electrical resistance, the percent of quenched value was used to correct for variations in the initial susceptibility of different specimens of the same alloy and also to allow the use of the same scale for both alloys. The plotting was facilitated by having the curves start at the same value for all aging temperatures. The actual values of susceptibility and resistance are given in the data sheets.

In considering the results, it should be remembered that all measurements at the same temperature, except hardness, were made on a single specimen. Hardness values represent an average of several specimens but they still show considerable scatter during the early stages of aging. This is inherent in the behavior of these alloys. On the other hand, resistance, susceptibility and remanence, being volume properties, show consistent results. The values given are for one specimen. Small differences were obtained from specimens aged at the same temperature, but the results were not suited to averaging.

## 2. Aging at 250° C

The results presented in Figures 24 and 25 show, first of all, that the property changes in both alloys at 250° C have the same direction and magnitude. The hardness results show a scatter which, in several cases, amounts to as much as 4 units. This is believed to be due to the non-uniformity of the aging process, which is exaggerated by the coarse grain size of the samples. For both alloys, straight

lines have been faired through the points and they show a slight increase over the thousand hours aging. In contrast to the hardness results, the other properties show very consistent values. These volume properties are not affected by grain size and microscopic non-uniformity of the aging process.

Resistance decreases 20 to 30 percent, an amount which is large for most age-hardenable alloys. However, when compared with the results at higher temperatures, this change appears rather small. No increase in resistance is noted in the early stages of aging. However, both alloys show a slight, but reproducible break, after about 0.1 hours, that can be explained by assuming two overlapping processes. A single resistance run at 100° C showed a drop of 2 percent after 100 hours. Susceptibility rises gradually in both alloys, with signs of a more rapid increase in the copper-cobalt alloy towards the end. The total increase of 15 percent for copper-iron and 40 percent for copper-cobalt appears small on the full logarithmic scale. During the first part of the increase in susceptibility, remanence remains constant. It starts to rise in both alloys at about 0.1 hours. This is where the break occurs in the resistance curves, but the connection, if any, is obscure.

The decreasing resistance indicates precipitation from the solid solution. The increasing susceptibility shows that the precipitate is ferromagnetic in both alloys. This is confirmed by the increase in remanence, since this property measures changes in the ferromagnetic portion only. The delayed increase in remanence may perhaps be due to the extremely small particle size of the first precipitate. Such



small particles might be ferromagnetic while in a magnetic field and yet fail to exhibit any remanent magnetization. An alternative possibility is that the first cobalt or iron-rich precipitate contains considerable amounts of copper.

### 3. Aging at 375° C

During aging at 375° C, the changes observed at 250° C proceed in the same direction until breaks occur, which mark the end of the first stage in the precipitation process. As shown in Figures 26 and 27, this first stage is characterized by a large decrease in resistance, a slight increase in hardness, a pronounced increase in remanence and a gradual increase in susceptibility. Identical changes are found in both alloys. These results indicate a ferromagnetic precipitate, and microscopic evidence, to be reported later, shows it is localized at the grain boundaries. The beginning of the second stage - that of general precipitation - occurs at about one hour. Hardness starts to increase at a more rapid rate with log time. Resistance shows an accelerated rate of decrease with log time and then drops more gradually. These breaks are sharper in the copper-cobalt alloy, due probably to the combined effects of less boundary precipitate, as shown by a smaller resistance drop, and less overlapping of the two stages.

Remanence shows a pronounced break in the copper-cobalt alloy at this time. When  $D/i$ , instead of  $\log D/i$  as in Figure 26, was plotted against log time, the break at one hour was even sharper and accurately reproducible in separate runs. Between 5 and 1000 hours, remanence increases at a much slower rate. On the other hand, susceptibility,

instead of slowing down, continues to rise in an uninterrupted, smooth curve. This indicates that susceptibility, which is now largely determined by the amount of the ferromagnetic precipitate, is not sensitive to differences between the grain boundary and the general precipitate. Hence, at the field strength used, either the magnetization of the two types of precipitate is the same or their amounts change in the correct proportions to give the same effect. But remanence is influenced by some difference between the two types such as size or composition, and so provides a means of distinguishing them at the start of general precipitation. The lag between susceptibility and remanence at this time is similar to the initial delay of remanence at 250° C and both phenomena may have the same origin.

In the copper-iron alloy, the changes in magnetic properties associated with the second stage depart widely from those of the copper-cobalt alloy. Remanence reaches a maximum at one hour and then remains constant, indicating the completion of ferromagnetic precipitation. But, from the continued drop in resistance, we infer that precipitation is still occurring and, from microscopic evidence at higher temperatures, that it is of the general type. Therefore, this precipitate must be non-ferromagnetic! Since the solution of 2.4 percent of iron in copper has given it a high paramagnetic susceptibility (as contrasted with its normal diamagnetism), precipitation of iron from solution should cause the susceptibility of the copper-rich solution to decrease.

Our ability to detect this decrease by measurements at a single field strength will depend upon the nature of the precipitate. Although this change must actually be occurring in both alloys during the first stage of precipitation, it is outweighed by the increase due to the ferromagnetism of the precipitate itself, and susceptibility rises. However, if the precipitate is paramagnetic, then the apparent susceptibility will be influenced chiefly by changes in the copper-rich solution which comprises over 98 percent of the sample, and it should decrease.

This decrease in susceptibility is shown in Figure 27 during the same period, between 1 and 1000 hours, when the remanence is constant. Thus, during the first stage, where the precipitate is ferromagnetic, susceptibility and remanence rise together and both reach a maximum at one hour. The general precipitation then commences and, since it is paramagnetic, the susceptibility decreases. This accounts for the great difference in the susceptibility results of the two alloys during the start of general precipitation. This difference will be discussed more fully later on, but it is important to note here that, despite differences in the magnetic properties of the precipitates, the basic aging process is quite similar in the two alloys.

#### 4. Aging at 550° C

Figures 28 and 29 show that at 550° C the first stage in the aging process is completed after the short period of 0.01 hours. During this interval the resistance of both alloys drops about 30 percent, while the hardness is unchanged. This substantiates the results at

lower temperatures which showed only slight hardening during the boundary precipitation stage. However, simultaneously with the start of general precipitation at 0.01 hours, the hardness rises sharply and reaches a maximum in both alloys at about 100 hours. Resistance shows its maximum rate of decrease at 0.01 hours and then drops gradually to an almost stable value after 100 hours.

The remanence changes in the copper-cobalt alloy duplicate those found at 375° C, and then proceed to a period of rapid increase commencing at one hour. This indicates that, after the general precipitate reaches a certain particle size or composition, the remanence is no longer influenced by these factors, but principally by its amount. Unfortunately, the susceptibility measurements could not be made at this temperature due to difficulties, inherent in the apparatus, in weighing strongly magnetic samples. It is believed that the results would show a continuation to higher values of the smooth curve found at 375° C.

The magnetic properties of the copper-iron alloy undergo in 0.1 hours at 550° C the same changes as in 1000 hours at 375° C. Susceptibility and remanence reach maximum values at about 0.01 hours. It will be noticed that remanence increases slightly after susceptibility starts to decrease. The probable explanation is that, in this sample, the general and localized precipitation are slightly overlapped. This causes the susceptibility maximum to be shifted to a lower value and a shorter time than at 375° C.

Upon further aging, susceptibility decreases due to the precipitation of iron in a paramagnetic form, and a minimum value is reached after 3 hours. Remanence also shows a slight drop during this period. This effect, not found in all specimens may be due to changes in composition or shape of the constant amount of ferromagnetic boundary precipitate. Susceptibility rises slowly at first and then rapidly after 200 hours. Remanence increases even slower at first, but then shows a decided jump at 200 hours. Since these changes occur at a time when minimum resistance has been nearly attained, they cannot be attributed to a new precipitate. Hence, they must be the result of the transformation of the paramagnetic precipitate, already present, to the ferromagnetic form.

This magnetic transformation probably overlaps the stage of general precipitation, a fact which, coupled with the absence of any noticeable effect on hardness or resistance, makes it difficult to determine when it starts. From the susceptibility results, we may assume that the process is continuous and progressing at a rate which increases, even on a full logarithmic scale. While susceptibility gives a smooth curve, remanence shows a decided break, that is even more pronounced at 700° C. In this case, although the precipitate is still small, as evidenced by maximum hardness, the particles have probably passed the critical size or composition which affected remanence on other occasions. However, if we picture the magnetic transformation as the result of a change in crystal structure from face-centered to body-centered cubic, we then have the formation of small particles of the new phase.

Hence, the situation is similar to that obtaining during the start of both stages of precipitation in the copper-cobalt alloy, and of the first stage in the copper-iron alloy. In all these cases, the remanence may be a sensitive indicator of the number of iron or cobalt atoms in an individual particle.

##### 5. Aging at 700° C

The results of aging at 700° C were affected by the appreciable solid solubility at this temperature of 1.0 percent cobalt and 0.5 percent iron in copper. By comparing Figures 30 and 31 with the corresponding ones for 550° C, it is seen that, at 700° C, the maximum hardness is lower and the minimum resistance is higher. These differences are undoubtedly due, in part, to the smaller amounts of cobalt and iron available for precipitation. As the results show, at 700° C, a scatter in the resistance and remanence values was obtained for the first time. In order to explain this scatter, the following experiment was performed.

Copper-iron and copper-cobalt specimens, which had been furnace cooled from the solution temperature, were aged at 700° C simultaneously with the regular quenched specimens. During the short aging intervals the specimens were all placed in the same holder and quenched together, but they were not in contact with each other. After a total aging time of 0.1 hours they were wrapped together in copper sheet for protection against corrosion. This caused the quenching to be less uniform. When the resistance results were plotted, they showed that all the specimens deviated from a smooth curve at the same time. The conclusion was that

these minor deviations were due to differences in the quench from the aging bath. In outward appearances, the quenching procedure was the same, and there was no way of predicting any deviations until the measurements were made. It was felt, however, that the scatter was satisfactorily explained and that a curve could be faired through the points.

In both alloys the resistance drops at a very rapid rate and reaches an almost stable value after one hour. Again we note that no hardening occurs during the greater part of this resistance drop. Some of this lag in hardness may be due to the slower heating of the larger specimen. Hardness rises sharply in both alloys at 0.01 hours and reaches a maximum at about 0.5 hours. In the copper-cobalt alloy, softening due to overaging takes place at a steady rate up to 300 hours. In the copper-iron alloy, softening is more rapid and the hardness levels off at 20 hours, while still considerably above its as-quenched value.

The magnetic properties do not show the breaks associated with the stage of grain boundary precipitation. Since this precipitate appears in the microstructure, the property changes accompanying it must occur in less than 3. seconds, which was the shortest aging time used. In fact, after this short interval at 700° C, the specimens are in the same state that they reached in about one hour at 550° C. No susceptibility measurements could be made on the copper-cobalt alloy since, as shown by the rapid rise in remanence, the specimens become strongly magnetic after a very short aging time.

The remanence results of the copper-cobalt alloy are interesting but difficult to interpret. A sharp maximum is reached at 3 hours or shortly after maximum hardness. Then, after decreasing smoothly, at 20 hours, the remanence suddenly levels off at a value of  $\log D/i$  of 2.8. These surprising results have been checked very closely in two independent runs. An annealed specimen aged for the same time at 700° C gives a  $\log D/i$  of 1.95, which is considerably lower, but the same resistance as the quenched and aged sample. According to the resistance values the quenched sample has reached equilibrium but, according to the remanence, it has not. Since the remanence is a more complex property with respect to structural changes, it is probable that the discrepancy is due to some difference in their past history.

In the copper-iron alloy, the magnetic results may be compared with those for copper-cobalt by noting that the lag between the occurrence of the general precipitate and its magnetic transformation serves merely to delay the period when the magnetic properties reach high values. For this reason it was still possible to measure susceptibility at 700° C and the values were comparable to those of copper-cobalt at 375° C. The remanence values reach the period of linear rise found in copper-cobalt at 550° C. Although the copper-iron alloy does not overtake the copper-cobalt in the length of this run, it will of course do so eventually. The break in the remanence curve, due to the magnetic transformation, occurs in 3 hours, or at the same stage of hardness and resistance as at 550° C. Although a very sharp break is observed, it is again accompanied by a smooth susceptibility curve.



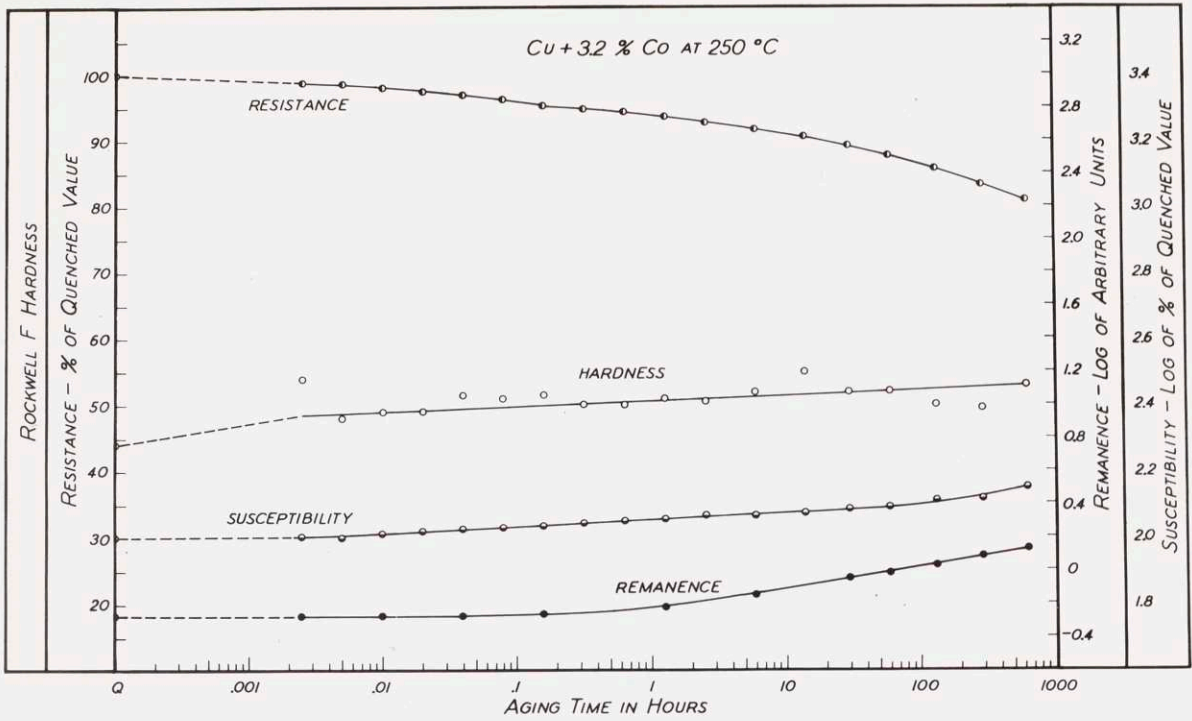


Fig. 24. Aging Curves of Copper-Cobalt Alloy at 250° C

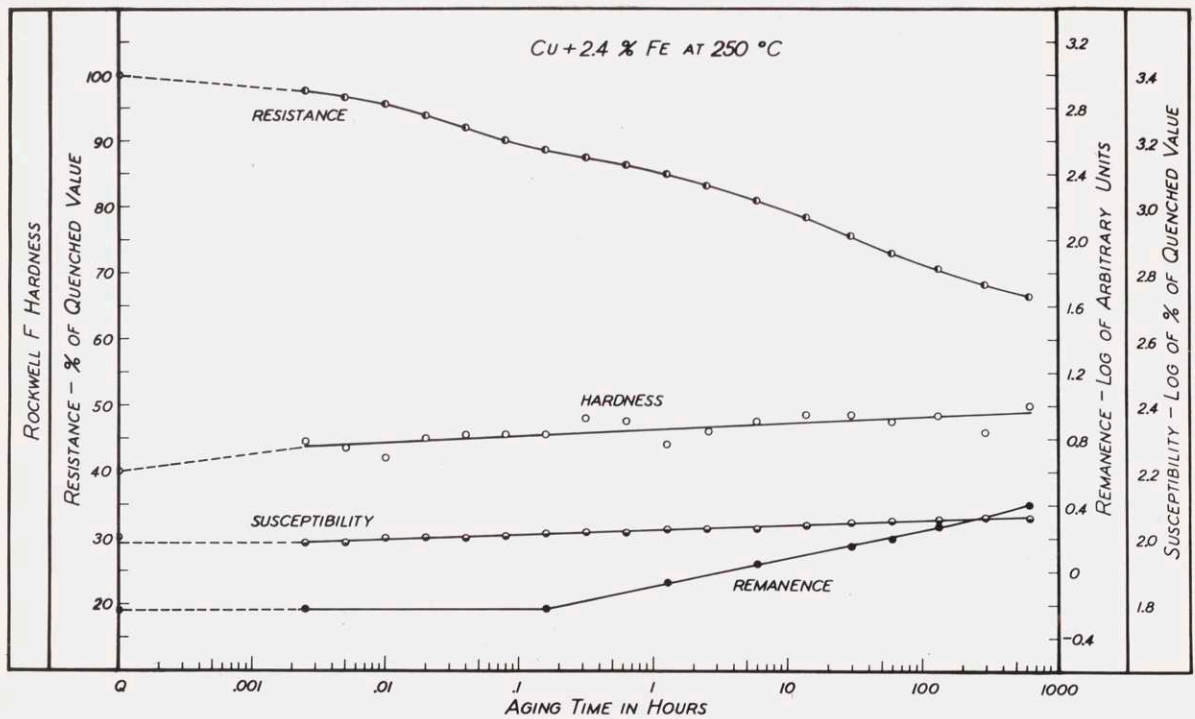


Fig. 25. Aging Curves of Copper-Iron Alloy at 250° C

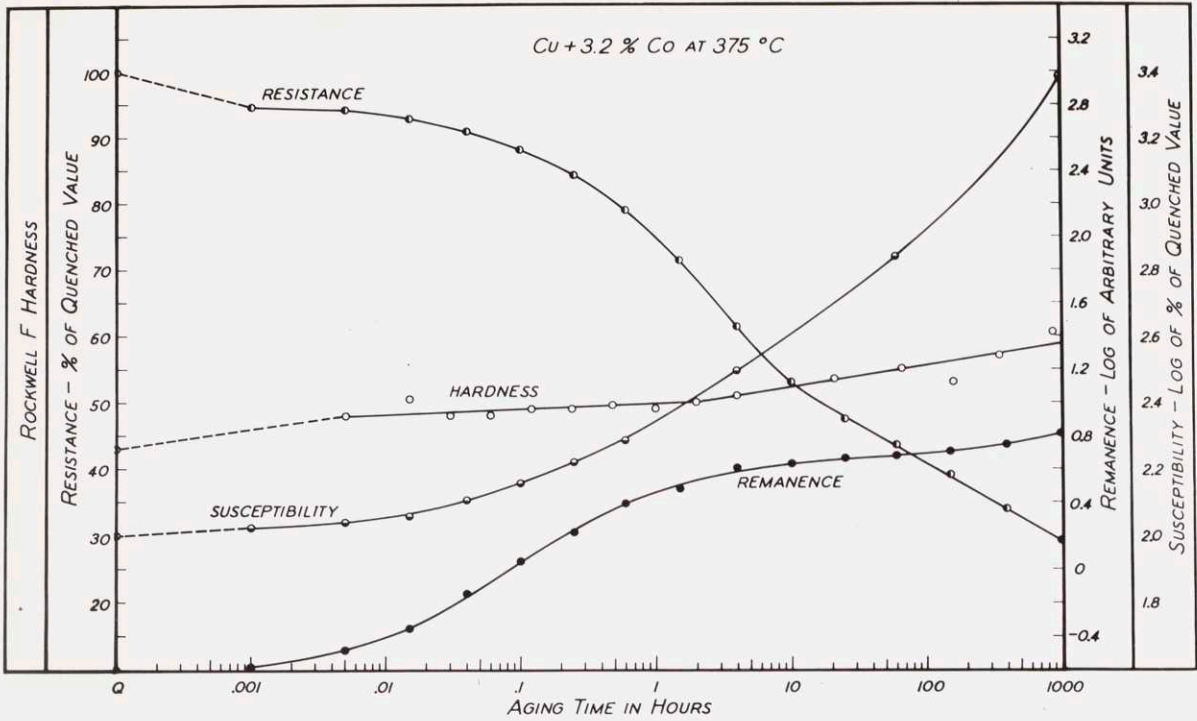


Fig. 26. Aging Curves of Copper-Cobalt Alloy at 375° C

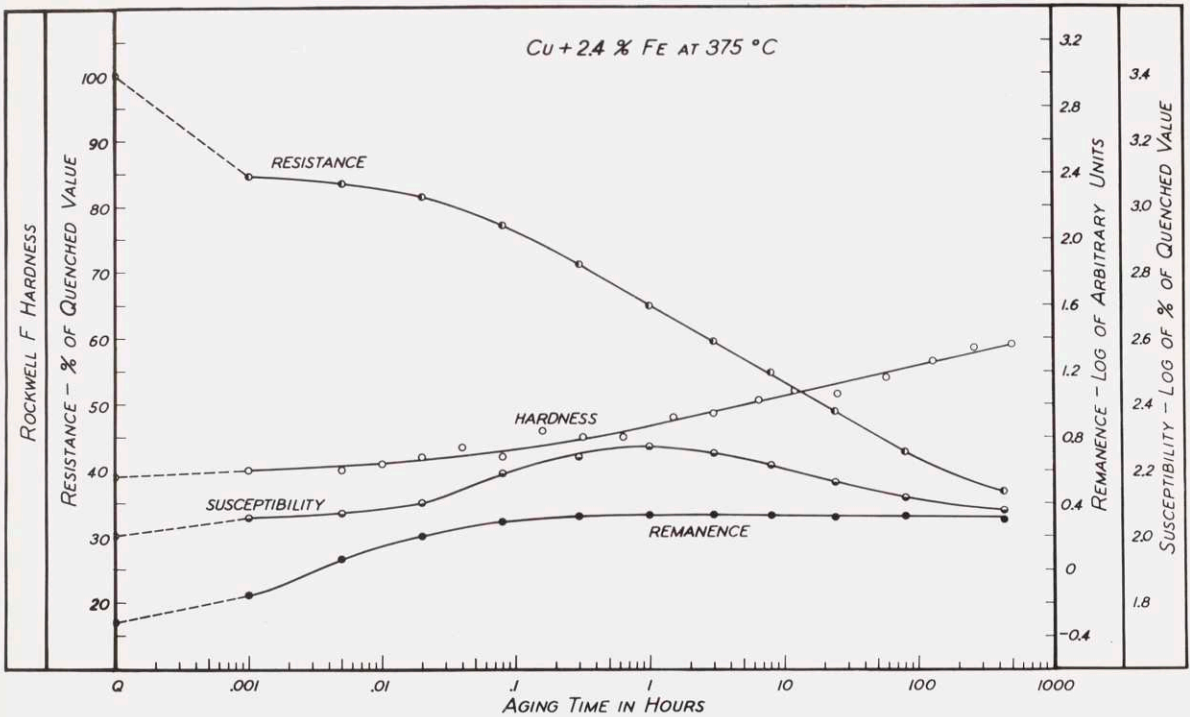


Fig. 27. Aging Curves of Copper-Iron Alloy at 375° C

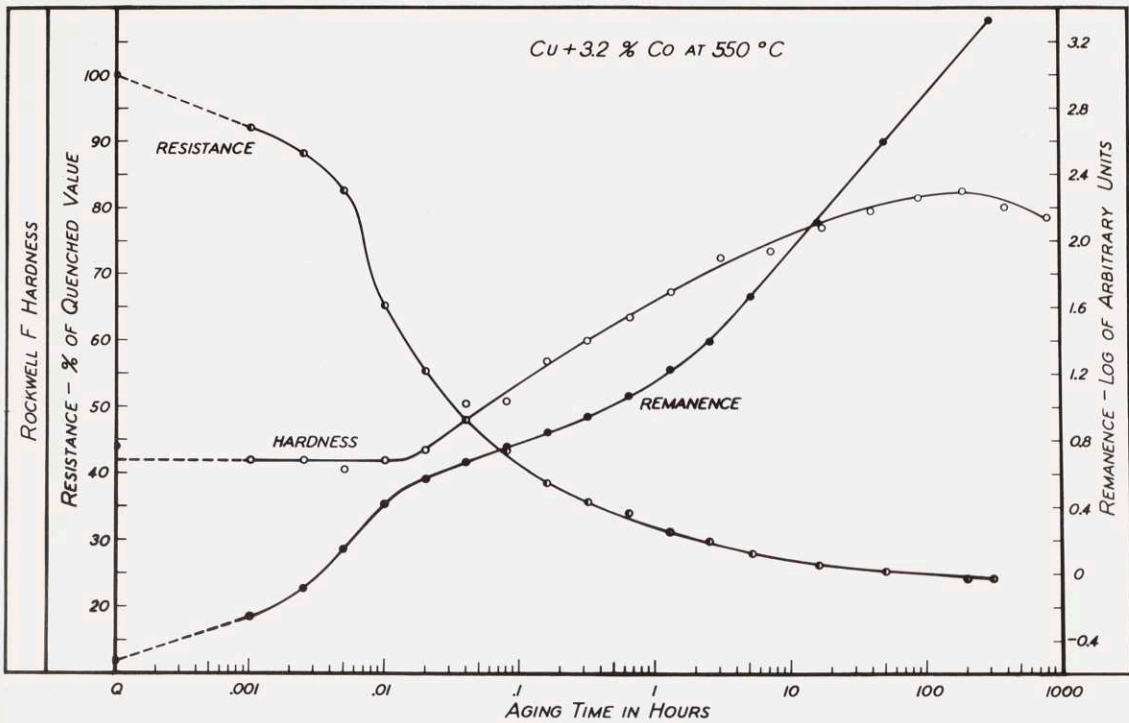


Fig. 28. Aging Curves of Copper-Cobalt Alloy at 550° C

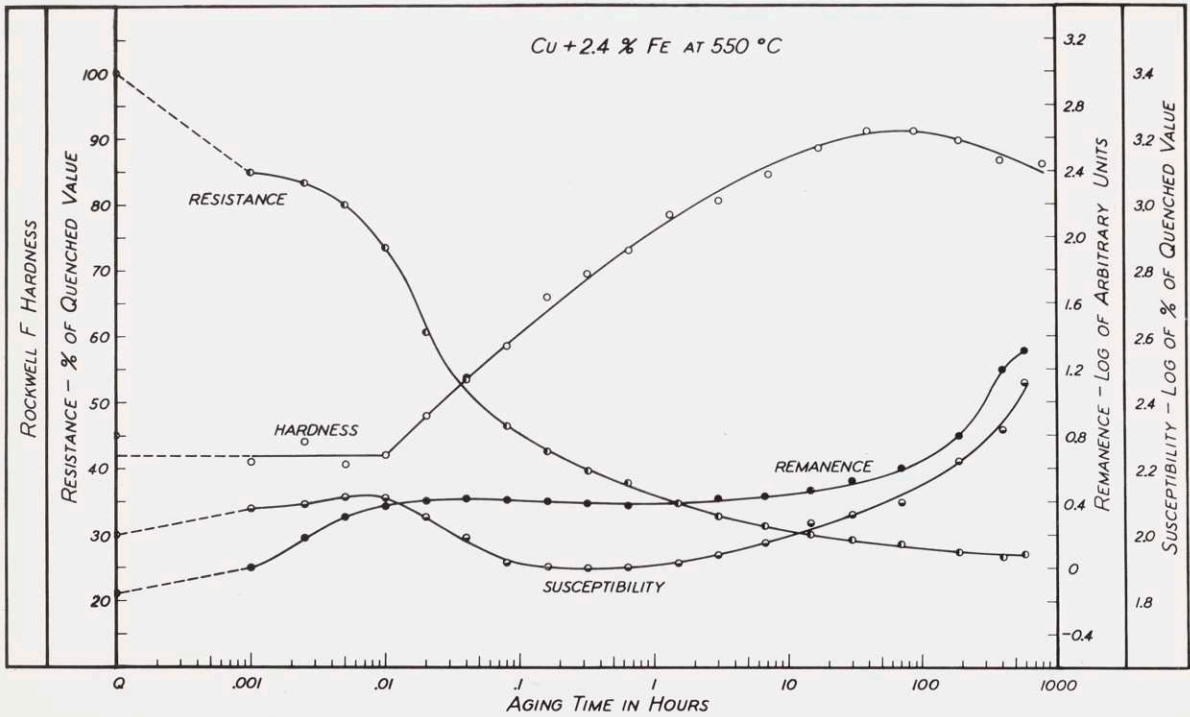


Fig. 29. Aging Curves of Copper-Iron Alloy at 550° C

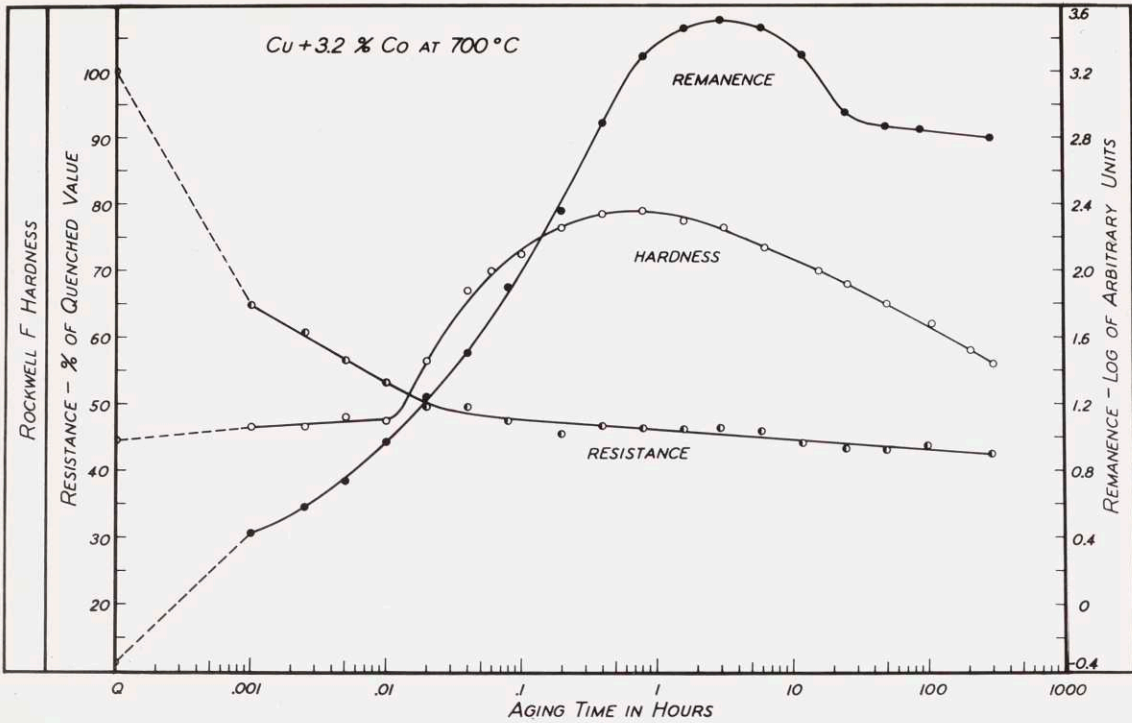


Fig. 30. Aging Curves of Copper-Cobalt Alloy at 700° C

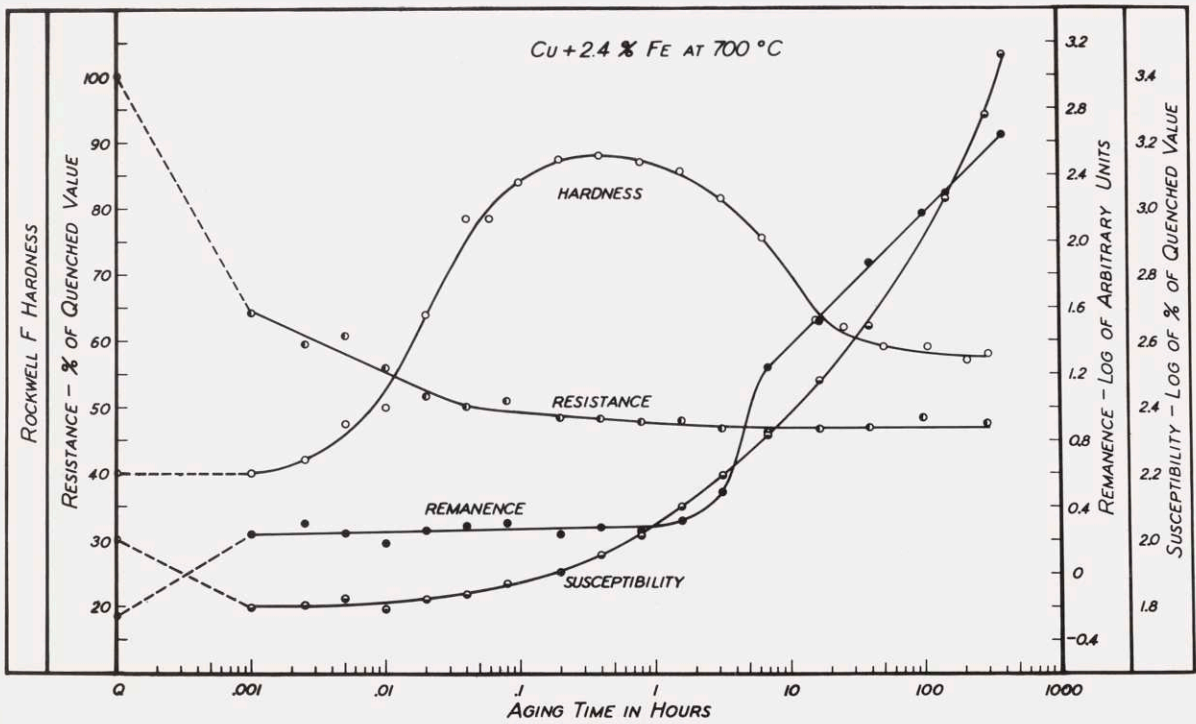


Fig. 31. Aging Curves of Copper-Iron Alloy at 700° C

## 6. Microstructure of Copper-Iron Alloy

The quenched structure is shown in Figure 32 (a). After 0.04 hours aging at 375° C a precipitate, as in Figure 32 (b), appears at the grain boundaries. These boundary areas, which consist of the stable copper-rich solid solution plus an iron-rich precipitate, then gradually grow into the grains. Although these areas are structureless at first because the precipitate is submicroscopic in size, they eventually show a sort of wave front like that of Figure 32 (c). The individual particles are still invisible but the effect of a large number is to produce a darkened zone.

During aging at 550° C the first boundary precipitate is visible after 0.02 hours and the structure is identical with that of Figure 32 (b). As this boundary fringe widens, a dark zone advances and leaves structure-less areas behind as in Figure 33 (a). In one spot the structure shown in Figure 33 (b) was observed at the advancing boundary. No actual particles are seen, even at 2500 diameters. The dark areas probably represent masses of tiny particles coming out of solution along certain crystallographic planes. While these first areas are growing, new ones are continuously forming until, after one hour, they cover about one-third of the total boundaries. At their greatest extent they cover not over 1 or 2 percent of the whole sample. After 7 hours particles are visible in the boundary areas at high magnification. The next appearance is that of resolvable particles of general precipitate in certain preferred areas such as twins. This is shown in Figure 33 (c) after 17 hours. The general precipitate grows until after 392

hours it is visible at 250 diameters as in Figure 33 (d). At higher magnification the whole surface is covered with precipitate but the particles are larger at the boundaries. This is shown in Figures 33 (e) and (f).

At 700° C the first boundary precipitate occurs at 0.0025 hours. These areas grow in the same manner, but more rapidly than at the lower temperatures. The general precipitate is apparent by a darkening of the grains after 0.04 hours as in Figure 34 (a). In some regions this precipitate seems to form wavy lines as shown in Figure 34 (b), while in others it lines up in regular lines which may have resulted from plastic deformation during the quench. New boundary areas continue to form up to 0.40 hours, at which time approximately half of the total boundaries are covered. Fairly coarse particles become visible in certain twin areas and, after 26 hours, even within the grains. The three types of precipitate: boundary, preferred general, and general, are clearly shown in Figure 34 (c).

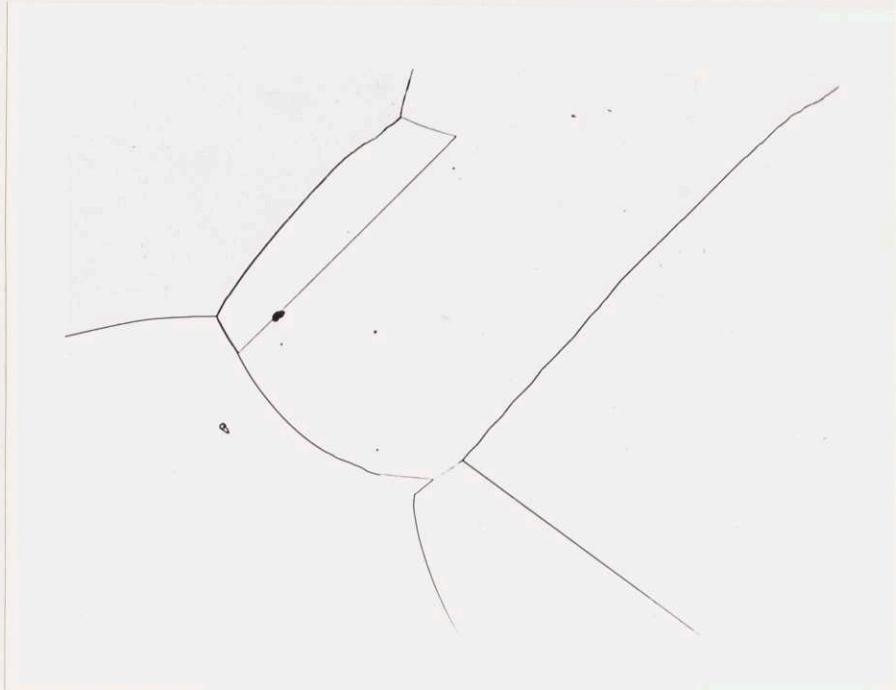
## 7. Microstructure of Copper-Cobalt Alloy

Due to the extremely rapid transformation rate, all the quenched copper-cobalt samples showed some evidence of grain boundary precipitate. This generally takes the form of slightly widened and rounded boundaries as shown in Figure 35 (a). During aging at 375° C, structureless grain boundary areas are formed and then grow into one of the adjacent grains. In some cases the original boundaries begin to disappear as shown in Figure 25 (b). No precipitated particles are visible.

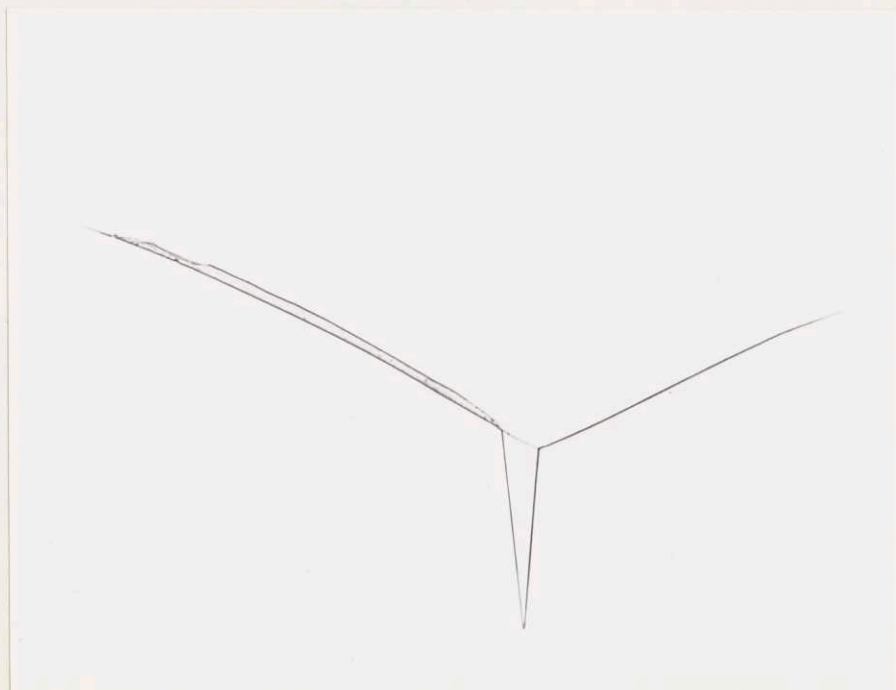
During aging at 550° C the same structureless boundary areas are formed as at 375° C. As seen in Figure 36 (a), these areas show no dark fringe like the copper-iron alloy. When general precipitation occurs the boundary areas are merged indistinguishably into the rest of the grain. The extent of their growth can be estimated by the size of the irregular bumps on the rounded grains. After one hour a string of tiny particles becomes visible along the grain boundaries. The general precipitate appears first in certain twin areas as in the copper-iron alloy and then at random throughout the grains. Figure 36 (b) shows the boundary particles and the preferred general precipitate, but the general precipitate is still too fine to resolve at 500 diameters.

The early stages of aging at 700° C show the same changes in microstructure as at the lower temperatures. Patches of general precipitate first appear after 0.04 hours. The boundary areas soon merge with the rest of the grains giving the structure shown in Figure 37 (a). After 6.4 hours particles appear in the bumps on the grain boundaries as shown in Figure 37 (b). Figure 37 (c) shows a general view of these dark patches at lower magnification. In addition to these globular particles, another acicular, type of precipitate appears after 109 hours. Figure 37 (d) shows these needles arranged in a sort of Widmanstätten structure. The exact nature of this precipitate remains to be determined, but it may be connected with the marked remanence changes occurring at the same time.

Fig. 32. Microstructure of Copper-Iron Alloy at 375° C



(a) As quenched 250X



(b) Aged 0.04 Hours 500 X



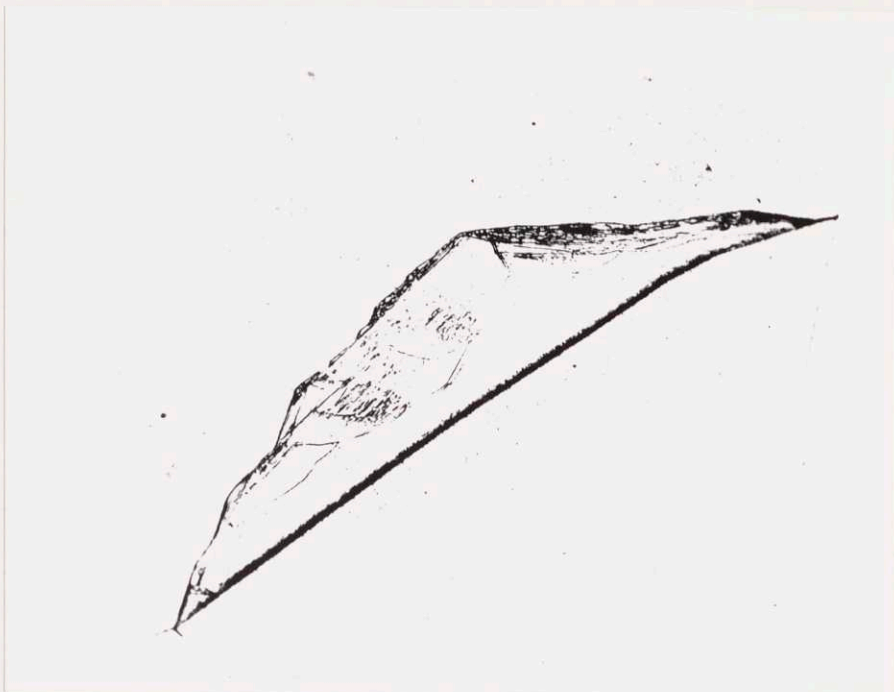
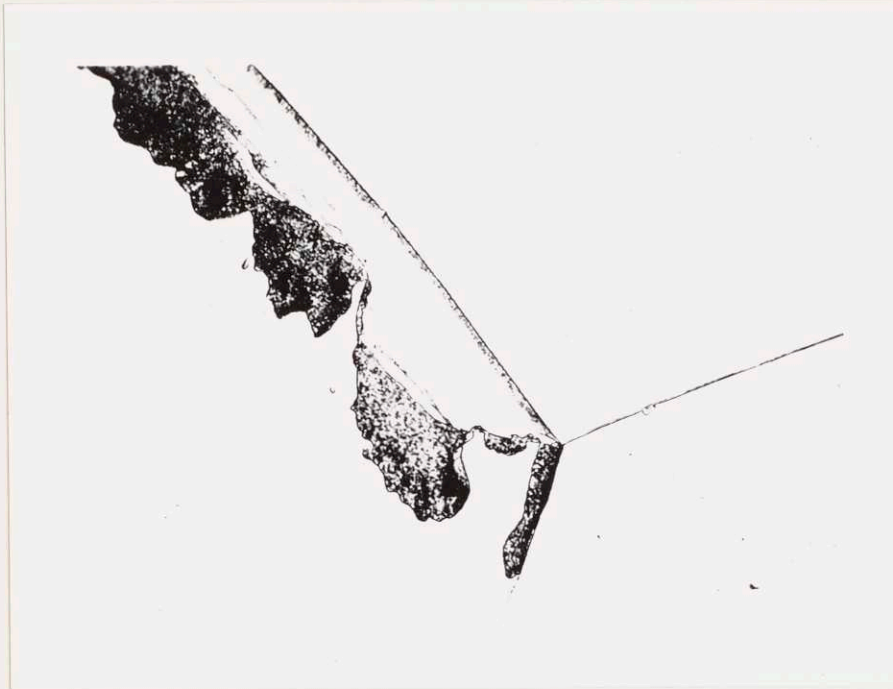
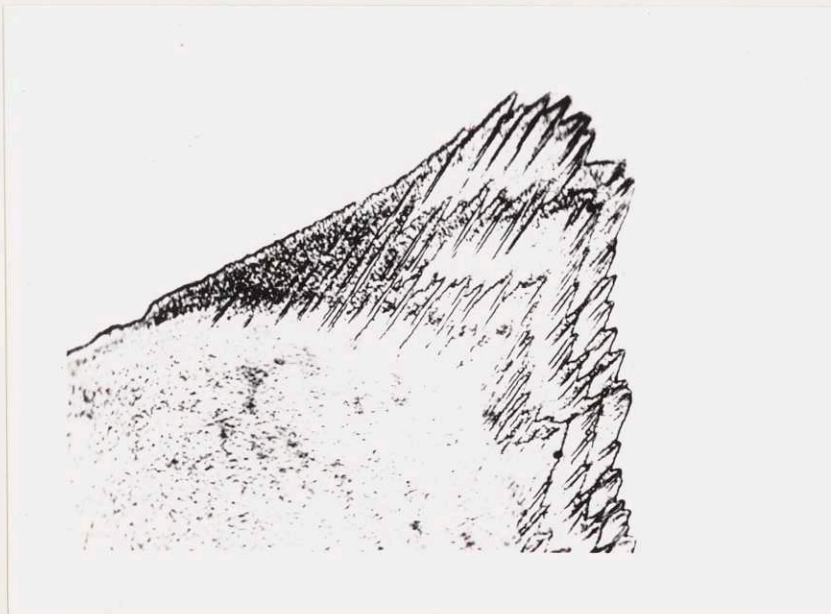


Fig. 32 (c). Aged 10 Hours 500X

Fig. 33. Microstructure of Copper-Iron Alloy at 550° C



(a) Aged 40 Hours 500X



(b) Aged 0.66 Hours 1200X

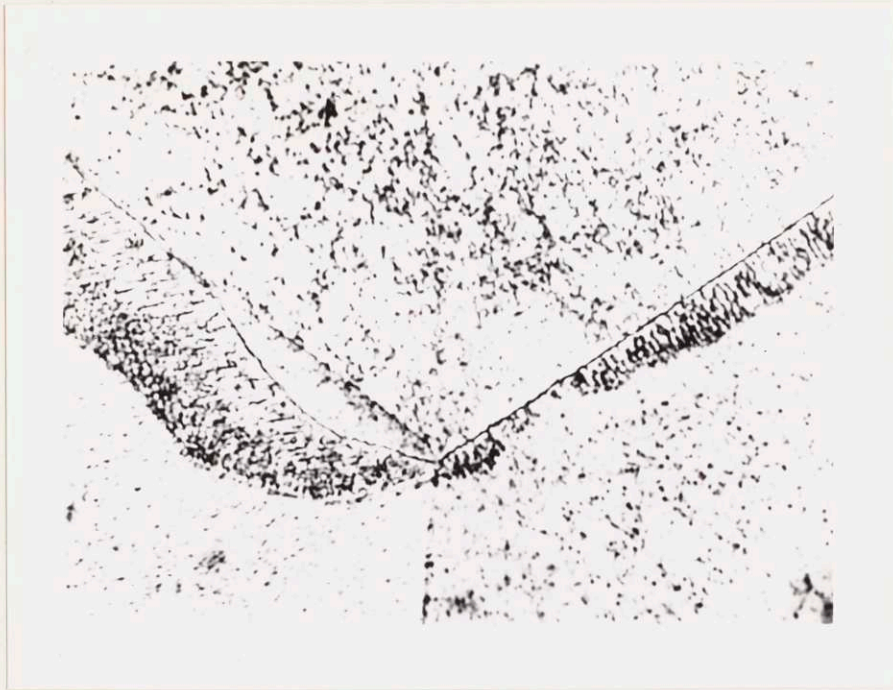


Fig. 33 (c). Aged 17.3 Hours 2000X

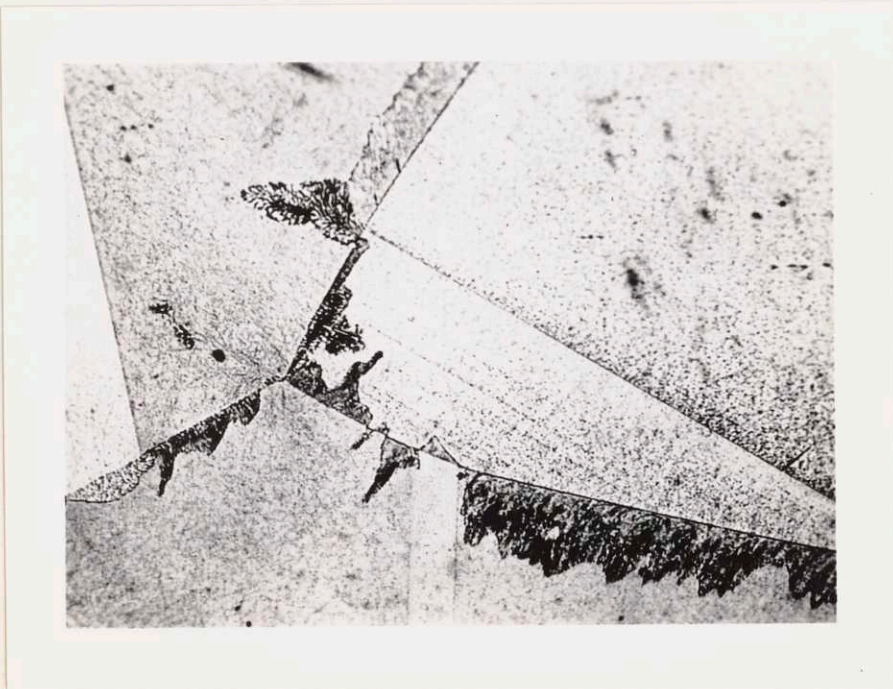


Fig. 33 (d). Aged 392 Hours 250X

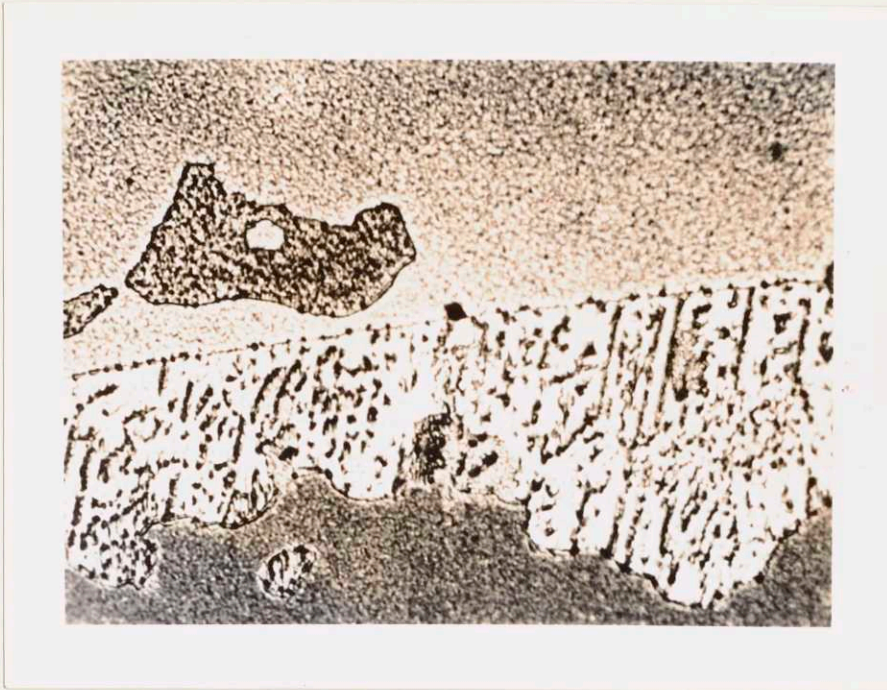


Fig. 33 (e). Aged 817 Hours 1000X

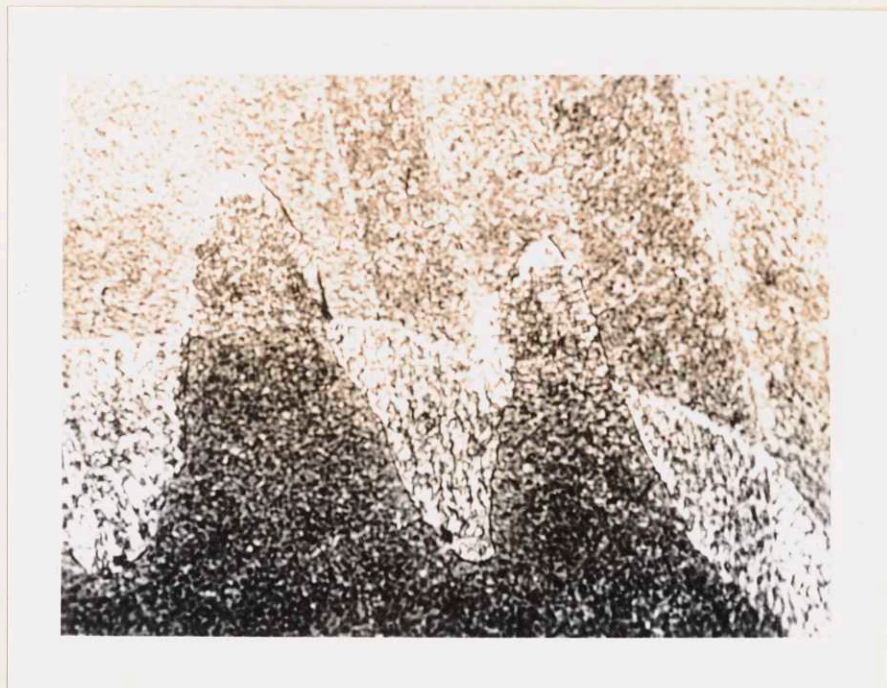
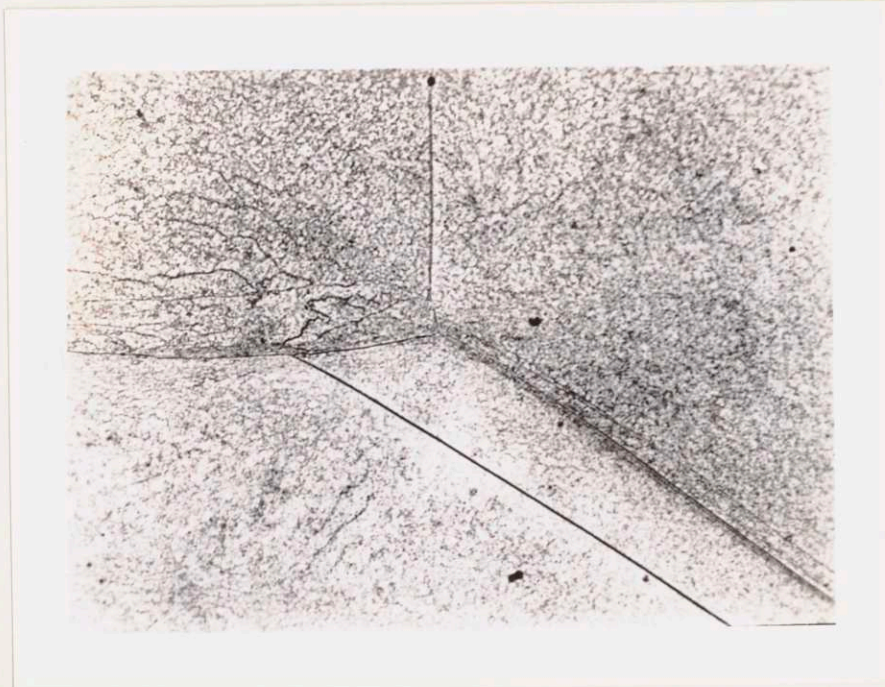


Fig. 33 (f). Aged 817 Hours 2000X

Fig. 34. Microstructure of Copper-Iron Alloy at 700° C



(a) Aged 0.04 Hours 500X



(b) Aged 0.10 Hours 250X

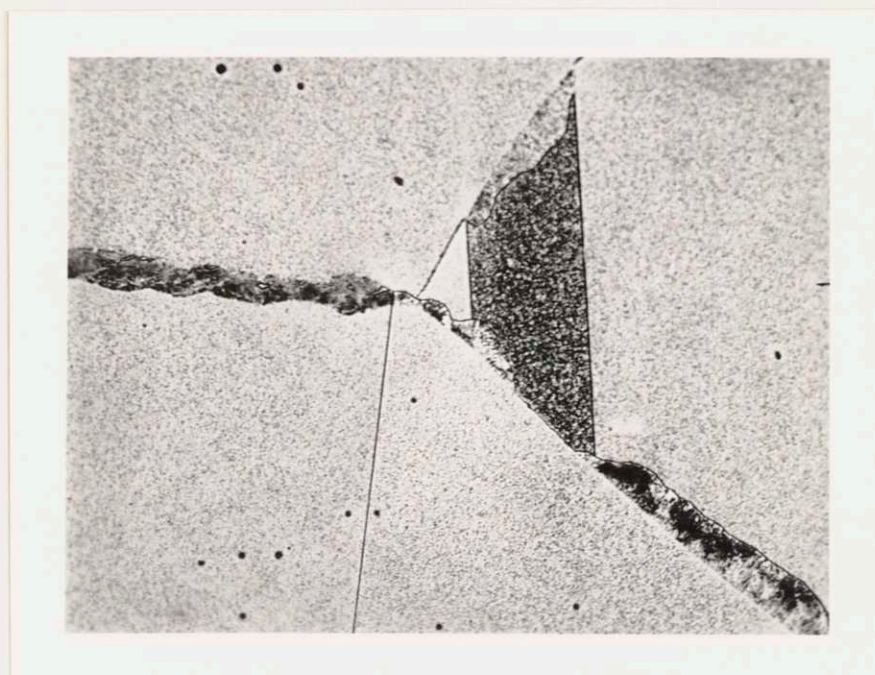
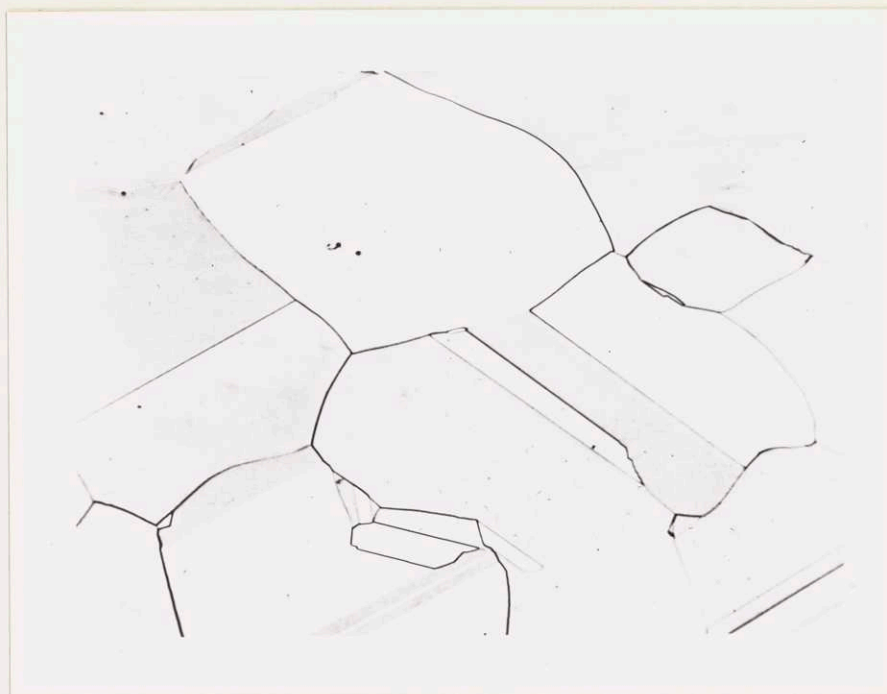
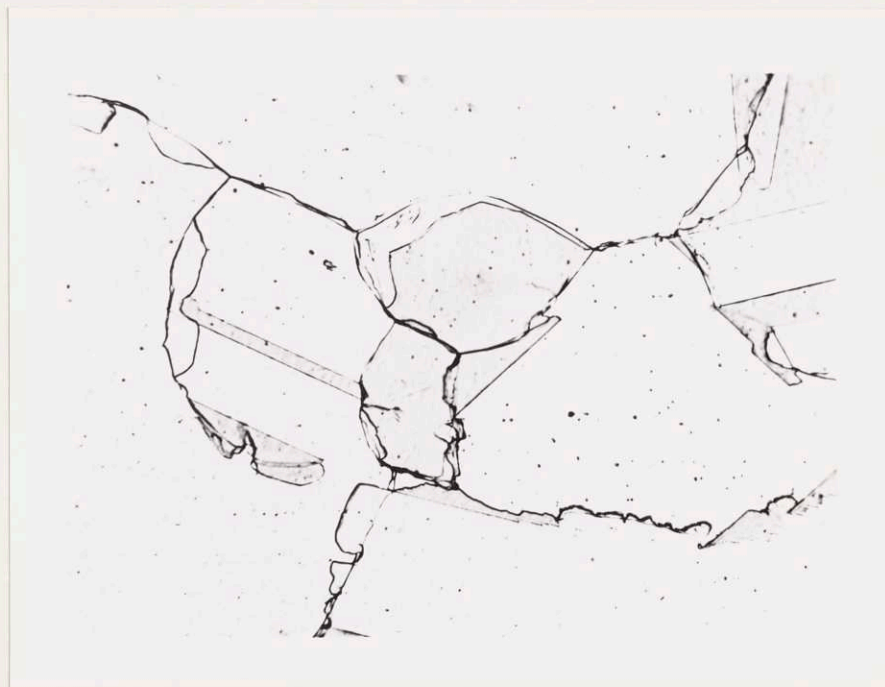


Fig. 34 (c). Aged 26 Hours 250X

Fig. 35. Microstructure of Copper-Cobalt Alloy at 375° C

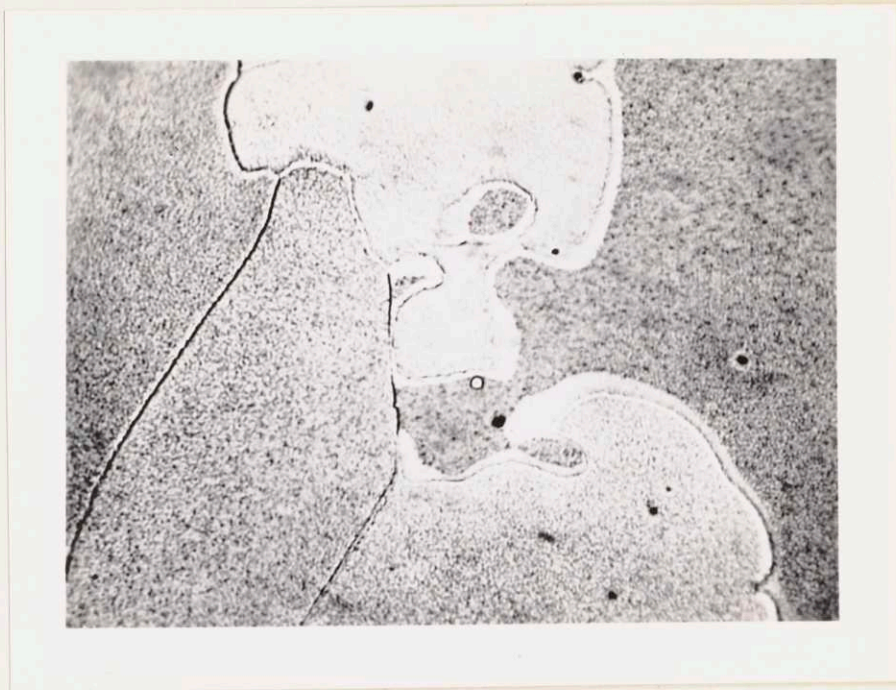


(a) As Quenched 150X

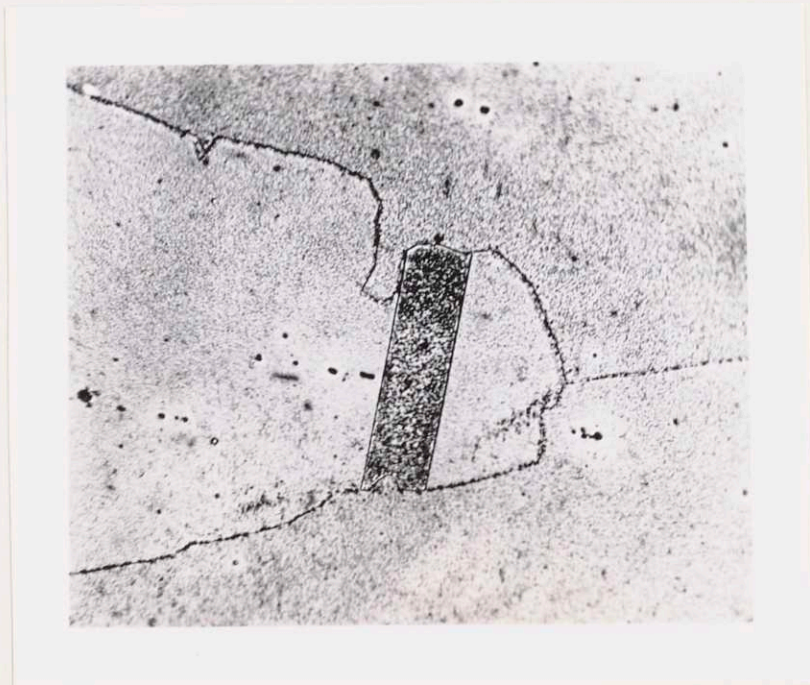


(b) Aged 10 Hours 250X

Fig. 36. Microstructure of Copper-Cobalt Alloy at 550° C



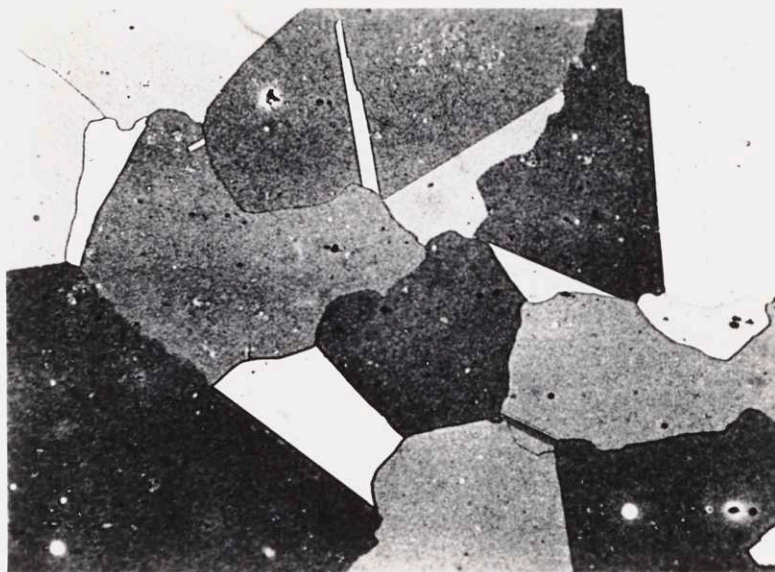
(a) Aged 0.16 Hours 1000X



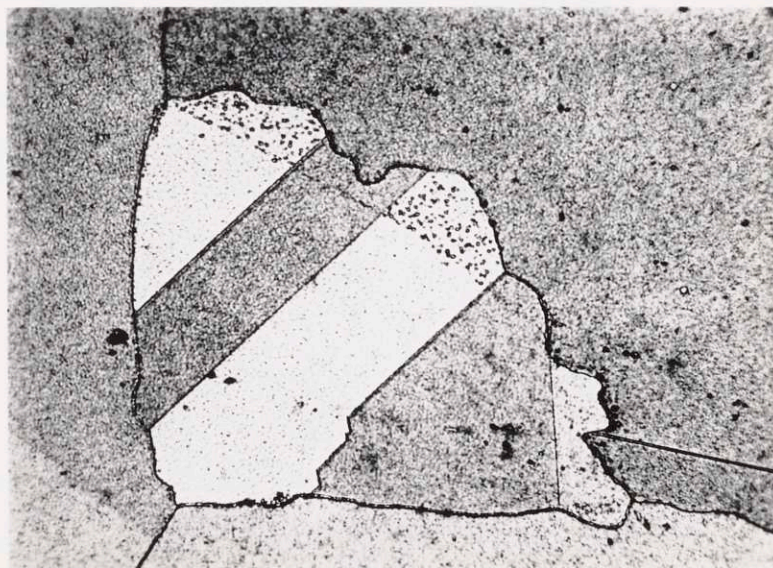
(b) Aged 817 Hours 500X



Fig. 37. Microstructure of Copper-Cobalt Alloy at 700° C



(a) Aged 0.10 Hours 250X



(b) Aged 6.4 Hours 500X

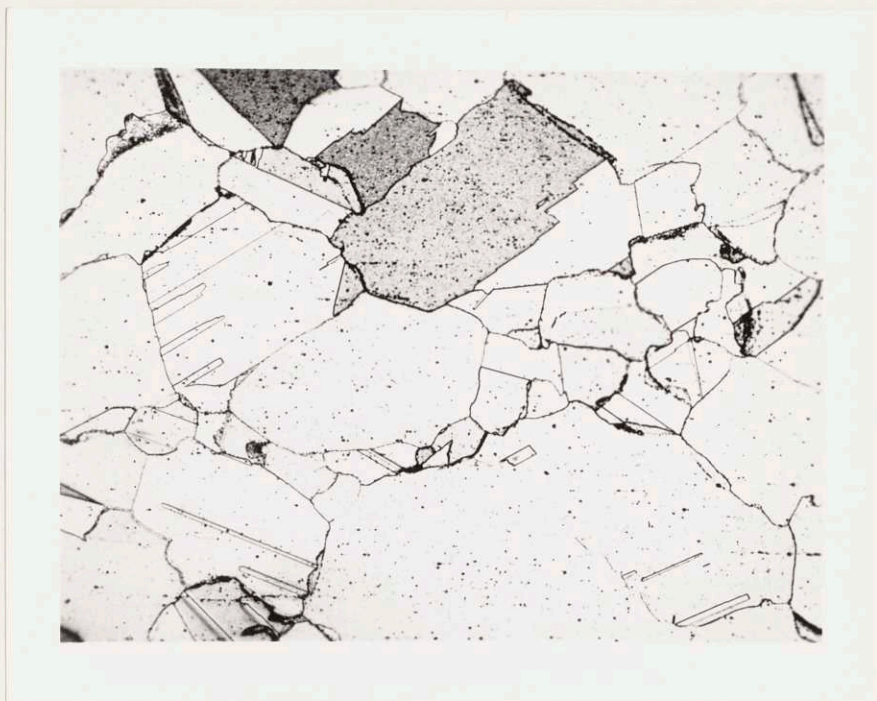


Fig. 37 (c). Aged 26 Hours 75X



Fig. 37 (d). Aged 212 Hours 250X

## VIII. CORRELATION AND INTERPRETATION OF RESULTS

### 1. Copper-Cobalt Alloy

The results of aging at four temperatures indicate that the copper-cobalt alloy undergoes a two-stage precipitation process. The aging curves at 250° C show only the first, while those at 700° C show only the second stage. At the intermediate temperatures of 375° or 550° C, the curves show both stages. Since the basic aging mechanism is the same, each successively higher temperature repeats the property changes of the lower temperatures and then adds further changes of its own. Aging proceeds very slowly at 250° C and the first stage is not completed in 1000 hours. At 375° C, the completion of the first stage and the start of the second are illustrated very clearly. During aging at 550° C, the first stage occurs rapidly, but the second is not completed. At 700° C, all of the first stage occurs before 0.001 hours and the second is virtually completed.

Remanence is the best indicator, among the properties measured, of the two stages in the precipitation process. It rises sharply during the first stage and levels off during the initiation of the second. It then goes through a period of rapid increase during the second stage, and finally reaches a maximum value at 700° C. Susceptibility is the only property not showing a break between the two stages. It rises smoothly at the two temperatures where it could be measured.

Hardness shows only a slight increase during the first stage, but increases markedly beginning with the second stage. It reaches its

maximum value after a long period at 550° C, when the resistance results indicate practically complete precipitation. This is interesting because it illustrates the very slow rate of growth of the precipitated particles.

Resistance decreases during both stages of precipitation. Only at 250° C is the aging process sufficiently slow so that the changes associated with the first stage may be studied. At this temperature a slight break occurs that might perhaps be attributed to "knot" formation preceding the second stage. The levelling off appears small on the scale used but is reproducible. It may be the result of two overlapping effects - one a decrease due to boundary precipitation and the other an increase due to "knot" formation. At higher temperatures a break occurs after the first three seconds, but it may only be the result of insufficient time for the specimens to reach the aging temperature. Although a considerable decrease in resistance occurs during the first stage, the maximum drop takes place at the start of the second stage. During the remainder of the second stage, the resistance drops gradually and approaches a stable value after long periods at 550° C.

Microscopic examination shows that the first stage is due to precipitation at the grain boundaries and that it occurs simultaneously with the property changes described above. It shows, further, that the second stage is one of general precipitation within the grains and that, in this instance, there is a time lag between the property changes and the appearance of the first signs of precipitation. In the first stage, the boundary areas may be easily detected at an early time when

they are still structureless due to the submicroscopic size of the particles. In the case of general precipitation, the grains are structureless originally, and no change is noticed until the particles have grown beyond the size that produces the property changes. The fact that new areas of boundary precipitate may still form after the property changes associated with the start of general precipitation, indicates that the two stages overlap to a certain extent.

The drop in resistance, during the period of grain boundary precipitation, is much greater than is to be expected from the amount of the precipitate and the resulting impoverishment of the copper-rich solid solution. However, the occurrence of this impoverished solution in the form of a continuous network at the grain boundaries, would produce a sort of short-circuiting effect. Again, during the beginning of general precipitation, a disproportionate drop in resistance occurs. Since the other properties indicate that this precipitation is probably fairly uniform, the conclusion is that the resistance is not a good measure of the rate of precipitation.

The magnetic properties show that both the grain boundary and the general precipitate are ferromagnetic. In fact, the alloy becomes so strongly ferromagnetic that it is impossible, in the apparatus used, to measure susceptibility at the two higher temperatures. With appreciable amounts of a ferromagnetic precipitate, the changes in the paramagnetism of the copper-rich solution have a negligible effect. Hence, the susceptibility value is determined by the amount of the pre-

precipitate and its saturation magnetization. From the smooth, uninterrupted rise of susceptibility between the two stages, the conclusion is either, that the magnetizations of the two types of precipitate are the same, or that their amounts change in the right proportions to produce the same effect.

While the resistance changes are due to the varying composition of the copper-rich solution, the changes in magnetic properties are caused by the cobalt-rich precipitate. As mentioned above, the susceptibility measures principally the amount of the precipitate. Remanence, on the other hand, shows more complicated changes, whose explanation must lie, not only in the amount of the precipitate, but also in its composition, size, shape and atomic arrangement. Changes in the first three factors certainly occur and possibly in the last two as well. Under equilibrium conditions, cobalt will dissolve about 10 percent copper, but the effects of temperature on this solubility are unknown. Hence, we cannot predict changes in the composition of the precipitate during aging. Above about 450° C, the cobalt-rich phase is face-centered cubic, while, at room temperature, the stable phase is hexagonal close-packed.

Entirely apart from equilibrium considerations, prior to precipitation, the solute atoms are located on the face-centered cubic host lattice and their most probable arrangement after precipitation would likewise be face-centered. If such a precipitate is actually formed, it should of course eventually transform into the stable hexagonal phase. Since both forms of cobalt are ferromagnetic, the transforma-

tion should cause only a small change in the magnetic properties. There is no data which will enable us to predict what to expect, but it may be that the unusual changes in remanence after long periods at 700° C are due, at least in part, to this transformation. These changes might, however, be caused by other factors such as composition, size, etc. The appearance of a new, acicular type of precipitate in the microstructure at about this time is additional evidence of some change in the precipitate.

No pre-precipitation effects of the type found in duralumin were noticed at any aging temperature. Resistance shows a continuous decrease, with the exception of a slight break at 250° C. Hardness begins to increase slightly with boundary precipitation and shows a large increase during general precipitation. However, this evidence does not necessarily support the simple precipitation theory, since it does not exclude the possibility of a "knot" stage. Because of the rapid transformation rate of this alloy, as shown by the appearance of grain boundary precipitate in severely quenched samples, it is possible that the pre-precipitation stage occurs during the quench. Subsequent aging will then show only the precipitation stages. This idea would be difficult to confirm experimentally. But even if a "knot" stage does occur during aging, any possible increase in resistance will be masked by the large decrease due to grain boundary precipitation.

If we can prove our postulate of a face-centered cubic transition phase, the indirect evidence of a pre-precipitation stage will be quite strong, since the formation of such a precipitate must be preceded by

segregations of solute atoms along the solid solution lattice. The experimental evidence for the copper-cobalt alloy is inconclusive. However, strong evidence confirming this point will be presented in the discussion of the copper-iron alloy immediately following.

## 2. Copper-Iron Alloy

The aging process in the copper-iron alloy is similar to that of copper-cobalt in that it involves a two-step precipitation process which occurs first at the boundaries and then throughout the grains. Moreover, the kinetics of the process is very nearly the same in both alloys. At all aging temperatures, the direction and magnitude of the changes in resistance and hardness are the same. Hence, the discussion of these two properties in the preceding section for the copper-cobalt alloy applies equally well here. The greater resistance drop in the copper-iron alloy during the first stage is probably due to the greater amount of boundary precipitate found under the microscope. However, because the initial resistance of the copper-cobalt alloy is 50 per cent greater, it shows a greater total decrease during aging. The slightly greater hardness increase in the copper-iron alloy may be the result of a better quench, as evidenced by the absence of grain boundary precipitate in the quenched samples.

The microstructure of the two alloys is similar in that both show a structureless boundary fringe at the start of the first stage. While in the copper-cobalt alloy this fringe tends to merge into the body of the grain with further aging, in the copper-iron alloy the boundary areas



remain distinct during all stages. The amount of the boundary precipitate appears to be greater in the copper-iron alloy, although such an estimate is necessarily difficult. Both alloys show the first microscopically resolvable particles of general precipitate in certain preferred areas such as twins. In spite of minor differences it is probable that the mechanism of precipitation is quite similar in the two alloys.

The magnetic results of the copper-iron alloy are complicated by the initial appearance of the general precipitate in a paramagnetic form and its ultimate transformation to the ferromagnetic state. The grain boundary precipitate is ferromagnetic and the changes in susceptibility and remanence during the first stage are identical with those of the copper-cobalt alloy. However, after the beginning of general precipitation, remanence remains constant for a long period and susceptibility decreases. These results, combined with those for resistance, prove conclusively that the general precipitate is paramagnetic\*. It is very likely that this paramagnetic iron-rich phase is face-centered cubic gamma iron! Here is the evidence for a transition phase that could not readily be shown in the copper-cobalt alloy. Because of the close similarities of the two alloys in all other respects, it is reasonable to presume that the face-centered transition phase appears in the copper-cobalt alloy as well. We thus have an illustration of the fact

---

\* This fact furnishes a satisfactory interpretation of the magnetic results of Tammann and Oelsen discussed in Section III - 5.

that the first precipitate in an age-hardening alloy is not necessarily the equilibrium phase.

Because the paramagnetic iron-rich phase is not stable either at the aging temperatures or at room temperature, we should expect it to transform ultimately into the stable ferromagnetic phase. This transformation does not begin until long periods of aging at 550° C and is not completed even after 300 hours at 700° C. This delay in the appearance of strong ferromagnetism enables measurement of susceptibility, as well as remanence, to be made at the higher aging temperatures. When the transformation does occur, the susceptibility rises rapidly, even on a full logarithmic scale, but it is the remanence which shows the most abrupt change. This is one more example of the greater structural sensitivity of remanence. It would be interesting to follow this change from the face-centered to the body-centered lattice with X-ray diffraction but, unfortunately, the amount of the iron is too small to detect. And even with large amounts of gamma iron, the lines in the X-ray pattern would be almost identical with those of the copper-rich solution.

The question as to why, in the copper-iron alloy, the boundary precipitate is ferromagnetic and presumably alpha iron, while the general precipitate is paramagnetic and presumably gamma iron, cannot be answered here. But several possible explanations for this phenomenon may be offered. The first is that during the quench a paramagnetic boundary precipitate forms and that it becomes ferromagnetic during subsequent aging. This is very unlikely since the remanence rises gradually during the first stage and simultaneously with a drop in resistance. In

other words, although some submicroscopic boundary precipitate may form during the quench, the property changes indicate that most of it occurs during aging.

A more plausible explanation is that the nuclei formed at the boundaries are larger than those within the grains. Then, when the precipitate forms, it is large enough to break away completely from the face-centered host lattice and assume its stable body-centered, ferromagnetic form. Both of these occurrences would be logical results of the greater mobility at the grain boundaries and they are in line with Masing's<sup>14</sup> explanation for the behavior of cobalt-nickel-copper alloys (see Section III - 3). Such a difference in particle size is actually observed microscopically during the later stages of aging. It also supplies a logical reason for the growth of the boundary areas at the expense of the rest of the grains. Of course, besides a difference in particle size, there may be a difference in composition. Thus, the general precipitate may be face-centered cubic because of the number of copper atoms in its lattice and, when enough of this copper has been removed, it assumes its normal body-centered form.

The above discussion may be applicable to the copper-cobalt alloy but, due to the similar magnetic properties of the two cobalt-rich phases, we have no proof that the boundary and general precipitates are different. But the fact that precipitation occurs much earlier at the boundaries, indicates that the conditions there are different from those within the grains.

The occurrence of a transition phase during general precipitation is quite probable in both alloys. Starting with this assumption, we can make some interesting speculations on the mechanism of precipitation. In the quenched condition, the supersaturated copper-rich solid solution will contain iron or cobalt atoms at random points on the face-centered lattice. During aging, diffusion of the solute atoms results in the formation of segregations or "knots" in the lattice where the concentration of solute atoms is greater. Since all three kinds of atoms have nearly the same size, we should not expect much additional lattice distortion as a direct result of this "knot" formation. This may explain why no increase in resistance is found as in duralumin, where the atomic sizes are quite different. Due to the continuity of the process depicted above, it is difficult to find a satisfactory criterion for the start of precipitation. However, this minor point should not concern us here, because of the non-uniformity of aging in the alloys studied. Eventually, there is enough difference in the lattice spacings so that the precipitate does break away from the host lattice. It is interesting to note that evidence of the general precipitate in the copper-iron alloy was observed microscopically before its transformation to the ferromagnetic state, indicating the remarkable stability of the transition phase. The final stage in the aging process involves the formation of the equilibrium phases and it may take a very long time for completion.

## IX. CONCLUSIONS

The following conclusions can be drawn from the results of this investigation:

(1) The aging process in both the copper-cobalt and the copper-iron alloy is one of two-stage precipitation.

(2) The first stage involves the precipitation, at the grain boundaries, of a cobalt or an iron-rich phase, both of which are ferromagnetic. The heterogeneous boundary areas grow to a certain extent into the adjacent grains and then stop.

(3) The second stage involves general precipitation within the center of the grains. In both alloys, the initial precipitate is probably a face-centered cubic transition phase. It is ferromagnetic in the copper-cobalt alloy and paramagnetic in the copper-iron alloy.

(4) The paramagnetic iron-rich phase transforms into a ferromagnetic form, probably body-centered cubic, after 200 hours at 550° C. This change is very clearly shown in the magnetic results. The initial cobalt-rich precipitate may likewise transform into its stable hexagonal phase, but the magnetic change is small since both forms are ferromagnetic.

(5) Hardness shows a slight rise during the first stage and a pronounced increase starting with the second stage. Maximum hardness is attained in both alloys after aging for 100 hours at 550° C.

(6) Resistance shows a continuous drop at all aging temperatures. It decreases markedly during the first stage and to an even greater

extent at the start of the second stage. Minimum resistance is virtually attained after 1000 hours at 550° C.

(7) Remanence is a sensitive indicator of the two-stage precipitation process. It also shows marked changes during the magnetic transformation in the copper-iron alloy and changes in the copper-cobalt alloy which may denote the appearance of the hexagonal phase.

(8) Apparent susceptibility shows a continuous increase in the copper-cobalt alloy at the two temperatures where it could be measured. In both cases its value is determined principally by the amount of the ferromagnetic precipitate. In the copper-iron alloy it shows the decreasing paramagnetic susceptibility of the copper-rich solution during the initial period of the general precipitation.

(9) The experimental results show none of the changes usually associated with a pre-precipitation stage. However, the probable occurrence of face-centered transition phases is indirect evidence in favor of a "knot" stage. The failure to detect this stage is probably due to the high transformation rate of these alloys during the quench and also to the microscopic non-uniformity of the aging process.

## X. RECOMMENDATIONS FOR FURTHER WORK

The present investigation has opened up a very promising field for further work. It is rather strange that the copper-cobalt and copper-iron alloys have so long escaped the attention of metallurgists for, as the results presented here have shown, these systems are extremely interesting from a theoretical standpoint. They are unique in their adaptability for magnetic measurements and in the unusual opportunity they present for studying transition phases. The results obtained so far indicate the importance of extending the work to include the following:

- (1) Determination of the equilibrium values of resistance and susceptibility at different temperatures for varying concentrations of the copper-rich solutions.
- (2) Determination of the magnetic properties of the cobalt and iron-rich phases with varying concentrations of copper.
- (3) Measurement of the field dependence of susceptibility during aging to enable quantitative calculation of the paramagnetic and ferromagnetic components.
- (4) Use of alloys with lower iron and cobalt contents in an attempt to obtain a more successful quench.
- (5) Study of alloys made from powders to determine effect of size and shape of ferromagnetic particles on the magnetic properties.
- (6) Continuation of aging at temperatures of 700° C or higher until the properties reach their equilibrium values.

(7) Additional microscopic work, using colloidal iron to show the ferromagnetic precipitate.

(8) Further work on X-ray diffraction.



XI

BIBLIOGRAPHY

1. M. Hansen - "Der Aufbau der Zweistofflegierungen", Springer, Berlin, 1936
2. Hanson and Ford - "Investigation of the Effects of Impurities on Copper, Part II - The Effect of Iron on Copper", J. Inst. Met. V. 32 (1924) pp. 335-361
3. Tammann and Oelsen - "Die Abhängigkeit der Konzentration gesättigter Mischkristalle von der Temperatur", Z. Anorg. Chem. V. 186 (1930) pp. 267-77
4. M. L. V. Gaylor - "Aging", Metallurgist Oct. 1938, p. 166, and Dec. 1938, p. 181
5. Merica, Waltenberg and Scott - "Heat Treatment of Duralumin", U. S. Bur. Std. Sci. Paper V. 15 (1919), p. 271
6. P. D. Merica - "The Age-Hardening of Metals", Trans. A. I. M. E. V. 99 (1932), pp. 13-54
7. M. Cohen - "Aging Phenomena in a Silver-Rich Copper Alloy", Trans. A. I. M. E., V. 124 (1937), p. 138
8. M. L. V. Gaylor - "The Theory of Age-Hardening", J. Inst. Met., V. 60 (1937), p. 249
9. Fink and Smith - "Age-Hardening of Aluminum Alloys, III - Double Aging Peaks", Trans. A. I. M. E., V. 128 (1938), p. 223
10. M. Cohen - "Age-Hardening of Duralumin" - Metals Technology, Oct. 1938, T. P. No. 978

11. Dehlinger - "Über den Verlauf von Ausscheidungen", Zeit f. Metallkde.  
V. 27 (1935), p. 209-12  
see also: Zeit f. Metallkde, V. 29 (1937), p. 401
12. Köster and Dannöhl - "Die Aushärtung der Gold-Nickel-Legierungen",  
Zeit f. Metallkde, V. 28 (1936), pp. 248-253
13. Volk, Dannöhl and Masing - "Die Entmischungsvorgänge in Co-Cu-Ni-  
Legierungen im festen Zustand", Zeit f. Metallkde, V. 30 (1938)  
pp. 113-122
14. Masing - "Der Zerfall der Mischkristalle in den Co-Ni-Cu-Legierungen  
im festen Zustand", Probleme Der Technischen Magnetisierungskurve,  
pp. 129-140, Springer, Berlin, 1938
15. M. G. Corson - "Copper Alloy Systems with Variable Alpha Range and  
Their Use in the Hardening of Copper", A. I. M. E. Proc. Inst. Met.  
Div., 1927, pp. 435-450  
Corson - "Systeme d'alliages de cuivre avec phase alpha et a limites  
variables et leur emploi pour le durcissement du cuivre", Rev.  
de Met., V. 27 (1930), pp. 83-101
16. C. S. Smith - "An Air-Hardening Copper-Cobalt Alloy", Min. and  
Met., V. 11 (1930), pp. 213-215
17. G. Tammann - "Die Vorgänge bei der Vergütung", Zeit f. Metallkde,  
V. 22 (1930), pp. 365-368
18. J. T. Norton - "Simplified Technique for Lattice Parameter Meas-  
urements", Met. and All. V. 6 (1935), p. 342
19. T. Ishiwara - "On the Magnetic Investigation of  $A_3$  and  $A_4$  Trans-  
formations in Pure Iron", Sci. Rep. Toh. Imp. Univ., V. 6 (1917),  
pp. 133-138

20. E. C. Stoner - "Magnetism and Matter", p. 508, Methuen, London, 1934
21. A. R. Kaufmann - "Current Balance for Measuring Magnetic Fields and Susceptibilities", Rev. Sci. Inst., V. 9 (1938), pp. 369-71
22. P. Jacquet - "Sur une nouvelle method d'obtention de surfaces metalliques parfaitement polies", Comp. Rend., V. 201 (1935), pp. 1473-1475
23. Lowery, Wilkinson and Smare - "Influence of the Polished Surface on the Optical Constants of Copper", Phil. Mag., V. 22 (1936) pp. 769-790

## XII. BIOGRAPHICAL NOTE

Robert Bruce Gordon was born in Rochester, New York, on May 26, 1915. Attended the public schools of Irondequoit, New York. Entered the University of Rochester in 1931 and was graduated in 1935, receiving the degree of Bachelor of Science in Mechanical Engineering with High Distinction. Elected to membership in Phi Beta Kappa.

Entered the Graduate School of the Massachusetts Institute of Technology in 1935 to pursue a course of study leading to the degree of Doctor of Science in Metallurgy, with a minor in Mechanical Engineering. Appointed Assistant in the Department of Metallurgy 1936 - 1939.

Presented to the Faculty of the Massachusetts Institute of Technology in May, 1939, a thesis entitled, "Age-Hardening of a Copper-Cobalt and a Copper-Iron Alloy".

XIII. APPENDIX

The following symbols and abbreviations have been used in the accompanying data sheets.

- R = Electrical resistance in ohms
- % R = Percent of quenched resistance
- $K_{15,000}$  = Apparent volume susceptibility in a field of 15,000 oersteds
- %  $K_o$  = Percent of quenched susceptibility
- Log %  $K_o$  = Logarithm of percent of quenched susceptibility
- D/i = Arbitrary units proportional to remanent magnetic moment
- H = Rockwell F Hardness

DATA FOR COPPER-COBALT ALLOY AT 250° C

(Figure 24)

Hours	$R \times 10^2$	% $R_o$	$K_{14,600} \times 10^6$	% $K_o$	Log % $K_o$	$\frac{D}{i}$	Log $\frac{D}{i}$
0	.3345	100	65.1	100.0	2.000	0.54	-.268
.0025	.3303	98.7	66.2	101.7	2.007	0.54	-.268
.005	.3297	98.6	65.0	100.0	2.000	—	—
.01	.3278	98.0	67.0	102.8	2.012	0.54	-.268
.02	.3258	97.4	68.3	104.8	2.020	—	—
.04	.3245	97.0	69.1	106.1	2.026	0.54	-.268
.08	.3222	96.3	69.7	107.0	2.029	—	—
.16	.3188	95.3	71.0	109.0	2.037	0.55	-.260
.32	.3172	94.8	71.9	110.3	2.043	—	—
.64	.3157	94.4	72.9	111.9	2.049	—	—
1.28	.3132	93.6	74.0	113.6	2.055	0.60	-.222
2.56	.3105	92.8	75.7	116.2	2.065	—	—
6.0	.3067	91.7	75.3	115.5	2.063	0.71	-.149
14	.3030	90.6	77.0	118.1	2.072	—	—
30	.2987	89.3	78.7	120.9	2.083	0.90	-.046
60	.2937	87.8	80.1	123.0	2.090	0.97	-.013
132	.2872	85.9	83.5	128.1	2.108	1.09	+ .037
295	.2785	83.3	85.0	130.7	2.116	1.22	.086
630	.2710	81.0	92.1	141.5	2.151	1.34	.127

DATA FOR COPPER-IRON ALLOY AT 250° C

(Figure 25)

Hours	$R \times 10^2$	% $R_o$	$K_{14,600} \times 10^6$	% $K_o$	Log % $K_o$	$\frac{D}{i}$	Log $\frac{D}{i}$
0	.2253	100	58.4	100.0	2.000	0.60	-.228
.0025	.2200	97.6	56.1	96.0	1.982	0.60	-.228
.005	.2175	96.5	56.1	96.0	1.982	—	—
.01	.2150	95.5	58.2	99.6	1.998	—	—
.02	.2113	93.8	58.7	100.4	2.002	—	—
.04	.2070	92.0	57.9	99.1	1.996	—	—
.08	.2025	90.0	58.8	100.6	2.003	—	—
.16	.1997	88.6	59.8	102.3	2.010	0.60	-.228
.32	.1970	87.5	60.3	103.2	2.014	—	—
.64	.1943	86.3	60.1	102.9	2.012	—	—
1.28	.1914	85.0	61.5	105.2	2.022	0.85	-.071
2.56	.1874	83.2	62.1	106.2	2.026	—	—
6.0	.1822	81.0	62.1	106.2	2.026	1.10	+.041
14	.1768	78.4	63.4	108.7	2.036	—	—
30	.1704	75.6	64.6	110.6	2.044	1.40	.146
60	.1645	73.0	65.6	112.2	2.050	1.55	.190
132	.1593	70.7	66.5	113.8	2.056	1.85	.267
295	.1537	68.2	68.2	116.9	2.068	2.10	.322
630	.1500	66.5	67.1	114.8	2.060	2.50	.398

## HARDNESS DATA AT 250° AND 375° C

250° C			375° C			
Hours	Cu - Co (Fig. 24)	Cu - Fe (Fig. 25)	Hours	Cu - Co (Fig. 26)	Hours	Cu - Fe (Fig. 27)
0	44	40	0	43	0	39
.0025	54	44.5	.005	48	.001	40
.005	48	43.5	.015	50.5	.005	40
.01	49	42	.03	48	.01	41
.02	49	45	.06	48	.02	42
.04	51.5	45.5	.12	49	.04	43.5
.08	51	45.5	.24	49	.08	42
.16	51.5	45.5	.48	49.5	.16	46
.32	50	48	1.0	49	.32	45
.64	50	47.5	2.0	50	.64	45
1.28	51	44	4.0	51	1.5	48
2.56	50.5	46	21	53.5	3.0	48.5
6.0	52	47.5	67	55	6.5	50.5
14	55	48.5	161	53	12	52
30	52	48.5	353	57	25	51.5
60	52	47.5	876	60.5	58	54
132	50	48.5	1308	61.5	129	56.5
295	49.5	46			262	58.5
630	53	50			500	59



DATA FOR COPPER-COBALT ALLOY AT 375° C

(Figure 26)

Hours	$R \times 10^2$	% $R_o$	$K_{15,000} \times 10^6$	% $K_o$	Log % $K_o$	$\frac{D}{i}$	Log $\frac{D}{i}$
0	.3610	100	52.1	100.0	2.000	0.25	-.602
.001	.3415	94.6	55.1	105.7	2.024	0.26	-.585
.005	.3400	94.2	57.0	109.3	2.039	0.33	-.481
.015	.3350	92.8	59.5	114.1	2.057	0.44	-.357
.04	.3292	90.9	66.0	126.7	2.103	0.71	-.149
.10	.3180	88.1	74.6	143.2	2.156	1.10	+.041
.25	.3039	84.2	86.1	165.1	2.218	1.65	.217
.60	.2852	79.0	100.2	192.0	2.283	2.45	.389
1.5	.2572	71.3	—	—	—	3.00	.477
4.0	.2212	61.3	163	312	2.494	4.00	.602
10	.1913	53.0	—	—	—	4.25	.628
25	.1717	47.5	—	—	—	4.55	.658
60	.1570	43.5	364	690	2.839	4.75	.677
151	.1409	39.0	—	—	—	5.00	.699
390	.1226	33.9	—	—	—	5.50	.740
990	.1053	29.2	1260	2420	3.384	6.50	.813

DATA FOR COPPER-IRON ALLOY AT 375° C

(Figure 27)

Hours	$R \times 10^2$	% $R_o$	$K_{15,000} \times 10^6$	% $K_o$	Log % $K_o$	$\frac{D}{i}$	Log $\frac{D}{i}$
0	.2408	100	53.5	100.0	2.000	0.48	-.319
.001	.2038	84.6	61.3	114.6	2.059	0.70	-.155
.005	.2010	83.5	62.8	117.4	2.070	1.15	+.061
.02	.1964	81.6	67.6	126.2	2.101	1.58	.199
.08	.1856	77.1	83.2	155.3	2.191	1.94	.288
.30	.1712	71.1	93.2	174.0	2.241	2.08	.318
1.0	.1562	64.9	88.5	186.0	2.270	2.14	.330
3.0	.1434	59.6	95.5	178.4	2.251	2.14	.330
8.0	.1320	54.8	87.6	163.7	2.214	2.12	.326
24	.1177	48.8	77.9	145.4	2.163	2.06	.314
80	.1033	42.8	70.1	131.0	2.117	2.10	.322
430	.0087	36.8	64.3	120.0	2.079	2.00	.301

DATA FOR COPPER-COBALT ALLOY AT 550° C

(Figure 28)

Hours	$R \times 10^2$	% $R_0$	$\frac{D}{i}$	$\text{Log } \frac{D}{i}$
0	.3525	100	0.30	- .523
.001	.3248	92.15	0.55	- .260
.0025	.3110	88.23	0.80	- .097
.005	.2910	82.57	1.40	+ .146
.010	.2295	65.14	2.60	.415
.02	.1917	55.40	3.70	.568
.04	.1697	48.10	4.70	.672
.08	.1534	43.50	5.80	.763
.16	.1364	38.70	7.10	.851
.32	.1264	35.86	8.80	.944
.64	.1203	34.13	11.75	1.070
1.28	.1103	31.30	17.05	1.232
2.56	.1058	30.0	25	1.398
5.15	.0990	28.06	46.5	1.667
16	.0930	26.35	130	2.114
50	.0895	25.37	400	2.60
200	.0860	24.40	—	—

DATA FOR COPPER-IRON ALLOY AT 550° C

(Figure 29)

Hours	$R \times 10^2$	% $R_0$	$K_{15,000} \times 10^6$	% $K_0$	Log % $K_0$	$\frac{D}{i}$	Log $\frac{D}{i}$
0	.2646	100	59.3	100.0	2.000	0.70	-.155
.001	.2249	85.0	71.2	120.1	2.080	0.99	-.004
.0025	.2203	83.3	73.0	123.2	2.091	1.52	+.182
.005	.2115	80.0	79.5	134.0	2.127	2.02	.305
.01	.1943	73.5	76.5	129.0	2.111	2.38	.377
.02	.1604	60.6	67.2	113.2	2.054	2.54	.405
.04	.1424	53.8	58.4	98.3	1.993	2.63	.420
.08	.1226	46.3	49.1	82.8	1.918	2.58	.412
.16	.1123	42.5	47.6	80.2	1.904	2.50	.398
.32	.1050	39.6	46.9	78.9	1.897	2.43	.386
.64	.0997	37.6	47.3	79.6	1.901	2.37	.375
1.50	.0922	34.8	48.5	81.7	1.912	2.45	.389
3.0	.0870	32.8	51.4	86.7	1.938	2.60	.415
6.7	.0826	31.2	56.0	94.4	1.975	2.70	.431
14.7	.0795	30.0	62.1	108.5	2.035	2.94	.468
30.4	.0776	29.3	68.1	114.8	2.060	3.33	.522
70.4	.0759	28.6	74.3	125.1	2.097	4.00	.602
190	.0722	27.3	99.0	166.8	2.222	6.25	.796
405	.0706	26.7	123.2	207.6	2.317	15.75	1.197
592	.072	27.3	171	288	2.459	20.5	1.312

## HARDNESS DATA AT 550° C AND 700° C

Hours	550° C		Hours	700° C	
	Cu - Co (Fig. 28)	Cu - Fe (Fig. 29)		Cu - Co (Fig. 30)	Cu - Fe (Fig. 31)
0	44	45	0	44.5	40
.001	42	41	.001	46.5	40
.0025	42	44	.0025	46.5	42
.005	40.5	40.5	.005	48	47.5
.01	42	42	.01	47.5	50
.02	43.5	48	.02	56.5	64
.04	50.5	53.5	.04	67	78.5
.08	51	58.5	.06	70	78.5
.16	57	66	.10	72.5	84
.32	60	69.5	.20	76.5	87.5
.66	63.5	73	.40	78.5	88
1.32	67.5	78.5	.80	79	87
3.07	72.5	80.5	1.6	77.5	85.5
7.3	73.5	84.5	3.2	76.5	81.5
17.3	77	88.5	6.4	73.5	75.5
40	79.5	91	16	70	63
90	81.5	91	26	68	62
194	82.5	89.5	51	65	59
392	80	86.5	109	62	59
817	78.5	86	212	58	57
			310	56	58

DATA FOR COPPER-COBALT ALLOY AT 700° C

(Figure 30)

Hours	$R \times 10^2$	% $R_0$	$\frac{D}{i}$	$\text{Log } \frac{D}{i}$
0	.3394	100	0.45	- .347
.001	.2200	64.8	2.65	+ .423
.0025	.2060	60.7	3.80	.580
.005	.1920	56.5	5.40	.732
.01	.1810	53.3	9.40	.973
.02	.1680	49.5	17.55	1.244
.04	.1683	49.6	32.5	1.512
.08	.1610	47.4	81.0	1.908
.20	.1546	45.6	230.5	2.363
.40	.1587	46.8	778	2.891
.80	.1574	46.4	1960	3.292
1.6	.1570	46.2	2870	3.458
3.0	.1577	46.4	3240	3.511
6	.1560	45.9	2870	3.458
12	.1500	44.1	1980	3.297
25	.1470	43.3	896	2.952
50	.1462	43.1	741	2.870
91	.1452	42.8	706	2.849
298	.1442	42.5	631	2.800

## DATA FOR COPPER-IRON ALLOY AT 700° C

(Figure 31)

Hours	$R \times 10^2$	% $R_o$	$K_{15,000} \times 10^6$	% $K_o$	Log % $K_o$	$\frac{D}{i}$	Log $\frac{D}{i}$
0	.2400	100	45.1	100	2.000	0.55	-.260
.001	.1540	64.2	28.1	62.3	1.795	1.72	+.236
.0025	.1430	59.6	28.2	63.5	1.803	1.98	.297
.005	.1460	60.9	30.0	66.7	1.824	1.72	.236
.01	.1343	56.0	27.8	61.7	1.790	1.51	.179
.02	.1240	51.6	29.8	66.0	1.820	1.79	.253
.04	.1203	50.1	30.8	68.5	1.836	1.90	.279
.08	.1225	51.0	33.2	73.8	1.868	1.98	2.97
.20	.1160	48.3	35.8	79.6	1.901	1.70	.230
.40	.1157	48.2	40.7	90.4	1.956	1.86	.270
.80	.1147	47.8	46.4	103.1	2.013	1.76	.246
1.60	.1150	47.9	56.7	126.0	2.100	2.06	.314
3.20	.1120	46.7	70.6	156.8	2.195	3.07	.487
7.0	.1110	46.2	93.4	207.	2.316	17.35	1.239
17	.1122	46.7	136	302.	2.480	33.0	1.518
40	.1125	46.9	198	440.	2.643	74.0	1.869
100	.1160	48.3	—	—	—	148	2.170
150	—	—	483	1070	3.029	196	2.292
298	.1140	47.5	860	1910	3.281	—	—
394	—	—	1310	2900	3.462	438	2.641

ABSTRACT

The object of this investigation was to study the mechanism of age-hardening in two alloys that were uniquely adapted for the use of magnetic measurements. These binary alloys of copper with 3.2 percent cobalt and 2.4 percent iron were in the form of paramagnetic solid solutions after drastically quenching from the solution temperature. Upon subsequent aging at suitable lower temperatures, a precipitate formed that was ferromagnetic in the copper-cobalt alloy and either ferromagnetic or paramagnetic, depending upon its location, in the copper-iron alloy. The accompanying changes in magnetic susceptibility and remanence were so marked that the precipitation process could be followed very nicely. From the changes in these properties and the more common ones of hardness, resistance and microstructure, a satisfactory qualitative picture of the aging mechanism has been obtained. Before presenting the results it will be desirable to discuss briefly the experimental details.

The alloys were made by melting in a clay-graphite crucible under a cover of charcoal and bottom-pouring into a chill mould. The raw materials were cathode copper of high commercial purity, electrolytic iron and commercial cobalt rondelles. Chemical analyses showed no segregation of cobalt or iron. The principal impurities were 0.02 percent carbon and 0.01 percent nickel. The copper-cobalt alloy contained 0.02 percent iron. The ingots were forged, hot rolled, then cold rolled to a strip 0.118 inches thick for hardness samples, and cold swaged to a



0.079 inch diameter rod for magnetic and resistance samples.

The specimens were given a solution treatment of several hours at 1040° C (1900° F) in a specially-built vertical tube furnace. This furnace was so constructed that the specimens could be heated and quenched in a hydrogen atmosphere in order to avoid oxidation of the surface. The specimens were suspended from a fine wire that was burned out by an electric current at the time of the quench. The specimens then fell by gravity into a bath of sodium hydroxide solution. Despite these efforts to avoid the effects of a high transformation rate, the alloys could not be given an entirely satisfactory quench, as was shown by a scatter in the properties of the as-quenched samples. The aging treatments were conducted in liquid baths at temperatures of 250°, 375°, 550° and 700° C. The specimens were quenched in water at suitable intervals and measurements made at room temperature.

Hardness measurements were made on the Rockwell F scale and were reproducible to  $\pm 2$  units. Electrical resistance was measured on a Kelvin double bridge and the results had a relative accuracy of about 0.1 percent. Magnetic susceptibility was measured by the Gouy method at a field strength of 15,000 oersteds. This property measured the magnetization of both the paramagnetic copper-rich solution and the ferromagnetic precipitate. In order to separate these two effects another property, remanence, dependent only on the ferromagnetic portion, was measured. The specimens were magnetized to saturation and then suspended by a glass fiber so as to be at right angles to the direction of a uniform magnetic field. The deflection of the specimen

when the field was applied was proportional to the remanent magnetic moment.

From the property changes at four temperatures the aging process in both alloys was found to involve two stages of precipitation. Aging at 250° C showed only the first stage, while 700° C showed only the second. The intermediate temperatures of 375° and 550° C showed both stages. During the first stage, hardness showed a slight increase, resistance a marked decrease, remanence a pronounced increase and susceptibility a gradual increase. The drop in resistance indicated precipitation and the increase in the magnetic properties showed that it was ferromagnetic. Microscopic examination of samples, polished and etched electrolytically to avoid extraneous effects, showed these changes were associated with precipitation at the grain boundaries.

During the second stage, where precipitation occurred generally within the grains, the hardness and resistance changes were similar in both alloys. Hardness increased about 50 Rockwell F units to a maximum after 100 hours at 550° C, while resistance, at the same time, nearly reached a minimum of about 30 percent of its initial value. The magnetic properties, on the other hand, showed striking changes between the two alloys. This was due to the fact that the general precipitate was ferromagnetic in the copper-cobalt alloy and paramagnetic in copper-iron. Thus, in the copper-cobalt alloy, susceptibility continued to increase strongly and remanence, after a delay in the early stages, did likewise. But in the copper-iron alloy, the remanence remained constant while susceptibility decreased as a result of the precipitation of iron from solution in a paramagnetic form.

These results indicated that both the cobalt and iron-rich precipitates were probably face-centered cubic transition phases. If this was true, their eventual transformation to stable forms was to be expected. Such a transformation was found in the copper-iron alloy after 200 hours aging at 550° C. The susceptibility and remanence showed marked increases due to the formation of a ferromagnetic phase, presumably body-centered iron. The susceptibility could not be measured at the two higher temperatures in the copper-cobalt alloy because of its strong ferromagnetism, but the remanence changes were very striking. The remanence reached a sharp maximum after 3 hours at 700° C, decreased to 20 hours and then levelled off suddenly. These changes might have been due to a transformation in the cobalt-rich phase similar to that of iron.

A correlation of the results showed that the aging mechanism was the same at all temperatures. Each successively higher temperature repeated the earlier changes and then carried them to a more advanced stage. No pre-precipitation effects of the type found in duralumin were observed. However, the probable occurrence of transition phases gave indirect evidence favoring a "knot" stage. The property changes due to "knot" formation may have been absent because of the rapid transformation during the quench or because of the non-uniformity of the aging process.